

# **Identification of B cell antigen receptor epitopes of mantle cell lymphoma B cells**

## **Dissertation**

Zur Erlangung des akademischen Grades Doctor rerum naturalium (Dr. rer. nat.)  
des Fachbereichs Chemie der Universität Hamburg

vorgelegt von

**Michael Fichtner**

Hamburg, 2016

*Der praktische Teil dieser Arbeit wurde im Zeitraum von Januar 2012 bis Dezember 2015 in der Arbeitsgruppe von Prof. Dr. Martin Trepel, der II. medizinischen Klinik und Poliklinik am Universitätsklinikum Hamburg Eppendorf, angefertigt.*

Gutachter: 1. Prof. Dr. Martin Trepel, Hamburg/Augsburg  
2. Prof. Dr. Edzard Spillner, Hamburg/Aarhus

Datum der Disputation: 30.09.2016

Datum der Druckfreigabe: 05.10.2016

# Table of Contents

Abstract.....	13
Zusammenfassung.....	14
1 Introduction.....	15
1.1 Overview over the human immune system.....	15
1.2 The B cell.....	16
1.2.1 B cell development.....	16
1.2.2 General structure of the B cell antigen receptor.....	17
1.2.3 Development of the immunoglobulin diversity.....	19
1.2.4 The theory of clonal selection.....	20
1.2.5 The BCR downstream signalling cascade.....	21
1.3 Non-Hodgkin-Lymphoma.....	23
1.3.1 Overview of B cell Non-Hodgkin lymphoma subtypes.....	23
1.3.2 The role of B cell receptors in Non-Hodgkin lymphomas.....	25
1.3.3 The mantle cell lymphoma.....	26
1.3.4 Inhibition of BCR signalling as a therapeutic opportunity.....	28
1.4 Superantigens.....	29
1.4.1 <i>Staphylococcus aureus</i> superantigens.....	29
1.4.2 Other known superantigens.....	31
1.5 Aim of this study.....	32
2 Materials.....	33
2.1 Laboratory devices.....	33
2.2 Kits.....	34
2.3 Media and Reagents.....	34
2.4 Enzymes.....	35
2.5 Antibodies.....	35
2.6 Oligonucleotides (Primer).....	36
2.7 Cells and bacteria.....	37
2.8 Animals.....	37
2.9 Software and online tools.....	38
2.10 General recipes.....	38
3 Methods.....	40
3.1 General molecular biological methods.....	40
3.1.1 RNA extraction.....	40

3.1.2	cDNA synthesis.....	40
3.1.3	Ethanol precipitation of DNA and RNA.....	41
3.1.4	Terminal transferase reaction.....	41
3.1.5	DNA and RNA quantification.....	41
3.1.6	Polymerase chain reaction (PCR).....	41
3.1.7	Agarose gel electrophoresis.....	43
3.1.8	Gel extraction.....	43
3.1.9	Cloning into pJet vector.....	43
3.1.10	Plasmid purification.....	44
3.1.11	DNA sequencing.....	44
3.1.12	Site directed mutagenesis.....	44
3.1.13	Cloning into pFastbacDual (pFBD) and pBud vectors.....	44
3.1.14	Next Generation Sequencing.....	47
3.2	Protein biological methods.....	49
3.2.1	Purification of recombinant antibodies and Fab fragments.....	49
3.2.2	Dialysis.....	52
3.2.3	Protein extraction.....	52
3.2.4	Protein Quantification.....	53
3.2.5	Sodium dodecyl sulfate polyacrylamide gel electrophoresis (SDS-PAGE).....	54
3.2.6	Coomassie staining of acrylamide gels.....	55
3.2.7	Western Blot.....	56
3.2.8	Far Western Blot.....	57
3.2.9	Enzyme linked immunosorbent assay (ELISA).....	58
3.2.10	Immunoprecipitation (IP).....	59
3.2.11	Preparation for mass spectrometry analysis.....	59
3.2.12	Dynamic light scattering.....	59
3.2.13	Random peptide phage display.....	60
3.3	Microbiological methods.....	67
3.3.1	Prokaryotic cell culture media and supplements.....	67
3.3.2	Propagation of <i>Escherichia coli</i> .....	68
3.3.3	Preparation of competent bacteria.....	69
3.3.4	Transformation of bacteria.....	70
3.3.5	DH10bac transformation and Bacmid purification.....	71
3.4	Cytological methods.....	72
3.4.1	Seeding of eukaryotic cells.....	73

3.4.2	Cryopreservation of cells.....	73
3.4.3	Cell counting.....	74
3.4.4	Isolation of peripheral blood mononuclear cells (PBMCs).....	74
3.4.5	Eukaryotic production of recombinant proteins.....	75
3.4.6	Immunofluorescence assay.....	77
3.4.7	Transduction of Burkitt lymphoma cell lines.....	78
3.4.8	Fluorescence-activated cell sorting (FACS).....	80
3.4.9	Flow cytometric cell analysis.....	80
3.4.10	Calcium influx measurement.....	81
3.4.11	Proliferation assay.....	81
3.5	Institutional approval.....	82
4	Results.....	83
4.1	Analysis of the MCL immunoglobulin sequences.....	83
4.1.1	The mantle cell lymphoma Ig repertoire.....	86
4.1.2	Comparison of the mutational load of NHL-Igs.....	88
4.1.3	Next-Generation Sequencing with two samples of the same patient.....	89
4.1.4	Prediction of N-glycosylation in MCL-Igs.....	91
4.2	Characterisation of mantle cell lymphoma-derived Igs.....	93
4.2.1	Production of recombinant antibodies with two expression systems.....	93
4.2.2	Epitope identification with random peptide phage display.....	94
4.2.3	Affinity and cross-reactivity of selected epitope mimics.....	96
4.2.4	Dynamic light scattering measurement of MCL-Igs.....	99
4.2.5	HEp-2 cell immunofluorescence assays.....	101
4.2.6	Western Blot with HEp-2 cell lysates.....	104
4.2.7	Immunoprecipitation using MCL-derived Igs.....	105
4.2.8	Mass spectrometry analysis of precipitated proteins.....	106
4.2.9	Vimentin binding capabilities of MCL-Igs.....	108
4.3	SpA as a potential superantigen for MCL BCRs.....	109
4.3.1	The SpA binding motif.....	109
4.3.2	Binding of SpA by NHL-derived Fab fragments.....	110
4.4	Generation of a model system for the analysis of BCR activation.....	112
4.4.1	Establishment of the surface immunoglobulin expression.....	114
4.4.2	Ca <sup>2+</sup> -Flux assay of transduced and untransduced Ramos cells.....	116
4.4.3	Ca <sup>2+</sup> -Flux assay of mantle cell lymphoma cell lines.....	118
4.4.4	Far Western Blot analysis of induced Ramos cells.....	119

4.4.5	Proliferation assay of stimulated Ramos cells.....	121
5	Discussion.....	123
5.1	The Ig repertoire of mantle cell lymphoma.....	123
5.1.1	MCL-derived Igs were only minimally mutated.....	123
5.1.2	Mantle cell lymphoma B cells showed a biased IGHV expression.....	124
5.1.3	MCL-Igs acquired no novel glycosylation sites.....	125
5.1.4	The MCL-Ig did not mutate over time.....	126
5.2	Identification of antigens and epitopes in NHL.....	127
5.2.1	Three MCL-Igs enriched epitope mimics during phage display selection.....	127
5.2.2	Most MCL-Igs did not bind to HEp-2 cell expressed auto-antigens.....	129
5.2.3	Cytoskeletal proteins are potential antigens for MCL-Igs.....	131
5.2.4	The NADP-dependent malic enzyme is a potential antigen recognised by MCL B cell receptors.....	132
5.2.5	MCL-Igs did not recognise themselves.....	132
5.2.6	Possible high throughput methods for antigen detection.....	133
5.3	Bacterial superantigens bind to MCL-Igs.....	134
5.4	MCL-Igs might be susceptible for further superantigens.....	136
5.5	Development of a cellular readout system for BCR activation.....	137
5.5.1	Ramos cells could be activated by a transduced IgM.....	138
5.5.2	Induction of the introduced BCR altered the cell behaviour.....	138
5.6	Conclusion and Outlook.....	140
6	References.....	142
7	Appendix.....	158
A	Permissions from the publishers.....	158
B	List of additional primers used in this study.....	159
C	Origin of the patient samples.....	162
D	Index of tables.....	163
E	Index of figures.....	164
F	Risk and safety statements.....	165
G	Hazardous chemicals used in this study.....	167
	Acknowledgements.....	170
	Eidesstattliche Versicherung.....	171

## Abbreviations

°C	degree Celsius
AA	amino acids
Ab	antibody
ABC/GCB	activated B cell like/germinal centre B cell like
Amp	ampicillin
APS	ammonium persulfate
b	base(s)
BCR	B cell antigen receptor
BL	Burkitt lymphoma
BLAST	basic local alignment search tool
bp	base pair(s)
BSA	bovine serum albumin
c	concentration
Ca <sup>2+</sup>	calcium (ion)
CaCl <sub>2</sub>	calcium chloride
CDR	complementarity determining region
CLL	chronic lymphocytic leukaemia
CMV	cytomegalovirus
CSR	class switch recombination
d	days
D (-gene segment)	diversity (-gene segment)
Da	Dalton
DAPI	4',6-diamidino-2-phenylindole
ddH <sub>2</sub> O	double-distilled water
DLBCL	diffuse large B cell lymphoma
DLS	dynamic light scattering
DMSO	dimethyl sulfoxide
DNA	deoxyribonucleic acid
dNTP	deoxynucleoside triphosphate
DZ	dark zone
<i>E. coli</i>	<i>Escherichia coli</i>
EDTA	ethylenediaminetetraacetic acid
ELISA	enzyme linked immunosorbent assay
Fab	Fragment antigen binding

FACS	fluorescence activated cell sorting
FBS	fetal bovine serum
F <sub>c</sub>	Fragment cristallisable region
FITC	fluorescein isothiocyanate
FR	framework region
GC	germinal centre
Gent	gentamycin
GHS	globally harmonised system of classification and labelling of chemicals
h	hour(s)
HCl	hydrochloric acid
HEPES	2-[4-(2-hydroxyethyl)piperazin-1-yl]ethanesulfonic acid
Ig	immunoglobulin
IGHV	immunoglobulin heavy variable (gene)
IGKV	immunoglobulin κ variable (gene)
IGLV	immunoglobulin λ variable (gene)
IMGT	international ImMunoGeneTics information system
IP	immunoprecipitation
IPTG	isopropyl β-D-1-thiogalactopyranoside
J (-gene segment)	joining (-gene segment)
Kan	kanamycin
KCl	potassium chloride
l	litre
LB	lysogenic broth
LZ	light zone
m	metre
M	molar
MALT	mucosa-associated lymphoid tissue
MCL	mantle cell lymphoma
MgCl <sub>2</sub>	magnesium chloride
mIg	membrane-bound immunoglobulin
min	minute(s)
NaCl	sodium chloride
Nb	number
NGS	Next-Generation sequencing
NHL	Non-Hodgkin lymphoma
OD	optical density



PAGE	polyacrylamide gel electrophoresis
PAMP	pathogen associated molecular pattern
PBMCs	peripheral blood mononuclear cells
PBS	phosphate buffered saline
PCNSL	primary central nervous system lymphoma
PCR	polymerase chain reaction
PE	phycoerythrin
PEG	polyethylene glycol
PEI	polyethylenimine
Pen	penicillin
polH	polyhedrin
PpL	<i>Peptostreptococcus magnus</i> Protein L
PRR	Pathogen recognition receptor
PVDF	polyvinylidene fluoride
RAG	recombination activating gene
RNA	ribonucleic acid
rpm	rounds/revolutions per minute
RT	room temperature
s	second(s)
<i>S. aureus</i>	<i>Staphylococcus aureus</i>
SDS	sodium dodecyl sulfate
Sf9	Spodoptera frugiperda (cell line)
sIg	surface immunoglobulin
SOB	super optimal broth
SOC	super optimal broth with catabolite
SpA	<i>Staphylococcus aureus</i> Protein A
Strep	streptomycin
SV40	simian virus 40
TAE	tris(hydroxymethyl)aminomethane-acetate-ethylenediaminetetraacetic acid
TB	terrific broth
TB	Tris borate
TBS(-T)	tris buffered saline (with Tween-20)
TE	tris(hydroxymethyl)aminomethane ethylenediaminetetraacetic acid
TEMED	tetramethylethylenediamine
Tet	tetracycline
U	units

UKE	University Medical Center Hamburg-Eppendorf
UV	ultra violet
V (-gene segment)	variable (-gene segment)
v/v	volume per volume
vol	volumes
w/v	weight per volume
WB	Western Blot
X-Gal	5-bromo-4-chloro-3-indolyl- $\beta$ -D-galactopyranoside

### **Abbreviations of nucleobases**

A	Adenine
C	Cytosine
G	Guanine
T	Thymine
N	random nucleobase

## Abbreviations of amino acids

A	Ala	alanine
C	Cys	cysteine
D	Asp	aspartate
E	Glu	glutamate
F	Phe	phenylalanine
G	Gly	glycine
H	His	histidine
I	Ile	isoleucine
K	Lys	lysine
L	Leu	leucine
M	Met	methionine
N	Ans	asparagine
P	Pro	proline
Q	Gln	glutamine
R	Arg	arginine
S	Ser	serine
T	Thr	threonine
V	Val	valine
W	Trp	tryptophan
Y	Tyr	tyrosine

## Prefixes

c	centi-
k	kilo-
M	mega-
m	milli-
n	nano-
μ	micro-



## Abstract

Mantle cell lymphoma (MCL) is an aggressive entity of B cell Non-Hodgkin lymphomas, which is associated with a poor prognosis. The impressive effectiveness of recently developed drugs, targeting the B cell receptor (BCR) signalling in this disease, suggest a major role of the BCR in the lymphoma development and progression. However, little is known about the bound epitopes and antigens of this molecule in MCL.

This study aimed to find specific antigens of MCL-BCRs to provide further insights into the pathogenesis of MCL. To accomplish this goal, MCL patient material was acquired and the variable regions of the tumour-associated immunoglobulins (Igs) were determined. Afterwards, the variable heavy and light chain regions of several MCL samples were cloned in an expression vector to produce IgGs and Fab fragments with the same binding properties as the MCL-BCRs.

It was shown that the BCR repertoire was strongly biased within the cohort of 24 analysed MCL samples. About 45% of all tumour B cells expressed an IGHV3-gene and one-third expressed an IGHV4-gene.

Immunoprecipitation and mass spectrometric analysis revealed two potential auto-antigens which were not associated with MCL to date:  $\beta$ -actin and the NADP-dependent malic enzyme. However, only a few MCL-derived antibodies bound to these proteins and random peptide phage display library screenings showed only limited success. By analysing the BCR repertoire of MCL samples, sequence features, which are indicative for a complementarity determining region (CDR)-independent recognition of the staphylococcal superantigen protein A (SpA), were found in all Igs harbouring an IGHV3-gene. Subsequent experiments demonstrated that all MCL-derived Fab fragments of this subgroup bound to SpA.

Moreover, a cellular readout system for BCR activation experiments was established. With this technique, it was possible to analyse whether an antigen is able to cross-link the BCR of a B cell and activates the BCR signalling cascade. This system was then used to demonstrate that SpA can induce B cells which express an IGHV3-gene. These results were also confirmed using the MAVER-1 and Jeko-1 MCL cell lines.

Consequently, the results of this study indicate that a *Staphylococcus aureus* infection might be an important hallmark in MCL pathogenesis. If the findings could be verified in patients, new promising approaches in MCL treatment or prevention could be developed.

## Zusammenfassung

Das Mantelzelllymphom (MCL) ist eine aggressive Entität des Non-Hodgkin-Lymphoms mit einer ungünstigen Prognose. Neue Medikamente, welche die Signalkaskade des B-Zell-Antigen-Rezeptors (BCR) inhibieren, zeigten in den letzten Jahren jedoch vielversprechende Behandlungserfolge. Diese Befunde verdeutlichten dabei auch die Schlüsselrolle des BCR bei der Tumorentstehung und -progression. Die Epitope und Antigene, welche durch die MCL-BCRs gebunden werden, sind bisher jedoch weitgehend unbekannt.

Ziel der vorliegenden Studie war es, neue Antigene der MCL-BCRs zu identifizieren und dadurch Einblicke in die Pathogenese des MCL zu erlangen. Dafür wurden MCL-Patientenproben gesammelt und die variablen Regionen der tumorassoziierten Immunglobuline (Ig) bestimmt. Anschließend wurden einige dieser Igs als rekombinante IgGs bzw. Fab-Fragmente produziert.

Es konnte gezeigt werden, dass das BCR-Repertoire der 24 Proben umfassenden Kohorte stark eingeschränkt war. Etwa 45% der untersuchten MCL-B-Zellen exprimierten IGHV3-Gene und ein weiteres Drittel exprimierte IGHV4-Gene.

Mittels Immunpräzipitationen und massenspektrometrischen Analysen konnten zudem zwei potentielle Auto-Antigene identifiziert werden, welche bisher noch nicht für das MCL beschrieben wurden. Dabei handelte es sich um  $\beta$ -actin und das NADP-abhängige Malatenzym. Allerdings zeigten nur wenige MCL-Igs eine Bindung an diese beiden Proteine und auch Phage-Displays mit randomisierten Peptidbibliotheken waren nur teilweise erfolgreich.

Es wurde daher auch nach Antigenen gesucht, welche Paratop-unabhängig gebunden werden. Dabei wurde entdeckt, dass alle Igs, die ein IGHV3-Gen exprimierten, ein Motiv aufwiesen, welches die Bindung des *Staphylococcus aureus* Protein A (SpA) ermöglichte. Anschließend konnte gezeigt werden, dass alle produzierten MCL-Fabs dieser bedeutenden Sub-Population an SpA binden.

Des Weiteren wurde eine Methode etabliert, die es ermöglichte zu untersuchen, ob ein Antigen den BCR-Signalweg induzieren kann. Mit Hilfe dieser Methode konnte dann gezeigt werden, dass SpA in der Lage ist B-Zellen, welche IGHV3-Gene exprimieren, zu aktivieren. Diese Ergebnisse wurden zudem in den MCL-Zelllinien MAVER-1 und Jeko-1 bestätigt.

Die Ergebnisse dieser Studie legen nahe, dass eine *S. aureus* Infektion eine entscheidende Rolle bei der Pathogenese des MCL spielen könnte. Wenn die Erkenntnisse dieser Studie im Patienten bestätigt werden, könnte dies neue Möglichkeiten für die Therapie oder Prävention des MCL eröffnen.

# 1 Introduction

## 1.1 Overview over the human immune system

The human body is persistently exposed to a plethora of pathogens. To counter these potential threats, the human immune system consists of two branches protecting the organism <sup>1</sup>. The innate immune system, evolutionarily older, protects the host in a generic way without specific adaptation. It responds immediately to infections or the disruption of mechanical or chemical barriers <sup>2</sup>. Pathogen recognition is thereby facilitated by so called pathogen recognition receptors (PRR), such as toll-like receptors <sup>3-5</sup>. PRRs are germline coded molecules able to detect pathogen associated molecular patterns (PAMPs), like lipopolysaccharides on bacteria, which are essential for the survival and infection of the pathogen, thus highly conserved <sup>1,3,6</sup>. As soon as a pathogen infects the host, neutrophilic cells and macrophages migrate to the infection site and try to ingest and eliminate the invading organism <sup>3</sup>. During this process, cytokines are released, attracting further immune cells to the infection site. In addition, antigen presenting cells (APCs), such as macrophages and dendritic cells migrate towards the lymph nodes where they present pathogen-associated antigens to the cells of the adaptive immune system, which represents the second branch of the human immune system <sup>1</sup>.

The cells of the adaptive immune system are separated into B and T lymphocytes, and derive from haematopoietic stem cells (HSC) <sup>7</sup>. In contrast to the cells of the innate immune system, lymphocytes are capable to engage pathogens specifically via receptors, formed by random rearrangement of specific gene segments (1.2.3) <sup>3,7</sup>. B lymphocytes develop in the bone marrow and provide the humoral immune response (1.2) <sup>7-9</sup>. T cells, on the other hand, mature in the thymus and are responsible for the cellular immune response <sup>7-9</sup>. The T cell receptors recognise peptides presented by the major histocompatibility complex (MHC I and MHC II) mostly expressed on APCs <sup>7</sup>.

Since the B and T cell receptors are highly adaptive, B and T lymphocytes are capable to bind nearly any given antigen, including self-antigens <sup>3,7</sup>. While binding of foreign antigens represents the intended function, self-reactivity must be suppressed by multiple complex mechanisms leading to a clonal deletion or clonal anergy of the auto-reactive lymphocyte <sup>3,7</sup>.

Moreover, the adaptive immune response leads to the creation of memory cells to quickly generate immune effector cells that eradicate pathogens that had been encountered previously <sup>7</sup>.

Therefore, the innate immune system facilitates the first line of defence and the activation of the adaptive immune system relies on the antigen presenting capabilities of the APCs<sup>1-3,7,10</sup>. Thus, both parts closely interact with each other via complex signalling mechanisms forming the human immune system to protect the body<sup>10</sup>.

## 1.2 The B cell

B cells (or B lymphocytes) are part of the adaptive immune system and represent its humoral branch, as they secrete soluble antibodies (or immunoglobulins, Igs) against pathogens<sup>10</sup>. A fully matured and antibody-secreting B cell is called plasma cell and produces Igs with a single defined specificity, which are constantly released into the body in order to bind and neutralise pathogenic molecules<sup>11</sup>. Igs are a major component of the blood accounting for about 20% of all plasma proteins<sup>11</sup>. The high level of specificity is achieved by a complex process of maturation.

### 1.2.1 B cell development

#### 1.2.1.1 Differentiation from haematopoietic stem cells in the bone marrow

In general, the main goal of B cell maturation is the development of a specific and functional B cell antigen receptor (BCR, 1.2.2) with a high affinity against a distinct antigen. During this process, the B cell passes through well defined developmental stages characterised by specific cell surface markers and recombination states of the BCR<sup>12</sup>.

To become a B cell, an HSC in the bone marrow differentiates into a multipotent progenitor-(MMP), early lymphoid progenitor- (ELP), and common lymphoid progenitor-cell (CLP) until it reaches pre-pro-B cell stage<sup>13-16</sup>. During this differentiation, important surface marker for B cell development, like the B220 isoform of CD45 and the interleukin-7 receptor (IL-7 $\alpha$ ), are upregulated and the recombination activating gene 1 and 2 (RAG1/2) expression increases<sup>17-20</sup>. However, neither the B cell characteristic CD19 nor a BCR is present at these early stages<sup>19</sup>.

The appearance of CD19 as well as the increasing activity of RAG1/2 and the terminal deoxynucleotidyl transferase (TdT) marks the entry into the pro-B cell stage<sup>12</sup>. At this point in time, the recombination of the heavy chain happens (see chapter 1.2.3). After the first genomic recombination, the B cell enters the pre-B cell stage defined by the presence of a pre-BCR on the cell surface<sup>21</sup>. This indicates a successful recombination of the Ig heavy chain gene. The pre-BCR is activated without an external antigen by self-aggregation of pre-BCRs, resulting in strong proliferation of the pre-B cells<sup>22</sup>. Self-aggregation is thereby facilitated via the surrogate light chain (SLC), formed by  $\lambda 5$  and VpreB, which is only present on pre-BCRs<sup>21-24</sup>. Furthermore, in the late



pre-B-cell stage the recombination of the light chain begins, ending up with the replacement of the surrogate light chain by the recombined kappa or lambda light chain <sup>25</sup>. At this stage, the BCR is fully assembled. Importantly, if the newly generated Ig binds to an auto-antigen, the B cell would undergo apoptosis (1.2.4). With a productively recombined BCR-Ig, the immature B cell leaves the bone marrow and migrates into the secondary lymphoid organs (lymph nodes and spleen). Of note, at this developmental stage the immature B cell has not yet encountered an antigen <sup>11</sup>.

### **1.2.1.2 Maturation in secondary lymphoid organs**

The bone marrow-derived naïve B cells are forming the B cell follicles in the lymph nodes and spleen <sup>12,26</sup>. After antigen encounter so called germinal centres (GC) develop quickly with the aid of T-helper cells <sup>27,28</sup>. During this process, naïve B cells which are displaced from the GC form an own compartment, the B cell mantle <sup>27</sup>. Distinguished by its microscopic appearance, the GC is divided into a dark zone (DZ) and a light zone (LZ) <sup>29</sup>. While the DZ contains almost only B cells with a big nucleus (resulting in a dark appearance), the LZ is populated by antigen-specific B cells, follicular dendritic cells and also some naïve B cells <sup>30,31</sup>. Functionally, the DZ is the site of B cell proliferation and BCR diversification, whereas the antigen presentation and selection happens in the LZ <sup>32</sup>.

In GC-B cells, the B cell lymphoma-6 protein (BCL-6) plays an important role as it influences multiple pathways and molecules, like BCL-2 and the DNA damage response mechanisms, to support somatic hypermutation (SHM) and prevent auto-immunity <sup>33</sup>. Furthermore, the activation induced deaminase (AID) is becoming active during GC-reaction resulting in affinity maturation of the B cells (1.2.3). Finally, also class switch recombination (CSR) of the Ig occurs during GC-reaction <sup>34</sup>.

Matured and positively selected GC-B cells are exported from the GC either as plasmablasts or as memory B cells <sup>35,36</sup>. Plasmablasts are still able to proliferate, but will finally differentiate into non-proliferating antibody secreting plasma cells, persistently secreting the specific hypermutated Ig <sup>37</sup>.

## **1.2.2 General structure of the B cell antigen receptor**

The BCR is a complex of intra- and extracellular proteins, which is responsible of binding a specific antigen and facilitates signalling into the cell to alter the cell behaviour <sup>38</sup>.

### 1.2.2.1 The immunoglobulin

To bind an antigen, the BCR contains a membrane-bound immunoglobulin (mIg) as a key molecule. It consists of four polypeptide chains, two identical heavy chains of about 440 amino acids (~50 kDa) and two identical light chains with about 220 amino acids (~25 kDa)<sup>39</sup>. Each light chain is bound to a heavy chain through disulfide bonds and the heavy chains are coupled by disulfide bonds as well, forming the Y-shaped Ig<sup>39</sup>.

Heavy and light chains are further subdivided into variable and constant domains of approximately 110-130 amino acids, each<sup>34</sup>. While heavy chains have three or four constant and one variable domain, the light chains always have one constant and one variable domain<sup>34</sup>. The variable regions are responsible for antigen binding, whereas the constant regions determine effector functions<sup>34</sup>. Five different classes of constant domains are known for the heavy chain constant regions, named after the greek letters  $\alpha$ ,  $\delta$ ,  $\epsilon$ ,  $\gamma$  and  $\mu$ <sup>40</sup>. Therefore, the immunoglobulin isotypes are called IgA, IgD, IgE, IgG and IgM, with IgG and IgA are subdivided into further subclasses (IgG1-IgG4, IgA1-IgA2)<sup>40</sup>. Every isotype has different functions facilitated by the binding of F<sub>C</sub>-receptors. For example, IgG binds to pathogens and can activate the complement system<sup>34</sup>. IgE, in contrast, plays an important role in inflammation, allergic reactions and asthma<sup>41</sup>. The first Ig a B cell usually produces is of the IgM or IgD isotype<sup>42</sup>. Only if the Ig binds an antigen, further B cell activation is induced and the isotype can change by class switch recombination (CSR)<sup>34,42</sup>.

For light chains only two types of constant domains exist named  $\kappa$  or  $\lambda$  and no CSR happens<sup>40</sup>.

The variable regions of heavy and light chains are located at the amino-terminal end of each of the peptide sequence and have three hyper-variable domains, named complementarity determining regions (CDR1-3)<sup>11,43</sup>. The specificity of an Ig is mainly based on the composition of these CDRs, which congregate and form the antigen binding site of the Ig, named paratope<sup>34,43</sup>. Between the CDRs are  $\beta$ -sheeted framework regions (FRs) which maintain the structural stability of the Ig<sup>44</sup>.

As a result, each Ig has two individual but identical antigen binding sites specific for a distinct region of an antigen, called epitope<sup>11</sup>.

### 1.2.2.2 The transmembrane protein CD79

The cytoplasmatic domains of membrane bound IgM and IgD molecules are very short with only three amino acids and thus, not able to facilitate downstream signalling<sup>21</sup>.

To transmit a signal into the cell, each mIg is non-covalently associated with the transmembrane heterodimer CD79. It is composed of the two proteins CD79a and CD79b (also known as Ig $\alpha$  and Ig $\beta$ ) which are linked by a disulfide bridge<sup>45</sup>. Both chains are part of the immunoglobulin

superfamily, having an extracellular Ig domain, a proximal spacer region, and a transmembrane domain <sup>46</sup>. In addition, the proteins have an intracellular domain bearing an immunoreceptor tyrosine-based activation motif (ITAM) <sup>47</sup>. Following activation, CD79 recruits further proteins to activate the downstream signalling cascade (1.2.5).

### 1.2.3 Development of the immunoglobulin diversity

The whole B cell antigen receptor repertoire in the organism has a diversity in the order of about  $10^{10}$ - $10^{11}$  different epitopes <sup>48</sup>. In contrast, the total number of protein coding genes in humans is in the range of 20.000 to 25.000 <sup>49</sup>. This means that the large diversity cannot be coded completely in the genome.

The high diversity is therefore achieved by four different mechanisms <sup>50</sup>. First is the combinatorial diversification. Variable regions of Ig heavy and light chains are assembled by random recombination of gene segments called variable (V)-, diversity (D)- and joining (J)-gene segments <sup>50</sup>. This process is called V(D)J-recombination and requires double strand breaks in the DNA introduced by RAG1 and RAG2 <sup>34</sup>. The V-,D- and J- gene segments for the heavy chains are coded on chromosome 14, the V-and J-gene segments forming the light chains are located on chromosome 2 and 22 for  $\kappa$  and  $\lambda$ , respectively <sup>34</sup>. During B cell maturation, the first step is the genomic recombination of a D- and a J-gene segment <sup>34</sup>. All unused segments between those segments are deleted <sup>34</sup>. Afterwards, this newly formed DNA complex is fused with a V-gene segment <sup>34</sup>. Consequently, all gene segments between the V-gene segment and the DJ-complex are erased. The generated VDJ-segment is then transcribed to an RNA transcript, which already contains the constant region gene <sup>11</sup>. The mRNA is spliced, deleting the remaining J-gene segments and fusing the gene which codes the constant region to the VDJ-region <sup>34</sup>. The same process builds up the light chain variable region with the exception of the missing D-gene segments in light chains <sup>34,40</sup>.

The second source of diversity is known as junctional site diversity <sup>40</sup>. It occurs as a result of imprecise joining of the mentioned gene segments <sup>40</sup>. Template independent insertion of nucleotides at the junction sites further increase the variety and is referred as junctional insertion diversity <sup>40</sup>. Importantly, the framework regions 1-3 as well as the CDR1 and 2 regions of the heavy chain are completely coded by the  $V_H$ -segment <sup>34</sup>. The CDR3-region, in turn, is assembled by the joined V-, D- and J- segments and thus has a very high diversity <sup>34</sup>.

Key enzymes facilitating the recombination are the recombination activating genes 1 and 2 (RAG1/RAG2), enzymes for the non-homologous end joining (NHEJ) and the terminal deoxynucleotidyl transferase (TdT) <sup>51</sup>. Together, they form a complex called VDJ-recombinase and

are almost exclusively expressed in lymphocytes<sup>51</sup>. The lack or mutation of proteins responsible for VDJ-recombination can lead to severe immune defects depending on the affected protein<sup>51</sup>. Of note, the V(D)J-recombination takes place in the bone marrow before antigen contact<sup>34</sup>.

Genomic recombination often results in an unproductive gene product. Due to the diploid genome, every B cell has two chances to create a functional B cell receptor<sup>52</sup>. If the recombination of the heavy or light chain fails a B cell cannot form a BCR and must undergo apoptosis<sup>53</sup>. Furthermore, if the recombination successfully created a productive Ig the unused chromosome must be disabled<sup>54</sup>. This process is called allelic exclusion and ensures that every B cell express only one Ig with a defined specificity<sup>54</sup>.

During ongoing antigen contact in the germinal centre, the Ig undergoes affinity maturation by introducing point mutations in the variable region to increase the affinity and specificity<sup>40</sup>. This somatic hypermutation takes place in the secondary lymphoid organs after stimulation of the B cell and is the fourth source of Ig diversity<sup>34,40</sup>. The basic mechanism is the deamination of cytosine to uracil by the activation induced deaminase (AID), also involved in class switch recombination<sup>34,55,56</sup>. Uracil is excised by DNA repair enzymes and replaced by an error prone DNA polymerase<sup>57</sup>. This process often ends up with the insertion of wrong nucleotides and results in the expression of an Ig with altered antigen specificity or affinity<sup>34</sup>.

### 1.2.4 The theory of clonal selection

As outlined above, the development of the antibody repertoire happens completely without antigen contact. Nevertheless, highly specific immunoglobulins against foreign antigens must be generated, while self-antigen recognition must be prevented.

The theory of clonal selection developed in 1957 by Frank Macfarlane Burnet explains the underlying mechanisms of this process and has become the widely accepted standard model<sup>58,59</sup>. It says that the organism is continuously producing B cells with random antigen specificities (in the bone marrow). Each B cell is thereby committed to a BCR with a defined specificity<sup>54</sup>. The antigen inexperienced B cells migrate into the secondary lymph organs where they come in contact with foreign antigens<sup>27,28</sup>. A B cell only proliferates if it can bind an antigen leading to a positive selection of this cell<sup>28</sup>. As described, expanded clones often undergo somatic hypermutation to increase the BCR affinities. If a clone loses its affinity to the antigen it gets eradicated, while clones with increased affinity will be expanded by further proliferation<sup>54</sup>.

Moreover, a B cell clone reactive against self-epitopes must be suppressed, to avoid autoimmune diseases<sup>28</sup>. Thus, B cells which bind self antigens with high affinity will most likely undergo apoptosis (clonal deletion)<sup>28</sup>. If the BCR has only low-affinity to the self-antigens, the B cell either

becomes unresponsive (anergic) and cannot proliferate or the BCR is edited in order to delete the self-reactivity (receptor editing)<sup>28,60-62</sup>.

Eventually, the most affine clones against a foreign antigen differentiate into memory and plasma cells<sup>54</sup>.

### 1.2.5 The BCR downstream signalling cascade

Unlike most cellular receptors with a clearly defined ligand, the BCR signalling must be induced by a great number of different antigens.

The classical activation theory of the BCR is based on the fluid mosaic model<sup>63</sup>. In brief, it assumes that all BCRs (and all other transmembrane proteins or complexes) in a resting B cell can float freely in the cell membrane bilayer. If an antigen is bound by a membrane-bound Ig (mIg), a second mIg of another BCR complex is recruited. This cross-linking finally leads to the activation of CD79 ITAMs. This cross-linking model (CLM) is supported by the observation that in most cases only bivalent F(ab)<sub>2</sub> but not monovalent Fab molecules can induce a B cell activation<sup>64</sup>. In addition, antigens harbouring only a single epitope are often not suitable as vaccines as they generate poor antibody titers<sup>65,66</sup>.

However, new findings are questioning the CLM due to studies showing that high antibody titers were also achieved by using monovalent antigens<sup>67,68</sup>. A possible alternative explanation is given by the dissociation activation model (DAM)<sup>69</sup>. The DAM suggests that the BCRs in resting cells are not monomers but form tightly packed oligomeric complexes<sup>70</sup>. If an antigen is bound by the mIgs the complexes open up and the CD79 ITAMs become accessible<sup>70,71</sup>.

To date, neither the CLM nor the DAM is completely falsified or verified. Nevertheless, if two BCRs reaching the necessary proximity, phosphorylation of the CD79 ITAMs by the LYN kinase is the next crucial step to signal into the cell<sup>72</sup>. Phosphorylated ITAMs then recruit the SYK kinase, activating further signalling proteins, such as SLP65 (also known as BLNK), phospholipase C $\gamma$ 2 (PLC $\gamma$ 2) and CD19 (Figure 1)<sup>73-77</sup>. In addition, also the phosphatidylinositol-3-kinase (PI3K) is phosphorylated by SYK<sup>78</sup>. Activated PI3K then phosphorylates phosphatidylinositol 4,5-bisphosphate (PIP<sub>2</sub>) forming phosphatidylinositol 3,4,5-trisphosphate (PIP<sub>3</sub>) which serves as docking site for the recruitment of brutons tyrosine kinase (BTK)<sup>79</sup>. Together, the whole protein complex is necessary to assemble the so called signalosome with BTK as a key molecule for further intracellular signalling (Figure 1).

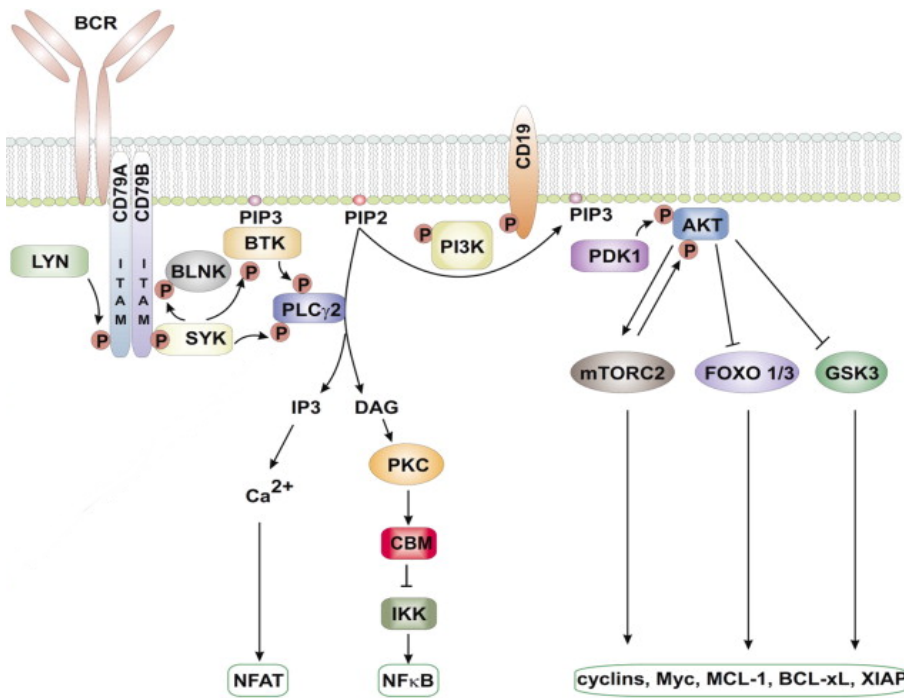


**Figure 1: Key molecules of the B cell antigen receptor signalling cascade.**

The image was obtained from Bojarczuk et al. (2015)<sup>168</sup> with permission from Elsevier (see Appendix A)

The formation of the signalosome and the activation of BTK results in the phosphorylation of PLC $\gamma$ 2<sup>80,81</sup> and the creation of the second messengers inositol 3,4,5-trisphosphate (IP3) and diacylglycerol (DAG) by hydrolysis of PIP2<sup>82</sup>. IP3 receptors on the endoplasmic reticulum (ER) bind IP3 resulting in an activation of Ca<sup>2+</sup> channels on the ER. This leads to an increased intracellular calcium level and to the opening of the membrane Ca<sup>2+</sup> channels, activating the nuclear factor of activated T cell (NFAT)<sup>83,84</sup>.

Moreover, DAG bind to Ras guanyl nucleotide-releasing protein (RasGRP) which in turn activates the protein kinase C $\beta$  (PKC $\beta$ ), finally leading to the activation of the NF- $\kappa$ B pathway<sup>85</sup>.

If both pathways are activated, the B cell proliferates and class switch recombination of the BCR occurs. If only NFAT but not NF- $\kappa$ B is activated, as happening in anergic cells, no B cell activation is possible<sup>86,87</sup>.

In B cells with class switched BCR-IgG, the initial BCR pathway activation is slightly different. In contrast to IgM, the cytoplasmatic IgG tail is longer and has two conserved motifs for intracellular signalling<sup>88,89</sup>. One of these motifs is the Ig tail tyrosine (ITT) motif which is bound by the growth factor receptor-bound 2 (GRB2), if phosphorylated by Syk. GRB2 then recruits BTK, leading into downstream signalling activation<sup>88,89</sup>. While IgM signalling usually favours survival and proliferation of the cells (activating the NF- $\kappa$ B pathway), a signal transduction via IgG triggers plasmacytic differentiation by ERK- and MAPK-pathways<sup>90-92</sup>.

## 1.3 Non-Hodgkin-Lymphoma

As outlined above, the development of mature B cells is a complex process with steps directly altering the DNA of the cell by introducing and repairing double strand breaks (1.2.3). Despite multiple control checkpoints during B cell maturation, erroneous DNA recombination can lead to B cell clones with uncontrolled proliferation, eventually forming a B cell lymphoma<sup>93</sup>. Historically, lymphomas are categorised into Hodgkin-(HL) and Non-Hodgkin-lymphomas (NHL). While HLs are characterised by the presence of Sternberg-Reed- or Hodgkin-cells in the lymphoid tissue, every lymphoma that is not a HL is called NHL<sup>93</sup>. Therefore, very diverse lymphomas are pooled in this group<sup>93,94</sup>.

NHLs currently account for about 4% of all cancers diagnosed in the western world<sup>95,96</sup>. More than 85-90% of all NHLs derive from B lymphocytes and only a small number coming from T or NK cells<sup>97</sup>. In general, NHL occur more often in white people and males and the incident rate increases exponentially with increasing age, with two-thirds of the patients older than 60 years<sup>97</sup>. Furthermore, the incidence rate of NHL has strong regional differences with the highest rates in northern America, Australia and Europe and the lowest in Asia<sup>98</sup>. However, some subtypes like the B cell lymphoma of mucosa-associated lymphoid tissue type (MALT lymphoma) have much higher incidence rates in Asia, which points towards a role of lifestyle, environmental factors, ethnogenomics and/or infections in the aetiology of different NHL subtypes<sup>98</sup>. To date, multiple risk factors, like viral and bacterial infections, tobacco and alcohol consumption as well as unhealthy diets were evaluated but have not been revealed as a general trigger in the majority of NHLs<sup>97,98</sup>.

### 1.3.1 Overview of B cell Non-Hodgkin lymphoma subtypes

NHL subtypes can be characterised by morphological and molecular analysis. Every subtype is an own lymphoma entity with an individual biological background, pathogenesis and incidence<sup>94,97-100</sup>. As shown in Figure 2, two subtypes, the diffuse large B cell lymphoma (DLBCL) and the follicular lymphoma (FL), accounted for more than the half of all NHL cases in the US<sup>98</sup>.

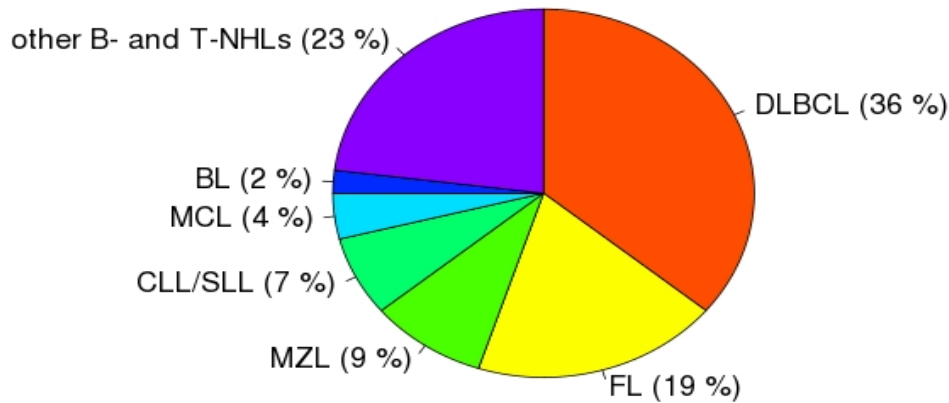


**Figure 2: Incidence rates of NHL subtypes in the USA (2000-2011).**

DLBCL: diffuse large B cell lymphoma; FL: follicular lymphoma; MZL: marginal zone lymphoma; CLL/SLL: chronic lymphocytic leukemia/small lymphocytic lymphoma; MCL: mantle cell lymphoma; BL: Burkitt lymphoma  
Adapted from Brian C.-H. Chiu and Ningqi Hou<sup>98</sup>.

Also, the aggressiveness of the diseases, prognosis and treatment options differ strongly between NHL subtypes (Table 1)<sup>97,99,100</sup>.

**Table 1: Common Non-Hodgkin-lymphomas categorised by indolent or aggressive behaviour.**

<b>Indolent B cell NHL</b>	<b>Aggressive B cell NHL</b>
Follicular lymphoma	Mantle cell lymphoma
Marginal zone lymphoma	Burkitt lymphomas
MALT lymphoma	Diffuse large B cell lymphoma

\*MALT: mucosa-associated lymphoid tissue type lymphoma

Depending on the developmental stage at which the B cell lymphoma arise, pregerminal, germinal and postgerminal centre lymphomas can be distinguished (Table 2)<sup>97</sup>.

**Table 2: B cell NHLs ordered by the suspected B cell development stage at genesis of the lymphoma.**

<b>Stage of B cell development</b>	<b>B cell NHL subtype</b>
Pregerminal centre	Mantle cell lymphoma
Germinal centre	Follicular lymphoma, Burkitt lymphoma, marginal zone lymphoma, GCB-DLBCL*
Postgerminal centre	Multiple myeloma, ABC-DLBCL*

\*GCB/ABC-DLBCL: germinal centre B-cell-like/activated B-cell-like diffuse large B-cell lymphoma



Lymphoma B cells of all NHLs shown in table 2 express a functional BCR<sup>93,94</sup>. As outlined above, the formation of heavy and light chains depends on DNA recombination (1.2.3). Although Ig-gene rearrangement is a tightly controlled process, RAG activity sometimes accidentally rearranges wrong non Ig-gene segments which can lead to chromosomal translocations<sup>93</sup>. Some NHL subtypes have characteristic translocations that can be used for classification, as well (Table 3)<sup>93,94</sup>.

**Table 3: Chromosomal translocations in B cell NHLs**

<b>Chromosomal translocation</b>	<b>Translocated gene</b>	<b>B cell NHL subtype</b>
t(8;14)(q24;q32)	MYC-gene	Burkitt lymphoma, DLBCL
t(11;14)(q13;q32)	CCND1-gene	Mantle cell lymphoma
t(14;18)(q32;q21)	BCL2-gene	Follicular lymphoma, DLBCL

As seen in table 3, the translocations juxtaposing oncogenes to chromosome 14q32, which bring these genes under the control of the Ig heavy chain promoter<sup>93</sup>. Since this promoter is highly active in B cells, the overexpression of an oncogene leads to a major dysregulation of the cell cycle. To a much lesser extent oncogenes translocate to the  $\kappa$ - or  $\lambda$ -promotor (chromosome 2 or 22 respectively)<sup>93,100</sup>. However, not all NHLs bear chromosomal translocations and also healthy individuals harbour B cells with such recombinations<sup>100-103</sup>. Therefore, additional pathogenic mechanisms are necessary for the pathogenesis of NHL.

### 1.3.2 The role of B cell receptors in Non-Hodgkin lymphomas

Most lymphoma B cells preserve the expression of the BCR suggesting an important role of this protein complex for the survival and proliferation of these cells<sup>93</sup>.

The functional activity and possible antigens, however, vary strongly between different NHL-entities. By analysing the gene profile of diffuse large B cell lymphoma (DLBCL), it was found that this disease must be differentiated into two types, called the activated B cell-type- (ABC-) and the germinal centre B cell-like- (GCB-) DLBCL<sup>104</sup>. ABC-DLBCLs rely on an active BCR signalling and show a genomic profile similar to *in vitro* stimulated B cells with an activated NF- $\kappa$ B pathway<sup>104-106</sup>. In contrast, GCB-DLBCLs are NF- $\kappa$ B independent and do not need the BCR signalling for survival<sup>105</sup>. These differences in BCR dependency can be a valuable prognostic factor since GCB-DLBCLs presumably have a better prognosis than ABC-DLBC<sup>104</sup>.

The analysis of the BCR also revealed two forms of chronic lymphocytic leukaemia (CLL). It was demonstrated that the clinical outcome differs between patients with mutated (M-CLL) and unmutated (U-CLL) BCR-Ig<sup>107</sup>. M-CLL showed a more indolent behaviour and favourable

outcome whereas U-CLL had an aggressive course of the disease <sup>107</sup>. Furthermore, CLL-B cells express only limited gene segments for the variable heavy chain, strongly indicating an antigen involvement in cancer development <sup>108</sup>. Similar observations were found for mantle cell lymphoma BCRs (1.3.3).

The ongoing BCR expression, the active BCR pathway and the limited BCR repertoire in some NHL cases led to the question which antigens are recognised by the lymphoma-B cells. Over the last decades, it was possible to identify multiple foreign and self-epitopes. It was shown that some CLL-Iggs bind to self-antigens and proteins that become exposed in apoptotic cells including vimentin and myosin heavy chain IIA <sup>109–112</sup>. A further remarkable activation mechanism of the BCR pathway in CLL is the cell autonomous signalling by self-recognition of BCRs <sup>113–115</sup>. In these cases, a BCR-Ig reacts with another BCR on the surface of the cell. This results in a constant signalling and cell activation <sup>113</sup>.

Another type of BCR activation was demonstrated in FL. Igs of FL cells are often highly mutated and display an acquisition of N-linked glycosylation sites in the antigen-binding region <sup>116,117</sup>. The introduced glycans at this site harbour mannose termini which can bind to lectins in the microenvironment <sup>118</sup>. It was further shown that lectins of *Pseudomonas aeruginosa* and *Burkholderia cenocepacia* are able to bind and activate FL cells <sup>119</sup>. These findings might lead to a novel treatment opportunity or help to prevent that lymphoma entity.

### 1.3.3 The mantle cell lymphoma

#### 1.3.3.1 Overview of the mantle cell lymphoma

Mantle cell lymphoma (MCL) is a rare disease and accounts for approximately 3-10% of all NHL cases in Europe and the US <sup>94,120</sup>. Despite recent advantages in therapy, MCL has a poor prognosis with a median survival of 3-4 years <sup>94,121</sup>. The median age of diagnosis is between 60-65 years and the disease occurs predominantly in males (ratio 2:1) <sup>94,121,122</sup>.

Based on cytology, MCL displays three typical growth patterns (mantle zone, nodular and diffuse) and four different cytological variants (classical, blastoid, small cell and pleomorphic) <sup>123</sup>. Further, MCL B cells display a distinct immunophenotype (CD19+, CD20+, CD22+, CD43+, CD79a+, CD5+, BCL-2+, CD23-, CD10-, CD200-, BCL6-) and a functional B cell receptor (1.3.3.2) <sup>124</sup>.

The genetic hallmark is the reciprocal chromosomal translocation t(11;14)(q13;q32), which leads to overexpression of CyclinD1, a cell cycle regulator normally not expressed in B lymphocytes <sup>125</sup>. Cyclins of the D-type can dimerise with cyclin dependent kinases (CDK4 and CDK6), leading to a phosphorylation of the tumour suppressor protein retinoblastoma (RB) <sup>126</sup>. As a result, affected cells

switches from G1 to S-phase, entering the cell cycle and proliferate <sup>126</sup>. In addition, various other mutations are present in MCL, including genes important for DNA damage response (i.e. ATM, P53) and cell cycle regulation (i.e. CDK4, RB1) <sup>127-129</sup>.

However, multiple studies also showed MCL cases without the CCND1 translocation but nevertheless displaying MCL mutation patterns and morphological features <sup>130-132</sup>. In many CCND1-negative cases, translocations of either CCND2 or CCND3 were found <sup>132-134</sup>. Since all proteins of the cyclin-family are cell cycle regulators, these translocations deregulate the proliferation of the B cells as well. To date, it is not completely known whether CCND1 negative variants have a different prognosis <sup>131,132</sup>.

Beside the very aggressive course of MCL, recent studies also demonstrated a few variants (10-15%) with an indolent behaviour and a long median survival <sup>135</sup>. These cases are often associated with a higher mutational load of the BCR, a non-complex karyotype and specific alterations in the MCL gene profile <sup>136</sup>. Furthermore, SOX11-negativity is suggested to be an important marker for indolent MCL but this remains controversial <sup>136-139</sup>.

### **1.3.3.2 The B cell antigen receptor in mantle cell lymphoma**

In recent years, the BCR of MCL B cells has gained increasing attention. It has been long thought that MCL develops from pregerminal B cells without antigen contact (1.2.1) <sup>140</sup>. Without the germinal centre reaction, the Igs are not somatically hypermutated and the variable heavy and light chain regions are nearly unmutated. Early studies sequenced the MCL-Igs and were able to confirm that they harbour mostly germline sequences <sup>141</sup>. As an antigen inexperienced naïve B cell has the ability of self-renewal and high proliferation rates, this theory partly explained the aggressive behaviour of MCL. Nevertheless, increasing evidence challenged this paradigm with multiple studies demonstrated the presence of mutated Ig sequences in about 20% of cases <sup>142-147</sup>. However, in contrast to the CLL, somatic hypermutation does not seem to have clinical or pathological relevance as mutated and unmutated cases have similar outcome <sup>147,148</sup>.

In addition, by analysing the BCR repertoire of different MCL cases, it was shown that many Igs consisted of similar variable heavy chains <sup>135,145-149</sup>. As a consequence, the BCR repertoire is strongly biased with four variable heavy chains (in order of abundance: IGHV3-21, IGHV4-34, IGHV1-8 and IGHV3-23) accounting for almost half of all cases <sup>149</sup>. A remarkable bias like that cannot be explained by chance and points towards an antigenic drive during MCL pathogenesis <sup>149,150</sup>.

Moreover, in some cases, subclones occurred, which underwent class-switch recombination<sup>150–152</sup>. Although the function and relevance is not completely understood, it was demonstrated that AID is expressed (1.2.3) and active in most MCL cases<sup>150–152</sup>. Since the expression levels and isoform expression of AID seems to vary between different tissues, it is likely that the tumour microenvironment plays a key role for the tumour behaviour<sup>126,150</sup>.

Additionally, Pighi et al.<sup>153</sup> demonstrated that several proteins of the BCR downstream signalling cascade are activated, which suggests an important role for the survival of the tumour.

Taken together, these findings emphasise an important selective pressure on MCL progenitor cells and probably an ongoing antigenic drive for MCL cells<sup>150</sup>.

However, despite this strong evidence for an antigen-driven pathogenesis of MCL and in contrast to other diseases like CLL or MALT-lymphoma, it remains unclear what kind of antigens are involved and what role they might play during tumourigenesis and progression.

As described in the next chapter, the BCR pathway inhibitors are very successful in treatment of MCL, further underlining the importance of BCR signalling (1.3.4).

### **1.3.4 Inhibition of BCR signalling as a therapeutic opportunity**

Treatment of NHL strongly depends on the respective entity<sup>99</sup>. Nevertheless, with the development of the anti-CD20 antibody Rituximab, the response rate and overall survival of patients with NHL dramatically increased. MCL patients, however, showed only limited response to Rituximab even if combined with chemotherapy and the progression-free survival was shorter, compared to other NHLs<sup>154–156</sup>.

As outlined before, multiple NHL entities, including the MCL, seem to rely on the BCR signalling pathway (1.3.2 and 1.3.3.2). The development of agents targeting intracellular processes might therefore be a promising way to improve the survival of patients.

One key element of the BCR pathway is the spleen tyrosine kinase (SYK), which is recruited directly after phosphorylation of the CD79 ITAMs (1.2.5)<sup>157</sup>. It was already shown, that SYK is overexpressed in multiple MCL tumour samples and also in some MCL cell lines<sup>153,158</sup>. Consequently, an inhibition of SYK *in vitro* led to an induction of apoptosis, especially in cell lines with high SYK expression<sup>153,158</sup>.

Phase 1 studies with the SYK inhibitor fostamitanib, however, revealed good objective response rates (ORR) in patients with relapsed CLL but only limited ORR in relapsed MCL<sup>159</sup>.

Another key molecule of the BCR signalling cascade is brutons tyrosine kinase (BTK). As described (1.2.5), activation of BTK directly affects proliferation and differentiation of the B cell. Due to its key role in this process, it is also an attractive target for inhibition<sup>160</sup>.

The highly selective BTK-inhibitor ibrutinib can bind covalently to Cys-481 of BTK, which results in an irreversible inhibition of its kinase activity <sup>161</sup>.

Compared to benign B cells, BTK is overexpressed in MCL cells, an observation also reported in CLL <sup>162,163</sup>. Thus, inhibition of the BTK signalling by ibrutinib treatment showed good clinical response rates in MCL and CLL <sup>164–166</sup>. Besides being a promising treatment option, these findings also highlight the BCR as an important research object.

Yet, about one third of the patients do not respond to ibrutinib and it was shown that most MCL cell lines had an intrinsic resistance against it <sup>126,167</sup>. These cell lines probably activate the NF- $\kappa$ B pathway through the BCR-independent NIK kinase pathway, which in turn might be a new valuable target for inhibition <sup>167</sup>.

Further inhibitors for proteins of the BCR signalling pathway (like PI3K and AKT) are currently being developed and multiple clinical trials are ongoing to test the effectiveness of these new drugs <sup>160,168</sup>.

In summary, the BCR seems to play a tremendous role during the development of multiple NHLs and the inhibition of the downstream signalling represents a promising new treatment option. The clinical success of these inhibitors might also help to foster the understanding of NHL development and highlight the BCR as a worthwhile research target.

## 1.4 Superantigens

The specificity and affinity of an immunoglobulin is enabled by the variable region at the amino-terminal end of the Igs (1.2.2.1). However, during co-evolution of the immune system and pathogens, some bacteria developed mechanisms to evade the host defence <sup>169</sup>. Normally only a few lymphocytes are induced by an antigen, but it was first shown in T cells that some bacterial and viral proteins can stimulate a large proportion of T cell-receptors <sup>169,170</sup>. This has led to the term superantigen, describing molecules which have a non-classical antigen-receptor-mediated interaction with multiple lymphocytes at once <sup>170</sup>.

Over the past two decades, multiple superantigens were also found to bind to the BCR.

### 1.4.1 *Staphylococcus aureus* superantigens

One of the best-characterised pathogen expressing superantigens is the gram-positive coccal bacterium *Staphylococcus aureus*. About 30-50% of healthy individuals are temporarily and up to 20% are persistently colonised with *S. aureus* <sup>171,172</sup>. Although frequently being a non-pathogenic

part of the bacterial colonisation, *S. aureus* can cause a variety of diseases such as skin infection, endocarditis, abscess and sepsis <sup>171</sup>.

Thereby, superantigens play an important role for *S. aureus* to circumvent the host immune defences. Two different well characterised superantigens are expressed, which are capable of binding to soluble or membrane bound Igs.

The *S. aureus* protein A (SpA) has become a model for superantigenic B cell activation <sup>173</sup>. It is a 42 kDa protein which consists of five highly homologous Ig binding domains and can be membrane bound or soluble <sup>174</sup>. Each domain binds with high affinity to the F<sub>C</sub> domain of IgGs <sup>175</sup>. Since the constant part of IgG is required for complement activation, the inverse binding of IgGs by SpA leads to an impaired immune response.

In addition, SpA bind a clearly defined binding motif in the framework region of the variable heavy chain domain <sup>174</sup>. This motif is present in nearly all genes of the IGHV3-family <sup>174</sup>. As shown in Figure 3, the binding occurs outside the complementarity determining regions and thus is completely independent of the CDR-mediated Ig binding ability.

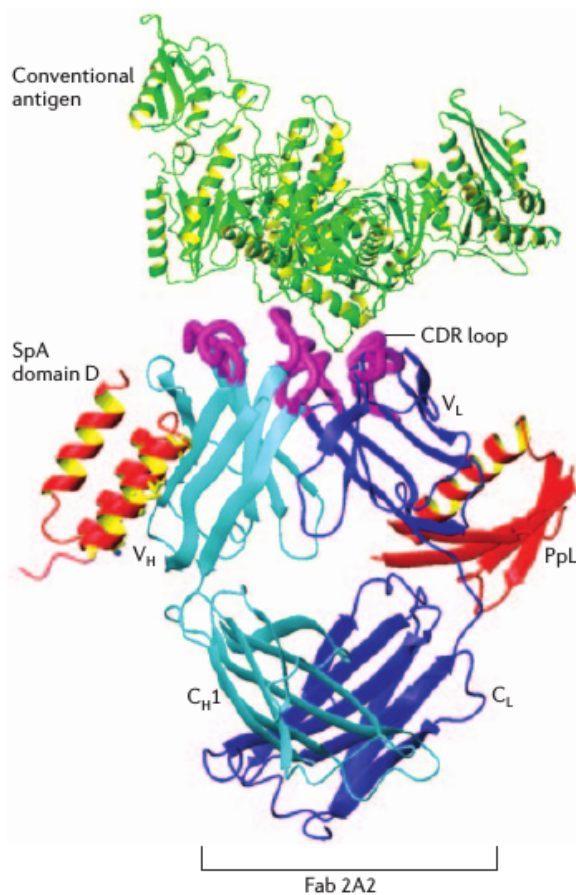


**Figure 3: Illustration of the complex between a Fab fragment, the SpA and PpL superantigens as well as a regular antigen.** Cartoon representation of the crystal structures of a Fab fragment (cyan: heavy chain, blue: light chain), the staphylococcal Protein A (SpA) and the *Peptostreptococcus magnus* Protein L (PpL). The superantigens are bound outside the CDR-regions (violet) and therefore do not impair the ability of the Fab to bind a classical antigen (green).

The picture was obtained from Silverman and Goodyear (2006)<sup>173</sup> with the permission of the NPG (<http://www.nature.com/nrmicro/index.html>).

*In vitro* experiments have shown a biased production of Igs harbouring a IGHV3 family after treatment of B lymphocytes with SpA <sup>176</sup>. However, *in vivo* SpA can heavily disrupt the B cell

repertoire by stimulating a large number of B cells at the same time <sup>177</sup>. Following this overstimulation, a large amount B cells requires secondary signals from the microenvironment (such as IL-4) for proliferation and differentiation <sup>173,177</sup>. As a result, cellular competition increases and essential factors for survival are consumed <sup>173,177</sup>. The shortage of pro-survival signals finally results in cell death of a large amount of B cells <sup>173,177</sup>.

Another superantigen expressed by *S. aureus* is the Staphylococcal enterotoxin D (SED). Besides being a superantigen of T cells it was found that SED can also bind to BCRs <sup>178</sup>. In a purified B cell system without T cells, it was able to induce the survival of B cells harbouring IGHV4-IgMs <sup>178</sup>. Nevertheless, the binding affinity of SED is much higher for TCRs than BCRs and to date, it is unknown whether the stimulation of BCRs by SED plays a significant role *in vivo* <sup>173,178</sup>.

### 1.4.2 Other known superantigens

The light chains of Igs are also targets for superantigens. *Peptostreptococcus magnus* protein L (PpL) is capable to bind a framework region present in most  $\kappa$ -light chains of the gene families 1, 3 and 4 (Figure 3) <sup>179,180</sup>. Similar to SpA, it has up to five homologous domains and each domain can bind to susceptible light chains <sup>180</sup>. PpL is therefore able to bind more than half of all human B cells harbouring a  $\kappa$ -light chain, although the binding affinities might vary <sup>181</sup>. It was shown *in vivo*, that this superantigen preferentially targets and activates B cells in the lymph nodes and spleen <sup>182</sup>. Moreover, *in vivo* activation by PpL seemed to induce apoptosis in a similar manner as seen by SpA <sup>183</sup>.

Besides bacterial molecules, also virus related superantigens were found. A prominent example is the gp120 molecule <sup>184,185</sup>. This molecule is part of the human immunodeficiency virus 1(HIV-1) and therefore present in HIV infected individuals <sup>184</sup>. It targets exclusively heavy chains of the IGHV3-gene family <sup>186</sup>. In contrast to SpA, it binds only a small subpopulation and the binding sites seem to differ <sup>186</sup>.

In conclusion, superantigens have the ability to activate whole B cell subsets in the organism. It was shown that they are able to quickly migrate to the secondary lymphoid organs and target a substantial proportion of B cells <sup>177,182,183</sup>. Stimulating B cells *in vitro* with superantigens resulted in a biased B cell repertoire with quick proliferation of the susceptible B cells <sup>176,186</sup>. *In vivo*, however, some experiments in mice have demonstrated a major depletion of superantigen induced B cells <sup>177,183</sup>.

## 1.5 Aim of this study

As outlined in chapter 1.3.3, mantle cell lymphoma cells (MCL) seem to be dependent on the B cell receptor signalling but the antigens bound by the BCR-IgG are still elusive. The aim of this study was to identify novel epitopes and antigens of the MCL-derived IgG. Furthermore, MCL-IgG should be characterised in the light of observations seen with other NHL-IgG to find similarities and differences between those entities.

To achieve this goal, lymphoma samples were collected and the respective variable heavy and light chains were determined. Afterwards, selectively chosen clones were produced as recombinant IgG and Fab fragments having the same epitope specificity as the MCL-IgG. With the antibodies in hand, random peptide phage displays were performed in order to find new epitopes and maybe novel potential antigens. In addition, further molecular biological approaches like immunoprecipitation and immunofluorescence assays were used to characterise the binding affinities of MCL-IgG and compare them with published data.

Finally, due to the rarity of primary MCL samples, a new cell based system should be established for a more flexible analysis of cellular activation and downstream signalling *in vitro*, without the need of primary patient material. Therefore, suitable cells were transduced with a vector containing MCL-IgMs of interest. This system is supposed to enable an *in vitro* analysis of BCR-antigen interaction like the BCR cross-linking abilities of an antigen.



## 2 Materials

### 2.1 Laboratory devices

Avanti® J-E refrigerated centrifuge	Beckman Coulter
Axioplan2 microscope with Axiophot2 imaging system	Carl Zeiss
Biomedical Freezer (-20 °C) and V.I.P. <sup>TM</sup> series freezer (-80 °C)	Sanyo Biomedical
Centrifuge 5424, 5810 and 5417 R (refrigerated)	Eppendorf
CK2 light microscope	Olympus
Curix 60 Blot developer	Agfa
Dynal magnet	Invitrogen
FACSAria <sup>TM</sup>	BD Biosciences
FACSCalibur <sup>TM</sup> cell analyser	BD Biosciences
Fusion SL3500 WL Digital Western Blot Imager	Vilber, Peqlab
Gene Pulser Xcell <sup>TM</sup> system	Bio-Rad
GeneGenius Bio Imaging System	Syngene
HERAcell 240	Thermo Fisher Scientific
HERASafe HS15 laminar flow workbench	Thermo Fisher Scientific
Illumina MiSeq <sup>TM</sup> next-generation-sequencing system	Illumina
Kelvitron® t microbiological incubator	Heraeus Instruments
Lab Style 3002 precisions balance	Mettler Toledo
Mastercycler® gradient	Eppendorf
Mastercycler® personal	Eppendorf
Microprocessor pH meter	WTW
Mini-PROTEAN® Tetra Cell electrophoresis system	Bio-Rad
Model G25 microbiological incubator and shaker	New Brunswick Scientific
Multiskan® Spectrum ELISA reader	Thermo Fisher
NanoDrop <sup>TM</sup> 2000c spectrophotometer	peqlab
PowerPac <sup>TM</sup> Basic power supply	Bio-Rad
Precellys Cell Homogeniser	peqlab
Spectrosize 300	Xtal Concepts
Sub-Cell® GT & Wide Mini Sub-Cell® GT electrophoresis system	Bio-Rad
Thermoblock	peqLab
Thermomix ME water circulation tank	B. Braun
Vi-CELL <sup>TM</sup> XR	Beckmann Coulter

Vortex Genie 2

Thermo Fisher Scientific

## 2.2 Kits

CloneJET PCR Cloning Kit

Thermo Fisher Scientific

GoTaq® DNA Polymerase

Promega

Mint-2 cDNA synthesis kit

evrogen

Omniscript reverse Transcription Kit

Qiagen

peqGOLD plasmid mini Kit

PeqLab

Ph.D.™-12 Phage Display Library Kit

New England Biolabs (NEB)

QIAquick® Nucleotide Removal Kit

Qiagen

QIAquick® PCR Purification Kit

Qiagen

QuikChange® Site-Directed Mutagenesis Kit

Stratagene

RNase-free DNase Set

Qiagen

RNeasy Mini extraction Kit

Qiagen

## 2.3 Media and Reagents

1 kb DNA ladder

New England Biolabs (NEB)

100 bp DNA ladder

New England Biolabs (NEB)

10x Trypsin/EDTA solution

PAA Laboratories

30% acrylamide/Bis-acrylamide solution (29:1)

Bio-Rad

6x DNA Gel Loading Dye

Thermo Fisher Scientific

2,2'-azino-bis(3-ethylbenzothiazoline-6-sulphonic acid) (ABTS)

Sigma Aldrich

Biocoll

Biochrom AG/Merck

cOmplete EDTA-free Protease Inhibitor Tablets

Roche

DMEM

Gibco

FBS

Gibco

HEPES

GE Healthcare

Intratect®

Octapharma

ISF-1

Biochrom AG/Merck

Ni-NTA-agarose beads

Thermo Fisher Scientific

PageRuler™ Prestained Protein Ladder

Thermo Fisher Scientific

Penicillin/Streptomycin

Gibco

Protein A Dynabeads®

Thermo Fisher Scientific

Protein A sepharose beads

GE Healthcare

pyruvat	Gibco
Roti®-Nanoquant	Carl Roth
RPMI-1640	Gibco
TransIT Insect reagent	Mirus
VECTASHIELD® mounting medium with DAPI	Vector Laboratories Inc.

Further reagents and chemicals used in this studies were obtained from the following companies: Affymetrix, BD Bioscience, Biorad, Carl Roth, Dako, Fermentas, Fluka, GE-Healthcare, Invitrogen, Merck, Serva, Sigma-Aldrich and Roche.

## 2.4 Enzymes

Antarctic phosphatase	New England Biolabs (NEB)
FastDigest™ Restriction enzymes	Thermo Fisher Scientific
Restriction enzymes for phage library generation	New England Biolabs (NEB)

## 2.5 Antibodies

Anti-goat-IgG HRP-labelled	Santa Cruz
Anti-human Fab HRP-labelled	AbD Serotec/Bio-Rad
Anti-human-IgM (WB von Elmar)	Southern Biotec
Anti-human-IgM FITC-labelled	Dako
Anti-human-kappa FITC-labelled	Dako
Anti-human-lambda PE-labelled	Dako
Anti-mouse-IgG HRP-labelled	Santa Cruz
Anti-mouse-IgM unlabelled	eBioscience
Anti-mouse-IgM FITC-labelled	eBioscience
Goat-anti-human-IgG	Caltag
mouse-anti-beta actin	Sigma-Aldrich
Mouse-anti-M13 HRP-labelled	GE Healthcare

## 2.6 Oligonucleotides (Primer)

For a comprehensive list of primer used for the amplification of the pBud, pFBD and pLeGO vector inserts as well as the utilised NGS-primer see Appendix B.

fUSE5 library primer	5'- TTCGGCCCCAGCGGCCCC
NEB -96 gIII sequencing primer	5'- CCCTCATAGTTAGCGTAAC
pJet Seq fw	5'- CGACTCACTATAGGGAGAGCGGC
pJet Seq rev	5'- AAGAACATCGATTTTCCATGGCAG
polH	5'- CACCATCGGGCCCCGG
CMV-fw	5'- CGCAAATGGGCGGTAGGCGTG
EF-1 $\alpha$	5'- TCAAGCCTCAGACAGTGGTTC
Seq_PlugO_3M_fw	5'- ACGCAGAGTGGCCATTACGGC
IgM rev nested	5'- CAGGAGACGAGGGGGAAAAG
Kappa rev nested	5'- GCTCATCAGATGGCGGGAAG
Lambda rev nested	5'- CAGAGGAGGGTGGGAACAG

***Primer used for the unbiased amplification of Ig sequences (adapted from Osterroth et al.<sup>187</sup>):***

BaPpC (fw)	5'- CTCTGCAGGATCCACGACCCCCCCCCCCCCC
BaP (fw nested)	5'- TCTGCAGGATCCACGACC
IgM rev	5'- CTCTCAGGACTGATGGGAAGCC
IgM rev nested	5'- CAGGAGACGAGGGGGAAAAG
Kappa rev	5'- CTGATGGGTGACTTCGCAG
Kappa rev nested	5'- GCTCATCAGATGGCGGGAAG
Lambda rev	5'- CGTGACCTGGCAGCTGTAG
Lambda rev nested	5'- CAGAGGAGGGTGGGAACAG

## 2.7 Cells and bacteria

Bacteria	
Name	Genotype
DH5 $\alpha$ <sup>TM</sup>	F <sup>-</sup> $\Phi$ 80 <i>dlacZ</i> $\Delta$ M15 ( <i>lacZYA-argF</i> ) U169 <i>deoR recA1 endA1 hsdR17</i> ( <i>r<sub>K</sub><sup>-</sup>, m<sub>K</sub><sup>+</sup></i> ), <i>phoA supE44 <math>\lambda</math> thi-1 gyrA69 relA1</i>
DH10bac <sup>TM</sup>	F <sup>-</sup> <i>mcrA <math>\Delta</math>(mrr-hsdRMS-mcrBC) <math>\Phi</math>80lacZ</i> $\Delta$ M15 <i><math>\Delta</math>lacX74 recA1 endA1 araD139 <math>\Delta</math>(ara, leu)7697 galU galK <math>\lambda</math> rpsL nupG/pMON14272/pMON7124</i>
XL1-Blue	<i>recA1 endA1 gyrA96 thi-1 hsdR17 sup44 relA1 lac</i> [F' <i>proAB Tn10 lacI<sup>q</sup> Z</i> $\Delta$ M15 (TetR)]

Eukaryotic cells:	
Name	Description
HEK-293T	Transformed human embryonic kidney cells
Sf9	<i>Spodoptera frugiperda</i> ovarian cells
Ramos	Human Burkitt lymphoma B lymphocytes
Namalwa.PNT	Human Burkitt lymphoma B lymphocytes
Namalwa.CSN	Human Burkitt lymphoma B lymphocytes
DG75	Human Burkitt lymphoma B lymphocytes
MCF-7	Human Breast cancer cells
HEp-2	HeLa contaminant carcinoma cells (human)
SK-BR3	Human mammary gland/breast cancer cells derived from metastatic site
MAVER-1	Mantle cell lymphoma B lymphocytes (human)
Jeko-1	Mantle cell lymphoma B lymphocytes (human)

## 2.8 Animals

For immunoprecipitation (3.2.10) murine lymph node protein lysates were used. The used lymph nodes were left over tissues of other projects and were obtained by Dr. Elmar Spies from FVB/N (immunocompetent inbred albino strain) mice.

## 2.9 Software and online tools

BLAST – basic local alignment search tool	<a href="https://blast.ncbi.nlm.nih.gov">https://blast.ncbi.nlm.nih.gov</a>
FlowJo 8.7	FlowJo
GeneSnap Viewer	Syngene
LibreOffice 5	The Document Foundation
MS Office 2010	Microsoft
OpenLab 5.0.2	improVision
Primer X	<a href="http://www.bioinformatics.org/primerx/">http://www.bioinformatics.org/primerx/</a>
PubMed	<a href="https://www.ncbi.nlm.nih.gov/pubmed/">https://www.ncbi.nlm.nih.gov/pubmed/</a>
R	The R Foundation
Spectro DLS software	Xtal Concepts
Vilber Lourmat Fusion 15.15	Vilber
Zotero	Roy Rosenzweig Center for History and New Media

## 2.10 General recipes

### 10x PBS (phosphate buffered saline):

80 g	NaCl	1.37 M
2 g	KCl	27 mM
17.8 g	Na <sub>2</sub> HPO <sub>4</sub> * 2H <sub>2</sub> O	100 mM
2.7 g	KH <sub>2</sub> PO <sub>4</sub>	20 mM
ad 1 l	ddH <sub>2</sub> O	

The pH was adjusted to 7.4 and the solution was sterilised at 121 °C for 20 min.

For 1xPBS 100 ml 10xPBS was filled up to 1 l with ddH<sub>2</sub>O.

### 1x PBS-T (0.05% Tween-20):

100 ml	10xPBS	10 % (v/v)
500 µl	Tween-20	0.05 % (v/v)
ad 1 l	ddH <sub>2</sub> O	

**10x TBS (Tris buffered saline):**

88 g	NaCl	1.5 M
2 g	KCl	27 mM
30 g	TRIZMA® base	250 mM
ad 1 l	ddH <sub>2</sub> O	

The pH was adjusted to 8.0 and the solution was sterilised at 121 °C for 20 min.

For 1xTBS 100 ml 10xTBS was filled up to 1 l with ddH<sub>2</sub>O and the pH was adjusted again to 8.0.

**1x TBS-T (0.2% Tween-20):**

100 ml	10xTBS	10 % (v/v)
200 µl	Tween-20	0.02 % (v/v)
ad 1 l	ddH <sub>2</sub> O	

The pH was adjusted to 8.0.

**10x TE buffer (Tris EDTA):**

100 ml	Tris-HCl (1 M, pH 7.5)	10 % (v/v)
20 ml	EDTA (500 mM, pH 8.0)	2 % (v/v)
ad 1 l	ddH <sub>2</sub> O	

For 1xTE buffer 100 ml 10xTE buffer was filled up to 1 l with ddH<sub>2</sub>O.

## 3 Methods

### 3.1 General molecular biological methods

Unless stated otherwise, master mixes and working solutions were prepared on ice.

#### 3.1.1 RNA extraction

Depending on the material (tissues or cells) samples were either pelleted by centrifugation (cells; 1 min, 500 g) and resuspended in lysis buffer or homogenised directly (tissue) in lysis buffer with the Precellys®24 cell homogeniser (Peqlab).

RNA was extracted using the RNeasy Mini Kit (Qiagen) according to manufacturer's instructions. A DNA digestion was always performed directly on the columns. To do so, 10 µl DNase I (Qiagen) diluted in RNase-free water, was added to 70 µl RDD buffer, gently mixed by pipetting up and down and transferred to the column. The column was incubated at room temperature for 15 min.

Finally, the RNA was eluted in 50 µl elution buffer and stored at -80 °C.

RNA of MCL samples starting from MCL4 ongoing were derived from the work-group of Prof. Wolfram Klapper (Kiel, Germany). These RNAs were extracted using the mirVana™ miRNA Isolation Kit (Thermo Fisher) according to manufacturer's instructions. All samples were fresh/frozen tissues and the origin of all samples is outlined in Appendix C.

#### 3.1.2 cDNA synthesis

Obtained RNA was transcribed into cDNA with an Oligo-dT primer. If the subsequent PCR amplification (3.1.6.1) was not successful, multiple cDNAs were generated using isotype specific primer (for  $\gamma$ -,  $\mu$ -,  $\kappa$ - and  $\lambda$ - isotypes). The general setup was:

X µl	1-2 µg sample RNA
2 µl	10x Buffer RT
2 µl	dNTP mix, 5mM each
2 µl	Oligo-dT primer or isotype specific primer
1 µl	RNase Inhibition (10 U/µl), diluted in RT Buffer
1 µl	Reverse transcriptase
ad 20 µl	RNase free water

The reaction mix was incubated at 37 °C for 1 h.



### 3.1.3 Ethanol precipitation of DNA and RNA

Ethanol precipitation was used for concentration and purification of DNA. Commonly, 1/10 volume sodium acetate (3 M, pH 5.2) and 2 volumes ethanol (96% (v/v)) were added to the sample and incubated for at least 30 min at -80 °C. Afterwards, the solution was centrifuged at 4 °C and full-speed (~20.000 g) for 20 min. The supernatant was carefully discarded, the pellet was washed with 70% ethanol (v/v) and centrifuged with full-speed at room temperature (RT) for 5 min. The supernatant was removed and the pellet was dried at RT until the ethanol completely vaporised. Finally, the pellet was diluted in ddH<sub>2</sub>O or the required buffer depending on the subsequent method.

### 3.1.4 Terminal transferase reaction

To add an oligo-G tail to the cDNA, the transcribed sample (3.1.2) was precipitated (3.1.3) and diluted in 20 µl ddH<sub>2</sub>O.

20 µl	cDNA
5 µl	10x TdT buffer
5 µl	CoCl <sub>2</sub> (2.5 mM)
1.5 µl	dGTP (10 mM)
0.5 µl	terminal transferase
ad 50 µl	ddH <sub>2</sub> O

The mixture was incubated for 30 min at 37 °C followed by enzyme inactivation at 75 °C for 20 min.

Eventually, the DNA was precipitated (3.1.3), dissolved in 50 µl ddH<sub>2</sub>O and the DNA concentration was determined (3.1.5).

### 3.1.5 DNA and RNA quantification

The nucleic acid concentration was determined by spectrophotometric measurement using a NanoDrop 2000c spectrophotometer (2.1). If the 260 nm/280 nm extinction ratio was above 1.8, the DNA/RNA was regarded as pure. Otherwise the DNA was precipitated again (3.1.3), to remove residual contaminations.

### 3.1.6 Polymerase chain reaction (PCR)

To amplify DNA fragments, the following setup was used as a standard PCR mix:

## Methods

X µl	template DNA (100 ng)
10 µl	GoTaq® 5x reaction buffer
1 µl	dNTPs (10 mM each)
1 µl	forward primer (10 mM)
1 µl	reverse primer (10 mM)
0.25 µl	GoTaq® DNA polymeras
<i>(optional) 1-2 µl</i>	<i>DMSO or formamide</i>
ad 50 µl	ddH <sub>2</sub> O

The run was performed with the following settings:

Step	Temperature	Time	Number of cycles
Initial denaturation	95 °C	3 minutes	1 cycle
Denaturation	95 °C	30 seconds	} 30 cycles
Annealing*	60 °C	30 seconds	
Extension	72 °C	35 seconds	
Final extension	72 °C	5 minutes	1 cycle

\*Annealing temperature depended on specific primer

### 3.1.6.1 Amplifications of heavy and light chain variable regions

To amplify the genes of the immunoglobulin heavy and light chain variable regions, a nested PCR was performed. The first PCR was done as described in GoTaq® colourless reaction buffer using BaPpC and the respective isotype specific primer (2.6).

For the second PCR, 10 µl of the first PCR were directly used as template DNA. The BaP and another isotype specific primer (within the first product) were used as primer. The second PCR was performed in GoTaq® 5x green reaction buffer.

If amplifications did not result in a specific product, the PCR protocol was adapted by altering the annealing temperature and/or the addition of DMSO or formamide.

### 3.1.6.2 Colony PCR

A colony PCR (cPCR) was used to check for successful transformations and to determine eligible plasmid inserts (3.1.9 and 3.1.13). Single colonies were picked from agar plates (3.3.2) with a pipetting tip and resuspended in 10 µl ddH<sub>2</sub>O. The used PCR mix was as described (3.1.6), but reduced to one-fourth of the standard setup, resulting in a total reaction volume of 12.5 µl per reaction mix. As DNA template 1 µl bacteria suspension was used.

### 3.1.7 Agarose gel electrophoresis

Depending on the expected product size (>1,000 bp or <1,000 bp), either a 1% or 2% (w/v) agarose gel was used. The agarose was melted in boiling 1x TAE buffer.

#### 50x Tris-Acetate-EDTA (TAE) stock solution (1 l):

242 g	Tris base (dissolved in ddH <sub>2</sub> O)	2 M
57.1 ml	EDTA solution (0.5 M, pH 8.0)	5.71 % (v/v)
28.55 ml	glacial acetic acid	28.55 % (v/v)
ad 1 l	ddH <sub>2</sub> O	

For 1x TAE buffer:

100 ml	50x TAE-stock solution
ad 1 l	ddH <sub>2</sub> O

The melted agarose solution was supplemented with 1 µl/ml ethidium bromide (Sigma, 10 mg/ml). DNA, amplified by PCR (3.1.6) using the GoTaq® 5x green reaction buffer, was loaded directly on the agarose gel. Otherwise, DNA was mixed with the appropriate volume of 6x loading dye (Thermo Fisher) and loaded to the gel. A 100 bp or 1 kb DNA-ladder (10 µl each, NEB) was used for size determination depending on the agarose concentration and expected product size.

The bands were analysed with UV-light (254 nm) using the GeneGenius Bio Imaging System (Syngene) and the Gene Snap software (2.9).

### 3.1.8 Gel extraction

To extract DNA from an agarose gel, the fragment of choice was cut out using a sterile scalpel (Braun) on a UV-light emitting table (364 nm). The PeqGOLD Gel extraction Kit (PeqLab) was used for DNA recovery, according to manufacturer's instructions.

### 3.1.9 Cloning into pJet vector

Amplified DNA fragments were cloned into a pJet1.2/blunt-vector using the CloneJET PCR Cloning Kit (Thermo Fisher) according to the manufacturer's instructions. Blunting of the DNA was performed in all cases. The ligated plasmids were transformed into *E. coli*-XL1-cells (3.3.4). A cPCR was (3.1.6.2) was performed with the supplied pJet-specific forward and reverse primer to determine DNA inserts of the correct length. Colonies with appropriate insert lengths were used to inoculate LB medium (3.3.2).

### 3.1.10 Plasmid purification

The PeqGOLD plasmid mini Kit (PeqLab) was used for plasmid purification according to manufacturer's instructions.

### 3.1.11 DNA sequencing

The sequencing of DNA took place in an external company (Seqlab). The following mixtures were prepared and sent to Seqlab:

X $\mu$ l	DNA (1.2 $\mu$ g plasmid DNA or 600 $\mu$ g single strand DNA)
3 $\mu$ l	sequencing primer (10 mM)
ad 15 $\mu$ l	ddH <sub>2</sub> O

### 3.1.12 Site directed mutagenesis

To clone the acquired sequences into a vector, distinct restriction enzyme were used (3.1.13). If an insert contained a recognition site for one of the required restriction enzymes, a site directed mutagenesis was performed to remove it. The point mutation was introduced without altering the coded amino acid and if possible with respect to the codon usage bias.

The QuikChange® Site-Directed Mutagenesis Kit (Stratagene) was used according to manufacturer's instruction. The pJet vector, carrying the respective sequence (3.1.9), was used as template.

The primer were designed with the help of the PrimerX online tool (2.9) and the general primer design guidelines of the kit.

Electrocompetent *E. coli*-XL1-bacteria were transformed with the mutated plasmid by electroporation (3.3.4.2). The transformed cells were expanded and the plasmid was purified (3.1.10). Finally, the plasmid was checked for presence of the required mutation by sequencing with a pJet primer (3.1.11).

### 3.1.13 Cloning into pFastbacDual (pFBD) and pBud vectors

Recombinant antibodies were produced in eukaryotic cells (3.4.5). Depending on the expression host, either a pFBD vector (Sf9 insect cells) or a pBud vector was used (HEK293T cells).

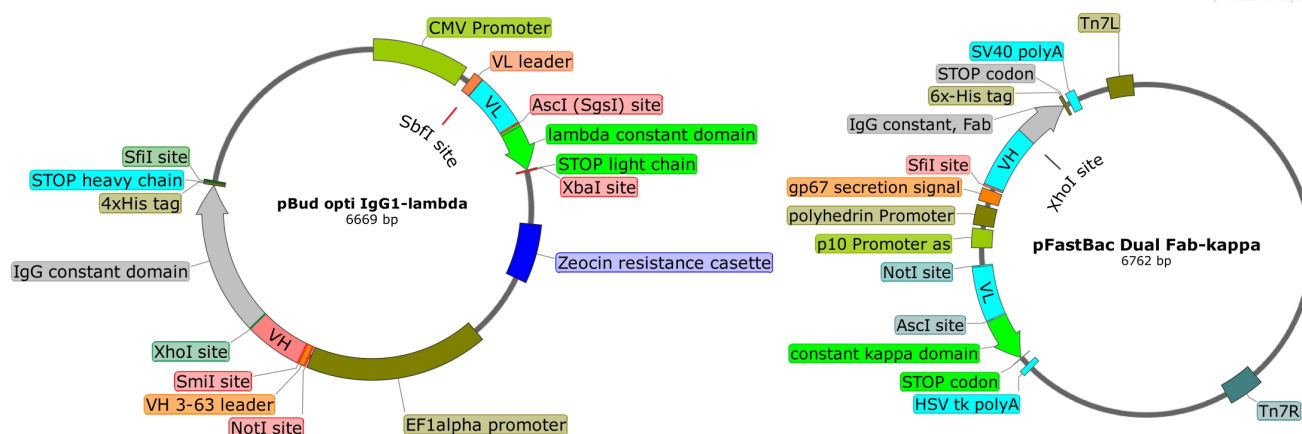


**Figure 4: Maps of the vectors used for expression of recombinant antibodies and Fab fragments.** The *pBud* vector (left) was used for protein production in HEK293T cells, whereas the *pFastBac Dual* (*pFBD*) vector was used for bacmid generation. For both constructs, four variants existed with a full length IgG1- or a Fab-constant heavy chain as well as either a kappa or lambda constant light chain gene.

Four different constructs of both vectors were designed, which harboured either the gene for the constant IgG1 region together with a  $\kappa$ - or  $\lambda$ -isotype gene, or the constant region of a Fab fragment and the  $\kappa$ - or  $\lambda$ -constant region gene (Figure 4).

### 3.1.13.1 Primer design and insert amplification

To append restriction site to the amplified variable regions of the Ig heavy and light chains, specific primer were designed for each sample. These primer sequences were based on the 5'- and 3'-end of the variable region sequence and spanned the whole variable region (3.1.11). All primers had the respective restriction enzyme recognition site to enable cloning into the vector and a short random sequence (GATC) at the 5'-end. For a list of all used primers see Appendix B.

Furthermore, the 3'-end of all primer was a guanine or cytosine base. To calculate the salt adjusted melting temperature ( $T_m$ ), the OligoCalc<sup>188</sup> online tool was used. The forward and reverse primer were adjusted to the same  $T_m$ . If one primer did not meet the criteria, both primer were adjusted until the  $T_m$  was similar.

The specific primers were used with a standard PCR mix (3.1.6) using 100 ng of the plasmid DNA as template. Since the primers were very long, the PCR program was adapted in order to reduce unspecific products:

Step	Temperature	Time	Number of cycles
Initial Denaturation	95 °C	3 minutes	1 cycle
Denaturation	95 °C	30 seconds	} 5 cycles
Annealing*	60 °C	30 seconds	
Extension	72 °C	35 seconds	
Denaturation	95 °C	30 seconds	} 25 cycles
Annealing + Extension	72 °C	40 seconds	
Final extension	72 °C	5 minutes	1 cycle

### 3.1.13.2 Plasmid insert digestion

The amplified plasmid inserts (3.1.13.1) were extracted from an agarose gel (3.1.7 and 3.1.8) and digested by the following restriction enzymes:

	pFBD	pBud
Heavy chain insert	SfiI + XhoI	XhoI + SmaI
Light chain insert	NotI + AscI	AscI + SbfI

The reaction mix was as follows:

25 µl	amplified insert
3 µl	10x FastDigest™ buffer
1 µl	Restriction enzyme 1
1 µl	Restriction enzyme 2

The mix was incubated for 30 min at 37 °C. If SfiI was needed as restriction enzyme, the digestion was performed in two steps. First, the reaction mix was prepared as described but without SfiI. After incubation for 30 min at 37 °C, the XhoI enzyme was heat inactivated at 80 °C for 15 min. Afterwards, SfiI was added and incubated for 30 min at 50 °C.

The whole reaction mix was purified with the QIAquickPCR Purification Kit (Qiagen).

### 3.1.13.3 Plasmid digestion and ligation

Depending on the light chain of the corresponding tumour Ig, a  $\kappa$ - or  $\lambda$ -vector was used, respectively. Four µg plasmid DNA was digested in the same way as described for the inserts (3.1.13.2). In general, the variable heavy chain was cloned first. Therefore, the vector was digested with the respective restriction enzymes for the heavy chain. The backbone was then

dephosphorylated by adding 3.5  $\mu$ l antarctic phosphatase buffer and 1  $\mu$ l antarctic phosphatase (NEB) to the reaction mix, followed by a further incubation for 30 min at 37 °C.

A gel electrophoresis was done to check for successful digestion and the upper band (linear backbone) was extracted (3.1.7 and 3.1.8).

Afterwards, the backbone and the variable heavy chain insert were ligated using a T4 DNA ligase (NEB). In general, the used backbone/insert ratio was 1:5. If this was not successful, different ratios were tried.

X $\mu$ l	Insert (~27 ng for 1:5 ratio)
Y $\mu$ l	Backbone (100 ng)
2 $\mu$ l	T4 DNA Ligase buffer (10x)
1 $\mu$ l	T4 DNA Ligase
ad 20 $\mu$ l	ddH <sub>2</sub> O

The reaction mix was incubated overnight at 16 °C. The next day, the whole reaction mix was transformed into bacteria (3.3.4.1). Zeocin (pBud) or ampicillin (pFBD) was used as selection marker for successful transformed bacteria. A cPCR (3.1.6.2) was made, with the specific primer used for insert amplification (3.1.13.1). Positive clones were inoculated in 4 ml LB medium, the plasmid was purified (3.1.10) and the plasmids were sequenced (3.1.11).

To clone the variable light chain region, the whole procedure was repeated with the respective enzymes and the light chain insert.

If the heavy chain insert contained a recognition site for one of the restriction enzymes used for the insertion of the light chain variable region, the cloning order was interchanged and the light chain was cloned first. Otherwise, a site directed mutagenesis was performed (3.1.12).

Successful cloned pBud vectors were used for transfection of HEK293T cells (3.4.5.1). The pFBD vectors were used for transformation of DH10bac cells (3.3.5).

### 3.1.14 Next Generation Sequencing

For next generation sequencing (NGS), RNA samples were transcribed into cDNA using the Mint-2 cDNA synthesis kit (evrogen) according to manufacturer's instructions.

After cDNA synthesis, three PCRs were performed using the Phusion® High-fidelity DNA Polymerase (NEB) to amplify the variable  $\mu$ -heavy chain region as well as the variable  $\lambda$ - and  $\kappa$ -regions. The PlugOligo-adaptor (supplied in the Mint-2 cDNA synthesis kit) and the respective reverse primer for the isotypes (IgM\_rev\_nested, kappa\_rev\_nested or lambda\_rev\_nested; see 2.6) were used. The following PCR mix was prepared:

## Methods

4 µl	5x Phusion® High-fidelity buffer
0.4 µl	dNTPs (10 mM)
1 µl	Plug-Oligo-3M adapter (15 µM)
1 µl	reverse isotype primer
1 µl	cDNA (transcribed with Mint-2 cDNA synthesis Kit)
0.2 µl	Phusion® Polymerase
ad 20 µl	ddH <sub>2</sub> O

The following PCR program was used:

Step	Temperature	Time	Number of cycles
Initial Denaturation	98 °C	2 minutes	1 cycle
Denaturation	98 °C	10 seconds	} 22 cycles
Annealing	66 °C	30 seconds	
Extension	72 °C	30 seconds	
Final extension	72 °C	10 minutes	1 cycle

A second PCR was carried out directly after completion of the first one. As template, 1 µl of the PCR product was utilised without additional purification. The Plug-Oligo-3M adapter and a specific isotype primer with an additional adapter sequence was used (see Appendix B):

4 µl	5x Phusion® GC buffer
0.4 µl	dNTPs (10 mM)
1 µl	Plug-Oligo-3M adapter (15 µM)
1 µl	reverse isotype primer with adapter sequence
0.6 µl	DMSO
1 µl	PCR product of first the PCR
0.2 µl	Phusion® Polymerase
ad 20 µl	ddH <sub>2</sub> O

An adapted two-step PCR program was used for the amplification.

Step	Temperature	Time	Number of cycles
Initial Denaturation	98 °C	2 minutes	1 cycle
Denaturation	98 °C	10 seconds	} 5 cycles
Annealing*	66 °C	30 seconds	
Extension	72 °C	30 seconds	
Denaturation	98 °C	10 seconds	} 15 cycles
Annealing + Extension	72 °C	60 seconds	
Final extension	72 °C	10 minutes	1 cycle



The whole PCR product was loaded to a 2% agarose gel and the band between 550 bp (light chains) and 700 bp (heavy chain) was extracted as described above (3.1.6.2 and 3.1.7). To add specific barcode sequences as sample identifier, a third PCR was done:

4 µl	5x Phusion® GC buffer
0.4 µl	dNTPs (10 mM)
1 µl	Linker_Seq_fw primer (10 mM) (Barcode primer fw)
1 µl	Linker_Bar_Seq_rev primer (10 mM) (Barcode primer rev)
0.6 µl	DMSO
X µl	extracted PCR product (2 ng)
0.2 µl	Phusion® Polymerase
ad 20 µl	ddH <sub>2</sub> O

The PCR program was as follows:

Step	Temperature	Time	Number of cycles
Initial Denaturation	98 °C	2 minutes	1 cycle
Denaturation	98 °C	10 seconds	5 cycles
Annealing*	52.2 °C	30 seconds	
Extension	72 °C	30 seconds	
Denaturation	98 °C	10 seconds	20 cycles
Annealing	63.5 °C	30 seconds	
Extension	72 °C	30 seconds	
Final extension	72 °C	10 minutes	1 cycle

After the PCR was finished, the reaction mix was loaded to a 2% agarose gel and the visible band was extracted as described earlier (3.1.7 and 3.1.8).

All samples were analysed by a Agilent 2100 Bioanalyzer system (Agilent Technologies) and pooled with other samples of the work-group of Prof. Mascha Binder.

The actual NGS run was done at the Next Generation Sequencing facility of the Heinrich-Pette-Institute (HPI). Acquired raw data was pre-selected by Malik Alawi at the HPI and analysed using the international ImMunoGeneTics information system® (IMGT®) HighV-Quest tool<sup>189,190</sup>.

## 3.2 Protein biological methods

### 3.2.1 Purification of recombinant antibodies and Fab fragments

The recombinant antibodies and Fab fragments which were produced in eukaryotic cells (3.4.5) carried an export signal and could therefore be directly purified from the cell culture supernatant.

The entire medium was collected and centrifuged (HEK293T: 5 min, 100 g; Sf9: 10 min, 500 g) to remove the cells. The medium was then soaked through a Filtopur V50 0.2 µm sterile filter (Sarstedt) to completely remove all cells. Full length antibodies were purified with Protein A sepharose (GE Healthcare) and Fab fragments were purified with Ni-NTA (Thermo Fisher). In both cases, the medium passed the beads by gravitational flow and the flow-through was collected and stored at 4 °C until the purification was completed.

### 3.2.1.1 Antibody purification with protein A

#### 1x PBS-high salt (1 l):

100 ml	10x PBS	10 % (v/v)
50.53 g	NaCl	in total: 1 M
ad 1 l	ddH <sub>2</sub> O	

An empty Poly-Prep® chromatography column (Bio-Rad) was filled with 1 ml protein A sepharose beads. The beads were washed with 10 ml PBS-high salt followed by continuously loading of the sterile cell culture medium to the column at 4 °C. Afterwards, the beads were washed with at least 50 ml PBS-high salt, until no residual protein was measurable in the flow through by photospectrometric analysis (3.2.4.1).

The antibodies were eluted with glycine (0.1 M, pH 3) and 1 ml eluate was directly mixed 25 µl Tris-HCl (1 M, pH 9) to neutralise the solution. Eventually, 110 µl glycerol (99.5% (v/v)) was added and the protein concentration was determined by a Bradford assay (3.2.4.2). To prevent repeated freeze and thaw cycles, the antibodies were separated in 100-200 µl aliquots and stored at -20 °C.

### 3.2.1.2 Fab fragment purification

All Fab fragments carried a His-tag at the heavy chain C-terminus. To purify a Fab-fragment produced in Sf9 cells, the medium had to be dialysed before Ni-NTA purification (3.2.2). The HEK293T medium did not interfere with the purification and was used without dialysis.

Fab fragment purification was always performed under native conditions. All recipes were adapted from the Ni-NTA Purification system manual (Thermo Fisher). The following solutions were used:

#### 10x Stock Solution A (1l):

27.6 g	sodium phosphate, monobasic (NaH <sub>2</sub> PO <sub>4</sub> )	200 mM
292.9 g	NaCl	5 M
ad 1 l	ddH <sub>2</sub> O	

**10x Stock Solution B (1 l):**

28.4 g	sodium hydrogen phosphate, dibasic (Na <sub>2</sub> HPO <sub>4</sub> )	200 mM
292.9 g	NaCl	5 M
ad 1 l	ddH <sub>2</sub> O	

**5x Native Purification Buffer (200 ml):**

7 g	sodium dihydrogen phosphate, monobasic (NaH <sub>2</sub> PO <sub>4</sub> )	250 mM
29.2 g	NaCl	2.5 M
ad 200 ml	ddH <sub>2</sub> O	

The 5x Native Purification Buffer was adjusted to pH 8.0 using NaOH.

**3 M Imidazole pH 6.0 (100 ml):**

20.6 g	imidazole	250 mM
8.77 ml	10x Stock Solution A	8.77 % (v/v)
1.23 ml	10x Stock Solution B	1.23 % (v/v)
ad 100 ml	ddH <sub>2</sub> O	

The pH was adjusted using NaOH or HCl.

**Native Binding Buffer with 10 mM imidazole (100 ml):**

333 µl	3 M imidazole, pH 6.0	250 mM
ad 100 ml	1x Native Purification Buffer	

The pH was adjusted to 8.0 using NaOH or HCl.

**Native Wash Buffer with 20 mM imidazole (100 ml):**

667 µl	3 M imidazole, pH 6.0	250 mM
ad 100 ml	1x Native Purification Buffer	

The pH was adjusted to 8.0 using NaOH or HCl.

**Native Elution Buffer with 250 mM imidazole (30 ml):**

2.5 ml	3 M imidazole, pH 6.0	250 mM
ad 50 ml	1x Native Purification Buffer	

The pH was adjusted to 8.0 using NaOH or HCl.

An empty Poly-Prep® chromatography column (Bio-Rad) was filled with 1.5 ml Ni-NTA agarose resin. The beads were washed with 6 ml ddH<sub>2</sub>O and equilibrated with 10 ml Native Binding Buffer. Afterwards, the cell culture medium was continuously loaded to the column at 4 °C. The beads were

then washed with at least 30 ml wash buffer until no protein was measurable in the flow through by photospectrometric analysis (3.2.4.1).

About 10 ml elution buffer was loaded on the column and 500 µl aliquots of the eluate were collected. Glycerol (99.5% (v/v)) was added and the concentration was determined by Bradford assay (3.2.4.2). Solutions with high protein concentrations (more than 0.2 mg/ml) were further split into smaller aliquots to avoid repeated freeze-thaw cycles.

The Fab fragment solutions were stored at -20 °C.

### 3.2.2 Dialysis

Since the Insect-Xpress cell culture medium interfered with Ni-NTA based Fab purification, a dialysis was performed prior column loading.

For a 300 ml production, three ZellTrans 6.0 dialysis tubes (Roth) with a length of about 35 cm were washed two times for 10 min with ddH<sub>2</sub>O. Afterwards the tubes were equilibrated in PBS for further 10 min. One side of each tube was carefully sealed with plastic clips, followed by loading the tube with the Fab fragment containing medium. After sealing the tube, it was transferred to 3 l PBS (10 times the production volume) and incubated overnight at 4 °C with constant stirring of the PBS.

On the next morning, the PBS was discarded, replaced by 1.5 l (5x medium volume) new PBS and again incubated at 4 °C for 3 h. Finally, the content of the tubes was transferred into a new flask and directly used for protein purification (3.2.1.2).

### 3.2.3 Protein extraction

To extract proteins from cell culture cells or tissues, the following buffer was used.

#### 1x Radioimmunoprecipitation assay buffer (RIPA) (100 ml):

1 ml	NP40	1 % (v/v)
0.5 ml	20% sodium dodecylsulfate (SDS)	0.5 % (v/v)
0.5 g	sodium deoxycholate	120 mM
ad 100 ml	PBS	

The buffer was stored in 10 ml aliquots at -20 °C. Prior use, 100 µl cComplete EDTA-free protease inhibitor (Roche) was added.

#### 3.2.3.1 Cell line lysis

To receive a sufficient amount of protein, cells were grown in two 175 cm dishes until reaching nearly 100% confluence. Then, the cell culture medium was removed and the cells were washed

two times with 20 ml PBS. Afterwards, 10 ml PBS were added and the cells were detached from the dish by gentle tapping or the use of a cell scraper followed by repeated resuspending using a pipette. The two cell solutions were merged in a 50 ml centrifugation tube and centrifuged for 5 min at 100 g. The supernatant was discarded, the cell pellet was resuspended in 4 ml and split into 2 ml reaction tubes. After centrifugation at 100 g for 5 min the supernatant was discarded and the pellets were resuspended in 2 ml lysis buffer (RIPA). The solutions were incubated on ice for 30 min followed by three freeze-thaw cycles.

Finally, the protein lysates were centrifuged at 10,000 g and 4 °C for 15 min and the protein-containing supernatant was transferred into fresh tubes. A Bradford assay (3.2.4.2) was performed to determine the protein concentration and the lysates were stored at -20 °C in 500 µl aliquots.

### **3.2.3.2 Tissue lysis**

Murine lymph nodes were acquired by Dr. Elmar Spies from FVB/N mice. The lymph nodes were extracted in addition to further organs used for other projects.

If necessary, the tissue was cut into small pieces on dry ice with a sterile scalpel. The frozen pieces were transferred into homogenisation tubes and an appropriate amount of lysis buffer (usually 1 ml) and ceramic beads (CK28, Precellys®, Peqlab) were added. For homogenisation of the lymph nodes the Precellys®24 tissue homogenizer (2x20 sec at 5,500 rpm, 20 sec break) was used.

After homogenisation, the tissue was incubated on ice for further 10 min and centrifuged at 500 g. The supernatant was transferred into a new tube and centrifuged at 10,000 g and 4 °C for 15 min. Afterwards, the protein lysate was transferred into a new tube, the protein concentration was determined (3.2.4.2) and the aliquots were stored at -20 °C.

## **3.2.4 Protein Quantification**

### **3.2.4.1 Photospectrometric quantification**

For a fast determination of the protein content in a solution, the extinction at 280 nm was measured with the NanoDrop 2000c spectrophotometer (2.1). The respective lysis buffer was used as blank. This method was primarily used to check for protein in the flow-through during protein purification (3.2.1).

### **3.2.4.2 Bradford protein assay**

For a more accurate determination of the protein concentration, the Roti®-Nanoquant (Carl Roth) solution was used according to manufacturer's instructions. Depending on the measured solution,

either different dilutions of BSA (protein lysates) or Intratect® (recombinant IgGs and Fabs) were used as calibration standards.

### 3.2.5 Sodium dodecyl sulfate polyacrylamide gel electrophoresis (SDS-PAGE)

The discontinuous Laemmli system with a stacking and separation gel was used <sup>191</sup>.

#### 5x protein sample buffer (adapted from Laemmli-et al. <sup>191</sup>):

1.67 ml	Tris-HCl (1.5 M, pH 6.8)	330 mM
2.5 ml	20% (w/v) SDS solution	5 %
5 ml	glycerol	50 %
1 ml	1% (w/v) bromophenol blue solution	0.1 %
ad 10 ml	ddH <sub>2</sub> O	

For reducing conditions, 5 µl β-mercaptoethanol were added per 100 µl before use.

#### Polyacrylamide separation gel (1 gel):

	8%	10%	12%
ddH <sub>2</sub> O	2.3 ml	2.0 ml	1.6 ml
30% acrylamide/Bis-acrylamide (29:1)	1.3 ml	1.7 ml	2.0 ml
Tris solution (1.5 M, pH 8.8)	1.3 ml	1.3 ml	1.3 ml
10% SDS solution	0.05 ml	0.05 ml	0.05 ml
10% ammonium persulfate (APS)	0.05 ml	0.05 ml	0.05 ml
Tetramethylethylenediamine (TEMED)	2 µl	2 µl	2 µl
Total volume:	5 ml	5 ml	5 ml

#### Polyacrylamide stacking gel (2 gels):

ddH <sub>2</sub> O	2.7 ml
30% acrylamide/Bis-acrylamide (29:1)	0.67 ml
Tris solution (1.5 M, pH 6.8)	0.5 ml
10% SDS solution	0.04 ml
10% ammonium persulfate (APS)	0.04 ml
Tetramethylethylenediamine (TEMED)	4 µl
Total volume:	5 ml

**10x running buffer (1 l):**

30 g	Tris base	250 mM
144 g	glycin	1.92 M
100 ml	10% (w/v) SDS solution	1 % (w/v)
ad 1 l	ddH <sub>2</sub> O	

The 10x running buffer solution was autoclaved at 121 °C for 20 min and diluted 1:10 in ddH<sub>2</sub>O prior use.

The gels were polymerised between two glass plates from Bio-Rad. A 10 lane comb was used to create the sample wells.

Up to 20 µl of the protein samples per lane were mixed with the appropriate amount of 5x protein sample buffer and incubated for 5 min at 70 °C. The electrophoresis apparatus was assembled with the SDS gel and the tank was filled with 1x running buffer. After carefully washing the wells, the protein samples and a protein marker (PageRuler™ Prestained Protein Ladder, Pierce) were loaded to the gel.

The electrophoresis run was started with a current of 80 V until the protein front entered the separation gel. Then, the voltage was increased to 120 V until the migration front reached the end of the gel or the expected protein was approximately in the middle of the gel.

The gel was removed from the apparatus and washed in ddH<sub>2</sub>O. Afterwards, it was either stained with colloidal coomassie (3.2.6) or used for Western blotting (3.2.7).

**3.2.6 Coomassie staining of acrylamide gels**

The colloidal coomassie recipe was adapted from Dyballa and Metzger<sup>192</sup>.

## Colloidal coomassie solution

100 g	aluminium sulfate-(14,-18)-hydrate	5 % (w/v)
200 ml	ethanol (96%)	10 % (v/v)
0.4 g	CBB G-250	0.02 % (w/v)
47 ml	orthophosphoric acid (85%)	2 % (v/v)
ad 2 l	ddH <sub>2</sub> O	

For best results, the preparation of the solution must have followed a specific order. At first, the aluminium sulfate was dissolved in ddH<sub>2</sub>O, followed by ethanol addition. After complete homogenisation, CBB G-250 was mixed to the solution. When the solution was completely dissolved, the phosphoric acid was added. At the end, the solution was filled up with ddH<sub>2</sub>O.

If everything was added in the right order the resulting solution had a “dark green-bluish appearance and [was] full of particles swimming around”<sup>192</sup>. If not, the solution had a more violet colour.

After the electrophoresis run, the gels were washed two times with ddH<sub>2</sub>O for at least 15 min. The gels were covered in colloidal coomassie solution and incubated overnight with constant shaking. The next day, gels were de-stained with ddH<sub>2</sub>O until the background was minimal.

Stained gels were scanned using a flat bed scanner.

### 3.2.7 Western Blot

#### 10x transfer buffer (1 l):

24.2 g	Tris base	200 mM
108.1 g	glycin	1.44 M
ad 1 l	ddH <sub>2</sub> O	

For 1x transfer buffer: 100 ml 10x transfer buffer and 100 ml methanol were mixed and filled up to 1 l with ddH<sub>2</sub>O.

A polyvinyl difluoride (PVDF) membrane (GE Healthcare) was incubated in 99.5% (v/v) methanol for at least one minute. In addition, four Whatman® filter paper and two foam pads were soaked with 1x transfer buffer. The holding cassette with the gel was assembled as follows:

cathode (-)
foam pad
Whatman® paper
gel
PVDF membrane
Whatman® paper
foam pad
anode (+)

The assembled cassette was transferred into the Blot apparatus which was filled with 1x transfer buffer. To prevent overheating, a frozen cool pack was placed in the tank.

The proteins were blotted for 2 h at 100 V or at 60 V overnight.

After protein transfer, the membrane was shortly incubated with methanol (99.5%) and stained with Ponceau S solution for 15 min. The Ponceau S was washed away by repeated washing with ddH<sub>2</sub>O and the Blot was documented using a flat bed scanner (Canon). Afterwards, the membrane was blocked with 5% milk (w/v) in TBS-T for 1 h.



If no Ponceau S staining was made, the membrane was directly blocked for 1 h in 5% milk ((w/v) in TBS-T) after methanol incubation.

Afterwards, the membrane was incubated with the primary antibody overnight at 4 °C. Different concentrations of the recombinant antibodies were used, ranging from 10 µg/ml to 0.1 µg/ml. All primary antibodies were diluted in 1% milk (w/v) in TBS-T.

The next day, the membrane was washed three times with TBS-T for 15 min, each. An HRP-labelled anti-human-Fab antibody (AbD-serotec), diluted 1:5,000 in 1% milk ((w/v) in TBS-T), was used as secondary antibody and incubated with the membrane for 1 h.

The membrane was washed again three times for 15 min with TBS-T. The Clarity™ Western ECL blotting substrate (Biorad) was used as HRP substrate according to manufacturer's instructions.

The chemiluminescence detection was performed either in a dark chamber using CL X-Posure films (Thermo Fisher Scientific) and the Agfa Curix 60 developer or with the Fusion SL3500 WL Digital Western Blot Imager (Vilber/Peqlab).

### 3.2.8 Far Western Blot

#### 10x TBE (1 l):

108 g	Tris base	892 mM
55 g	boric acid	890 mM
ad 900 ml	ddH <sub>2</sub> O	
40 ml	EDTA-solution (0.5 M, pH 8.8)	0.04 % (v/v)
ad 1 l	ddH <sub>2</sub> O	

Per well, 25 µg of the proteins (SpA, anti-human-Fab- or anti-mouse-IgM-antibody) were mixed in 100 µl sterile 1x TBE. Each well of six-well-plate was coated with the respective protein solution for 20 min at 37 °C. To coat the wells, the solution was evenly distributed in the well using a pipette tip but the walls were spared.

In total,  $1 \times 10^7$  transduced and untransduced Ramos cells (in 2 ml medium) were added to each well and incubated for 2 h. Afterwards, the cells were transferred in a 15 ml centrifugation tube and centrifuged for 5 min at 200 g. The supernatant was discarded, the cells were resuspended in PBS and transferred to a 2 ml reaction tube. The cells were centrifuged again at 100 g for 2 min, the supernatant was discarded and the pellet was frozen at -80 °C.

The further processing of the far Western Blot was performed by Helwe Gerull and Prof. Peter Nollau at the Research Institute Children's Cancer Center and Clinic of Pediatric Hematology and Oncology (University Medical Centre Hamburg-Eppendorf).

In short: The pelleted cells were lysed in KLB-lysis buffer (150 mM NaCl, 25 mM Tris-HCl (pH 7.4), 5 mM EDTA, 1% Triton X-100, 10% glycerol, 10 mM sodium pyrophosphate, 1 mM sodium ortho-vanadate, 10 mM  $\beta$ -glycerolphosphate, 1 mM PMSF, 1 mM DTT, 0.2 mg/mL aprotinin, 10 mM sodium fluoride and 0.1 mM freshly prepared sodium pervanadate). Fifteen  $\mu$ g of the protein extract were separated on 4-12% SDS-PAGE gradient gels (Invitrogen), transferred to a PVDF-membrane and blocked in 10% skim-milk (in TBS-T) at 4 °C overnight. Subsequently, membranes were probed with 1  $\mu$ g/mL of biotinylated GRB2- or SHP2- SH2 domains precomplexed with streptavidin-horseradish peroxidase (Pierce).

### 3.2.9 Enzyme linked immunosorbent assay (ELISA)

ELISAs were used to determine the yield of antibody production in monoclonal cells after transfection and to measure binding affinities to antigens. The following table summarises the general ELISA setup for these experiments.

	Coated protein	Ligand	Detection antibody [Dilution]
supernatant ELISA	2 $\mu$ g anti-human-IgG	cell culture supernatant	HRP-labelled anti-human Fab (AbD-Serotec) [1:4,000]
Phage ELISA	2 $\mu$ g recombinant lymphoma IgG	selected phages	anti-M13 antibody (GE Healthcare) [1:5,000]
SpA* ELISA	4 $\mu$ g SpA	lymphoma Fab fragments	HRP-labelled anti-human Fab (AbD-Serotec) [1:4,000]

\*SpA = staphylococcal protein A

All ELISAs were performed in immunolon microtiter 96-well plates (Falcon). Per well, 2-4  $\mu$ g of the respective proteins were diluted in 75  $\mu$ l TBS and coated overnight. Except for the production ELISA, at least triplicates for all samples were used. The wells were washed once with TBS-T and blocked with 150  $\mu$ l 3% BSA (in TBS-T) for 1 h. Ligands were diluted in 1% BSA (in TBS-T) to a total volume of 75  $\mu$ l and incubated with the coated (and blocked) protein for 1 h. Afterwards, the wells were washed three times with 150  $\mu$ l TBS-T followed by the incubation with the detection antibody (in 75  $\mu$ l 1% BSA) for 1 h. All wells were washed again three times with 150  $\mu$ l TBS-T.

The detection buffer (Citric acid, ABTS) was supplemented with 2.5  $\mu$ l hydrogen peroxide per ml and 75  $\mu$ l detection buffer were given into each well. After a short incubation (5-15 min), the extinction at 405 nm was measured using a Multiskan® Spectrum ELISA reader (Thermo Fisher).

### 3.2.10 Immunoprecipitation (IP)

To precipitate antigens from a protein solution, Protein A Dynabeads® (ThermoFisher) were used. The bead solution was homogenised and 50 µl beads per precipitation were transferred to a 1.5 ml reaction tube. A Dynal magnet (Invitrogen) was used to separate the beads from the supernatant and the supernatant was discarded. The beads were loaded with 4 µg antibody (diluted in 200 µl TBS-T) for 15 min. The beads were then precipitated using the magnet and the supernatant was discarded. Up to 500 µl RIPA protein lysate (500-1,000 µg) was added and incubated with the loaded beads overnight at 4 °C with constant rotation.

The next day, the beads were precipitated, the supernatant was discarded and the beads were washed three times with 400 µl TBS-T. After the last washing step, the beads were carefully dissolved in 100 µl TBS-T and transferred to a new reaction tube. Using the magnet, the beads were precipitated and the supernatant was removed. Finally the beads were resuspended in 50 µl denaturing Laemmli buffer and the precipitated proteins were separated by SDS-PAGE (3.2.5).

### 3.2.11 Preparation for mass spectrometry analysis

To reduce contamination with foreign peptides, the glass plates, the glass chamber for the coomassie staining and the Bio-Rad Mini-Protean® electrophoresis systems was washed with 5% (v/v) hydrogen peroxide for 20 min. In addition, all solutions were made fresh. Protecting hand gloves were worn at all times.

The precipitated proteins were separated by SDS-PAGE (3.2.10 and 3.2.5) and the gel was stained with fresh colloidal coomassie solution overnight. Afterwards, the gel was destained with ddH<sub>2</sub>O multiple times until no background was visible.

Precipitated bands were carefully extracted using a sterile scalpel and transferred into separate reaction tubes. For each band another scalpel was used.

The samples were further processed at the Core Facility mass spectrometry & proteome analysis of the UKE.

### 3.2.12 Dynamic light scattering

The concentrations of all IgGs were adjusted to 1 mg/ml. Prior measurement, all samples were centrifuged at full speed and 4 °C for 20 min.

All measurements were performed with kind assistance of Dr. Sven Falke from the work-group of Prof. Betzel at the DESY (Deutsches Elektronen-Synchrotron).

For measurement, at least 12 µl of the sample was transferred into a quartz cuvette (Hellma). The sample volume was always obtained from slightly below the surface. The cuvette was placed in a Spectrosizer 300 DLS instrument (Xtal concepts) and the sample was irradiated by a red light laser ( $\lambda = 690 \text{ nm}$ , 10-50 mW). The scattered light was detected at an angle of 90 degree.

The scattering was analysed using the Spectro software (Xtal concepts), which was also used for the calculation of the theoretical hydrodynamic size and molecular weight. This calculation used the acquired fluctuation in the intensity of the scattered light and therefore determined the translational diffusion coefficient ( $D_0$ )<sup>193</sup>. The hydrodynamic radius ( $R_h$ ) could then be calculated using the Stokes-Einstein equation<sup>193</sup>:

$$R_h = \frac{KT}{6\pi\eta D_0} \quad K = \text{Boltzmann constant, } T = \text{temperature; } \eta = \text{viscosity}$$

### 3.2.13 Random peptide phage display

#### 20% PEG/NaCl (1 l):

200 g	polyethylene glycol (PEG 8000)	20 % (w/v)
147 g	NaCl	2.5 M
ad 1 l	ddH <sub>2</sub> O	

Four different random peptide phage libraries were used. Three of them (X12, X18 and  $\beta$ -sheet) based on the fUSE5 system described by Scott and Smith<sup>194</sup>. The fUSE5 libraries were mostly generated by Dr. med. Fabian Müller and Mareile Cordes. The protocol is outlined below.

The fourth library, which was used for selection, was the Ph.D.<sup>TM</sup>-12 phage display library (NEB). It was used according to manufacturer's instruction with the supplied *E. coli* K12 ER2738 bacteria.

#### 3.2.13.1 General generation of a fUSE5 library

The fUSE5 library backbone was digested with SfiI to enable the insertion of the respective random oligonucleotides.

Oligonucleotides coding the degenerated insert sequence were commercially synthesised (Metabion). The insert sequences always followed the NNK-rule. Therefore, the first two nucleotides were completely random, whereas the last nucleobase was either guanine or thymine.

The following insert oligonucleotides were ordered:

X12	5'-CACTCGGCCGACGGGGCT- (NNK) <sub>12</sub> -GGGGCCGCTGGGGCCgAA
X18	5'-CACTCGGCCGACGGGGCT- (NNK) <sub>18</sub> -GGGGCCGCTGGGGCCgAA
$\beta$ -sheet	5'-CACTCGGCCGACGGGGCT- (NNK) <sub>4</sub> (TGC)(NNK) <sub>6</sub> (TGC)(NNK) <sub>4</sub> -GGGGCCGCTGGGGCCGAA

The flanking sequences harboured a BglI restriction site. All oligonucleotides were resuspended in H<sub>2</sub>O to a final concentration of 1 µg/µl.

The Sequenase 2.0 Kit (Amersham) was used with the fUSE5 library primer. Four reactions were prepared with the following scheme:

2 µg	oligonucleotide
4 µg	fUSE5 library primer
2 µl	5x sequenase reaction buffer
ad 10 µl	ddH <sub>2</sub> O

The reaction mix was incubated in a PCR cycler at 65 °C for 2 min and slowly cooled down with a ramp time of 10 min from 65 °C to 40 °C. Each tube was filled up to following elongation reaction mix:

10 µl	sample
2 µl	dNTPs (Fermentas, 10 mM)
5 µl	DTT (0.1 M)
2 µl	diluted Sequenase (according to manufacturers instructions)
ad 50 µl	enzyme dilution buffer

The mix was incubated at 37 °C for 1 h.

Afterwards, the double-stranded oligonucleotides were purified using the QIAquick Nucleotide Removal Kit (Qiagen) according to manufacturer's instructions. In total, three columns were used. Prior elution, 100 µl of the manufacturer's elution buffer (10 mM Tris-HCl, pH 8.5) was diluted 1:3 in ddH<sub>2</sub>O. DNA was eluted with 50 µl per column using the diluted elution buffer, followed by a second elution with 30 µl (total elution volume: 240 µl).

The whole eluate was used for the subsequent BglI digestion:

240 µl	eluted DNA
30 µl	NEB 3 buffer (10x)
3 µl	BSA (NEB, 100x)
30 µl	BglI (NEB, 10,000 u/ml)

The reaction mix was evenly distributed in three reaction tubes and incubated at 37 °C for 4 h.

After complete digestion, the DNA was purified using three columns of the QIAquick Nucleotide Removal Kit and eluted in 50 µl diluted elution buffer per column. If not used directly for the test ligation, the samples were frozen immediately.

### Test ligation of insert and library plasmid backbone

A small scale test ligation was performed to determine the best molar ratio between library backbone and insert. Three ratios were used (plasmid/insert): 1:10, 1:30 and 1:100. The ligation was performed as described, using 500 µl plasmid DNA (3.1.13.3). To determine the background ligation rate, further ligations were performed with DNA-free Tris-HCl as sample. After the ligation was completed, the mix was precipitated with ethanol (3.1.3) and dissolved in 25 µl diluted elution buffer. An electroporation was done with 1 µl ligated plasmid and 25 µl DH5α bacteria (3.3.4.2). For each sample, three different dilutions of the electroporated cells were spread on a LB<sub>Tet</sub> agar plate and incubated at 37 °C overnight. By counting the colonies on the plates, the best molar ratio for ligation with the lowest background was calculated. If no sufficient ratio was observed, different further ratios were tested.

### Large scale ligation

The best molar ratio of library backbone to insert was used for large scale ligation. Therefore, the calculated amount of insert was mixed with 10 µg library backbone, incubated for 2 min at 65 °C and cooled down on ice for at least 5 min. Then, the sample was filled up to the following reaction mix:

X µl	backbone/insert mix
50 µl	T4 ligase buffer (NEB, 10x)
30 µl	T4 DNA ligase (NEB, 400,000 U/ml)
ad 500 µl	ddH <sub>2</sub> O

The reaction mix was evenly distributed to ten reaction tubes and incubated overnight at 16 °C. Afterwards, the ligation mix was precipitated and the pellet was dissolved in 200 µl diluted elution buffer.

### Large scale electroporation

For 10 µg of the ligated plasmid, 100 electroporations were needed. Therefore, 200 ml SOC medium in four 50 ml aliquots was pre-warmed to 37 °C. In addition, 3.8 l (38 ml per ligation) pre-warmed LB medium (with 20 µg/ml tetracycline and 100 µg/ml streptomycin) was split into four aliquots, transferred into 2 l Erlenmeyer flasks and prewarmed to 37 °C. Also, 16 LB<sub>Tet</sub> agar plates were prepared.

The electroporations were performed as described with 2 µl plasmid and 50 µl DH5α bacteria (3.3.4.2). To achieve the maximum electroporation speed, and therefore a high quality library, three

persons worked together on the electroporations. Electroporated cells were collected and after every 25 electroporations (50 ml cell solution), the bacteria were placed in an incubator and shook at 37 °C and 200 rpm for 1 h.

After the 1 h reconstitution in SOC medium, the whole bacteria solution was transferred into the prepared 950 ml LB medium. An aliquot of 120 µl was obtained and 100 µl were directly spread on an LB<sub>Tet</sub> agar plate. Three dilutions (1:10, 1:100 and 1:1,000) were made (100 µl each) and also spread on LB<sub>Tet</sub> agar plates. All 16 plates were incubated overnight at 37 °C and the colonies were counted the next day to determine the library diversity.

#### Phage precipitation

When the saturation of the 1 l LB medium cultures reached an  $OD_{600} \geq 2$ , the cell suspensions were centrifuged two times at 10,000 rpm for 20 min and the supernatant was collected. To precipitate the phages, 10 g PEG8000 and 7.5 g NaCl was added per 250 ml supernatant. The phage solutions were then stirred overnight at 4 °C. The next day, the precipitated phages were centrifuged at 10,000 g for 20 min at 4 °C and the supernatant was discarded. The tubes were centrifuged again (10,000 g, 10 min, 4 °C) and the remaining supernatant was removed. The pellets of all tubes were resuspended in a total volume of 30 ml TBS and dissolved by shaking for 15 min at 37 °C. All phage solutions were pooled (total volume: 30 ml) and centrifuged for 5 min at 7,000 g and room temperature. The supernatant was transferred into a clean tube and 4.5 ml 20% PEG/NaCl solution was added, mixed and incubated overnight at 4 °C. Afterwards, the suspension was centrifuged at 10,000 g for 20 min at 4 °C, the supernatant was discarded and the pellet was dissolved overnight in 500 µl TBS (with 0.02% sodium azide). Finally, the phage library solution was centrifuged at 17,900 g and room temperature for 5 min and the supernatant was transferred in a new tube. To store the library, it was split into aliquots and either kept at 4 °C for up to 6 month or supplemented with glycerol (50% total volume) and stored at -20 °C.

To determine the amount of phages per batch, the library was titrated (3.2.13.5).

### **3.2.13.2 Phage panning**

#### Fuse5 library selections

K91 bacteria were streaked out on an LB<sub>Kan</sub> agar plate (3.3.1) and grew overnight at 37 °C. In addition, 4 µg of the target antibody (in 75 µl TBS) was coated per well of a 96 well plate overnight.

The well was washed with TBS and blocked with 3% BSA (in TBS) for 1 h. For the first round,  $2 \times 10^9$  phages were diluted in 1% BSA to a total volume of 75  $\mu$ l. The well was washed with TBS and incubated with the phages for 2 h. Meanwhile, 10 ml TB<sub>Kan</sub> (3.3.1) medium was inoculated with K91 bacteria and the bacteria were shaken until the optical density at 600 nm (OD<sub>600</sub>) of a 1:10 dilution was between 0.16 and 0.2. The well was washed six times with TBS-T and three times with TBS. Afterwards, 200  $\mu$ l of the bacteria were added to the well and incubated for 1 h at room temperature without moving the plate. The bacteria were then transferred into 10 ml LB medium with 0.5  $\mu$ g tetracycline per ml (1  $\mu$ l of a 5 mg/ml stock solution in 10 ml) (3.3.1) and shaken for 20 min at room temperature and additional 39  $\mu$ l tetracycline solution were added (final concentration 20  $\mu$ g/ml). 250  $\mu$ l of the bacteria culture were obtained and the 10 ml culture was incubated at 37 °C and 200 rpm overnight. From the obtained bacteria, 1  $\mu$ l, 10  $\mu$ l and 100  $\mu$ l were streaked out on LB<sub>Tet</sub> agar plates and incubated at 37 °C to determine the amount bound phages. The next day, the suspension culture was centrifuged for 10 min at 8,000 g and 4 °C. The supernatant was transferred to a fresh tube and 2 ml 20% PEG/NaCl were added. The phages were precipitated (3.2.13.3) and the second round was started (3.2.13.4).

### Ph.D.<sup>TM</sup>-12 library selection

*E. coli* K12 ER2738 were streaked out on a LB<sub>Tet</sub> agar plate and grew overnight. One well of a 96 well plate was coated with 4  $\mu$ g of the target antibody in 75  $\mu$ l TBS. The well was washed with TBS, blocked in 1% BSA for 1 h, washed again and  $2 \times 10^9$  phages were added and incubated for 2 h. In parallel, 20 ml LB<sub>Tet</sub> medium was inoculated with the K12 ER2738 bacteria and shaken at 37 °C and 200 rpm, while the OD600 was carefully monitored to not exceed 0.01-0.05 (early-log phase). The well was washed six times with TBS-T and three times with TBS. To elute the phages, 100  $\mu$ l 0.2 M Glycin-HCl (pH 2.2) was added to the well and incubated for 5 min. The solution was then transferred into a new tube and neutralised with 15  $\mu$ l 1 M Tris-HCl (pH 9.1). For titration, 1  $\mu$ l was obtained and used to infect 200  $\mu$ l of the bacteria. After 10 min of incubation, the infected bacteria were spread on LB<sub>IPTG/X-Gal</sub> agar plates in 1:10, 1:100 and 1:1,000 dilutions (100  $\mu$ l each) and incubated overnight at 37 °C. The next day, the blue colonies were counted to determine the output.

The remaining 114  $\mu$ l of the phage solution were directly used to infect the 20 ml K12 bacteria culture (in early log phase) and the phage/bacteria mixture was incubated for 4 h at 37 °C and 110 rpm.



Afterwards, the culture was transferred in a centrifugation tube and centrifuged for 10 min at 8,000 g and 4 °C. The supernatant was transferred to a new tube and 4 ml 20% PEG/NaCl was added to precipitate the phages overnight. After phage purification, the second round was started (3.2.13.3 and 3.2.13.4).

### **3.2.13.3 Phage precipitation and purification**

After PEG/NaCl addition the phages were precipitated for at least 2 h at 4 °C, but preferably overnight at 4 °C. The precipitated phages were then centrifuged for 20 min at 10,000 g and 4 °C, the supernatant was discarded and the pellet was centrifuged again (20 min, 10,000 g, 4 °C). Residual supernatant was removed, the phages were resuspended in 200 µl TE buffer and transferred into a new tube. The solution was centrifuged again for 5 min at 10,000 g and room temperature and the phage-containing supernatant was transferred in a clean 1.5 ml reaction tube. Phages were stored at 4 °C for up to two month. For long term storage, the equal volume sterile glycerol (final concentration 50%) was added and the phages were stored at -20 °C (usually only monoclonal phages and unselected libraries).

Prior use, the phages were titrated to determine the concentration of infectious virions (3.2.13.5).

### **3.2.13.4 Further selection rounds**

Beginning with the second selection round, pre-selected phage libraries were also negatively selected against the polyclonal human-IgG serum Intratect®. The handling and amplification of the phages and bacteria remained the same as in the first round. For that reason, only the differences are described.

In addition to the target antibody, three wells were coated with 4 µg polyclonal IgG (Intratect®), per well (in 75µl TBS). The next day, the first well with coated polyclonal IgG was washed with TBS, blocked with 3% BSA, washed again and incubated for 1 h with  $2 \times 10^9$  phages (in 75 µl 1% BSA) of the pre-selected library from the previous selection round. Meanwhile, the second well with coated polyclonal IgG was blocked with 3% BSA. The phage solution from the first well was transferred to the second well and incubated for 1 h, again. Within this incubation step, the remaining two wells were blocked. The negatively selected phage solution was evenly distributed to the two wells and 1% BSA was added to a final volume of 75 µl solution per well. The phages were incubated for 30-60 min (2<sup>nd</sup> round: 60 min, 3<sup>rd</sup> round: 45 min, 4<sup>th</sup> and 5<sup>th</sup> round: 30 min).

Following that incubation, the phages were handled similar to the first round (3.2.13.2). Phages which were incubated with polyclonal IgG were only used to determine the output of unspecific phages and were not amplified.

The next day, all colonies on the agar plates were counted. The amount of (blue) colonies acquired by selection with the target antibody was divided by the amount of colonies from the incubation with polyclonal IgG. The resulting number was the enrichment score.

### **3.2.13.5 Phage Titration**

Depending on the used library, 10 ml medium were inoculated with K12 or K91 bacteria until mid-log-phase was reached (K12:  $OD_{600} \sim 0.5$ ; K91:  $OD_{600} \sim 0.16-0.2$  for 1:10 dilution).

Using a serial dilution, the phages were diluted 1:1,000,000 in TBS. Then, 20  $\mu$ l of the diluted phages were transferred to a well of a 96 well plate. A 10-fold and 100-fold dilution of these phages were made, filled up to 20  $\mu$ l with TBS and were transferred to the 96-well plate wells, too.

As soon as the bacteria reached the desired  $OD_{600}$ , 100  $\mu$ l of the bacteria solution were transferred to each well. After incubation (K12: 10 min; K91: 60 min) the infected cells were streaked out on LB-agar plates (K12: with IPTG/X-Gal; K91: with tetracycline) and the plates were incubated overnight at 37 °C. The (blue) colonies were counted on the next day.

### **3.2.13.6 Sequence identification of selected peptides**

If the enrichment score after 4 rounds was sufficient ( $>10$ ), 20 colonies were randomly picked to inoculate 10 ml LB medium (for K91 with tetracycline), each. All cultures grew overnight at 37 °C and 200 rpm.

The next morning, the bacteria cultures were centrifuged for 10 min at 8,000 g and 4 °C. The supernatant was split and 9 ml were transferred in a new tube. The remaining 1 ml were transferred into a further tube. To precipitate the phages, 1/6 volume 20% PEG/NaCl (1.5 ml or 200  $\mu$ l) was added to the respective tubes and incubated overnight at 4 °C. The larger of the two mixes was purified as described (3.2.13.3). The cell pellets of the bacteria, infected with amplified phages derived from the Fuse5 library, were frozen and stored at -20 °C.

An anti-phage ELISA was performed with the obtained monoclonal phages to determine the best binders (3.2.9). DNA of up to ten of the best binders were purified in order to sequence the peptide insert.

The frozen cell pellets of the bacteria, infected with Fuse5 phages, were used for a Plasmid Mini-Prep (3.1.10) with the PeqGOLD plasmid mini Kit (PeqLab) according to manufacturer's instructions.

To isolate the DNA of Ph.D.<sup>TM</sup>-12 phages, the small scale phage precipitation was used. Precipitated phages were centrifuged with 10,000 g at 4 °C for 20 min. The supernatant was discarded, the pellet was centrifuged again and the remaining supernatant was carefully removed. The pellet was dissolved in 100 µl 4 M NaI solution and 250 µl ethanol (96% (v/v)) was added. The mix was incubated for 15 min at room temperature. The following steps were performed as described for DNA precipitations (3.1.3).

The dry pellet was dissolved in 30 µl TE buffer and used for DNA sequencing (3.1.11). Depending on the used phage library, either the "Fuse55 rev" or the "NEB -96 gIII sequencing" primer (2.6) was used.

### 3.3 Microbiological methods

#### 3.3.1 Prokaryotic cell culture media and supplements

If not stated otherwise, all media were autoclaved for 20 min at 121 °C directly after preparation.

##### LB (lysogeny broth) medium (1 l):

10 g	Bacto <sup>TM</sup> tryptone
5 g	Bacto <sup>TM</sup> yeast extract
10 g	NaCl
ad 1 l	ddH <sub>2</sub> O

Optional (for LB-agar plates):

15 g	Bacto <sup>TM</sup> agar
------	--------------------------

##### TB (terrific broth) medium (1 l):

12 g	Bacto <sup>TM</sup> tryptone
24 g	Bacto <sup>TM</sup> yeast extract
4 ml	99.5% (v/v) glycerol
ad 900 ml	ddH <sub>2</sub> O

After sterilisation with the autoclave 100 ml sterile TB-supplement was added.

**TB-supplement (500 ml):**

11.57 g	KH <sub>2</sub> PO <sub>4</sub> monobasic	170 mM
82.14 g	K <sub>2</sub> HPO <sub>4</sub> * 3 H <sub>2</sub> O	720 mM
ad 500 ml	ddH <sub>2</sub> O	

The solution was sterilised by sterile filtration using a Filtopur V50 0.2 µm sterile filter (Sarstedt).

**SOB (super optimal broth) medium (1 l):**

20 g	Bacto™ tryptone
5 g	Bacto™ yeast extract
0.5 g	NaCl
2.5 ml	KCl (1 M)
ad 1 l	ddH <sub>2</sub> O

**SOC (SOB with catabolite repression) medium (1 l):**

10 ml	MgCl <sub>2</sub> (1 M)
20 ml	glucose (1 M)
ad 1 l	SOB medium

**Antibiotics/Supplements added to 1 l medium, if necessary:**

Ampicillin (Amp) 1 ml stock solution (150 mg/ml in ddH <sub>2</sub> O)
Gentamycin (Gent) 0.7 ml stock solution (10 mg/ml in ddH <sub>2</sub> O)
Kanamycin (Kan) 1 ml stock solution (50 mg/ml in ddH <sub>2</sub> O)
Tetracyclin (Tet) 2 ml stock solution (5 mg/ml in ethanol)
Zeocin (Zeo) 500 µl stock solution (100 mg/ml, supplied by InvivoGen)
IPTG/X-Gal* 1 ml stock solution (40 mg/ml IPTG in ddH <sub>2</sub> O; 40 mg/ml X-Gal in DMF#)

\* Isopropyl β-D-1-thiogalactopyranoside / 5-bromo-4-chloro-3-indolyl-β-D-galactopyranoside

# Dimethylformamide

Antibiotics and supplements were always added after sterilisation at a temperature ≤ 50 °C.

**3.3.2 Propagation of *Escherichia coli***

All bacteria, transformed with a plasmid containing one or more antibiotic resistance genes, were selected with the respective antibiotics in the media.

### 3.3.2.1 Cultivation on agar

After pipetting the bacteria solution on the agar plate, the bacteria were spread by shaking the plate with glass beads. The agar plate was incubated for more than 16 h at 37 °C until single colonies became clearly visible. Monoclonal bacteria were picked for further use. Agar plates sealed with Parafilm® could be stored for several weeks.

### 3.3.2.2 Cultivation in suspension

LB medium was inoculated with single clones from agar plates or glycerol stocks overnight and was incubated at 37 °C, while constantly shaking with 200 rpm. Transformed bacteria, designated to plasmid miniprep, grew in 5 ml LB medium. For large cultures, as used for protein production, a pre-culture was done overnight followed by the inoculation of the required amount of medium.

### 3.3.2.3 Glycerol stocks

For long term preservation, bacteria clones were cryopreserved as glycerol stocks. A 5 ml suspension culture was centrifuged at 5,000 g for 2 min. The supernatant was discarded, the bacteria pellet was resuspended in 1 ml cryo-medium (0.5 ml 99.5% (v/v) glycerol + 0.5 LB medium), aliquoted if necessary and frozen at -80 °C. When needed, a small amount of cells were scraped from the cryo stock and used to inoculate 5 ml LB-medium overnight.

## 3.3.3 Preparation of competent bacteria

### 3.3.3.1 Chemocompetent bacteria (Calcium chloride method)

Bacteria from a glycerol stock were plated on LB<sub>Tet</sub> agar and grew overnight at 37 °C. A single colony was used to inoculate a pre-culture with 50 ml LB<sub>Tet</sub> medium. The bacteria were shaken overnight with 200 rpm at 37 °C. Then, 950 ml LB<sub>Tet</sub> medium was evenly distributed to six Erlenmeyer flasks and inoculated with 0.5 ml pre-culture per flask. The bacteria grew at 37 °C and 200 rpm until the optical density at 600 nm (OD<sub>600</sub>) reached 0.6. To cool the cells, the flasks were placed on ice. Afterwards, the bacteria suspensions were transferred into pre-cooled 250 ml centrifugation bottles and centrifuged at 4 °C and 1950 g for 5 min. All solutions for the following steps were pre-cooled on ice. The supernatant was discarded and the bacteria in each bottle were resuspended with 150 ml CaCl<sub>2</sub> solution (100 mM). After incubation for 30 min on ice, the suspensions were centrifuged again for 5 min (4 °C, 1950 g). The supernatant was discarded, the

bacteria were resuspended in 10 ml CaCl<sub>2</sub> solution (100 mM) per centrifugation bottle and pooled afterwards. The merged suspension was centrifuged for 5 min (4 °C, 1950 g), the supernatant was discarded and the bacteria were carefully resuspended in 2.5 ml CaCl<sub>2</sub>/glycerol-solution (50 mM CaCl<sub>2</sub>/20% glycerol). Finally, 100 or 200 µl aliquots of the solution were distributed to pre-cooled 1.5 ml reaction tubes and frozen either on dry-ice or liquid nitrogen. The competent bacteria were finally stored at -80 °C.

### **3.3.3.2 Electrocompetent bacteria**

In contrast to the generation of chemocompetent cells, the bacteria grew in SOB medium and not LB medium. Apart from this, the first steps were similar. The bacteria were streaked on an agar plate, a single colony was used for pre-culture and 6 flasks, with 950 ml medium in total, were inoculated with the pre-culture and grew until the OD<sub>600</sub> was 0.6. Thereafter, the flasks were cooled on ice for about 15 min and the bacteria suspensions were transferred in pre-cooled 250 ml centrifugation bottles. The bottles were centrifuged at 385 g and 4 °C for 15 min and the supernatant was carefully removed. The cells were resuspended in 150 ml ice-cold HEPES (1 M, pH 7) per bottle and centrifuged again for 15 min (4 °C, 385 g). The bacteria were resuspended again in 60 ml HEPES per bottle and were pooled in two centrifugation bottles (180 ml each). Then, the bacteria were centrifuged (15 min, 4 °C, 385 g), the supernatant was discarded and the cells were resuspended in 15 ml ice-cold 10% (v/v) glycerol per bottle and eventually pooled in one bottle. The pooled bacteria were centrifuged at 860 g and 4 °C for 10 min and the supernatant was discarded. The pellet was resuspended in 2-3 ml ice-cold glycerol (10% (v/v)), distributed to pre-cooled 1.5 ml reaction tubes in 100 µl aliquots and frozen on dry ice.

The electrocompetent cells were stored at -80 °C. To test the quality of the new cells, a test electroporation was performed.

### **3.3.4 Transformation of bacteria**

#### **3.3.4.1 Heat shock transformation**

Competent bacteria (3.3.3.1) were thawed on ice for a few minutes, 50 µl of the bacteria were transferred into a tube (containing the plasmid) and incubated for 20 min on ice. Afterwards the plasmid/bacteria mix was transferred into a 42 °C warm water bath for 45 sec. Immediately after that incubation, the suspension was cooled on ice for further 2 min. Between 200 µl (XL1) and 1 ml (DH10bac) SOC medium was added and the bacteria were incubated for 1 h (XL1) or 4 h

(DH10bac) at 37 °C and 200 rpm. Finally, the bacteria were spread on LB agar plates with the appropriate supplements (i.e. antibiotics or/and IPTG/X-Gal) and incubated overnight at 37 °C.

### 3.3.4.2 Electroporation

Electrocompetent bacteria were thawed on ice. Up to 3 µl salt free DNA was added to the thawed bacteria and mixed gently. The mixture was transferred into a pre-cooled electroporation cuvette (1 mm, Biorad), the cuvette was wiped dry at the outside and quickly put into the ShockPod™ cuvette chamber of the Gene Pulser Xcell™ system (Biorad). A pulse with the following setting was used for electroporation:

Electrode gap:	1 mm
Voltage:	1,800 V
Capacitance:	25 µF
Resistance:	200 Ω

After the pulse, the bacteria were quickly transferred into 2 ml pre-warmed SOC medium and incubated at 37 °C and 200 rpm for 1 h. Different dilutions of the transformed bacteria were plated on LB agar (containing the appropriate supplements) and were incubated overnight at 37 °C.

### 3.3.5 DH10bac transformation and Bacmid purification

#### Solution 1 (100 ml):

182.1 mg	Tris-HCl (pH 8)	15 mM
372.2 mg	Na <sub>2</sub> -EDTA * 2H <sub>2</sub> O	10 mM
ad 100 ml	ddH <sub>2</sub> O	

Prior use 5 µl RNase A (10 mg/ml, Peqlab) was added per 1 ml Solution 1.

#### Solution 2 (100 ml):

800 mg	NaOH	200 mM
10 ml	10% SDS-solution	1 % (v/v)
ad 100 ml	ddH <sub>2</sub> O	

#### Solution 3 (100 ml):

29.4 g	potassium acetate	3 M
ad 100 ml	ddH <sub>2</sub> O	

The pH of solution 3 was adjusted to pH 5.5.

DH10bac cells were transformed with 100 ng pFBD vector (3.1.13) by heat-shock transformation as previously described (3.3.4.1). After transformation, the cells were spread on LB<sub>IPTG/X-Gal</sub> agar plates with kanamycin, gentamycin and tetracycline antibiotics and were incubated for two days until distinct blue and white colonies became visible. Only white clones were picked and a cPCR with the respective insert primer was performed (3.1.6.2). At least two positive colonies were cultivated in 5 ml LB medium (with kanamycin, gentamycin and tetracycline) overnight.

The next day, the cells were pelleted by centrifugation at 7,000 g for 5 min, the supernatant was discarded and the pellet was resuspended in 500 µl Solution 1 (with RNase I). Afterwards, 500 µl Solution 2 was added and the tube was gently inverted. The mix was incubated for 5 min at room temperature followed by the addition of 500 µl Solution 3 and a 10 min incubation on ice. Thereafter, the mix was centrifuged for 15 min at 17,000 g and room temperature. The supernatant was evenly split and transferred into two new 2 ml reaction tubes, followed by precipitation of the DNA with 800 µl isopropanol per tube. Washing and drying of the DNA precipitation was performed as described for ethanol precipitations (3.1.3). The dry DNA pellet was resuspended in 100 µl TE buffer and the bacmid concentration was measured (3.1.5). All bacmids were stored at 4 °C for up to one year and were used for the subsequent transfection of Sf9-insect cells (3.4.5.2).

### 3.4 Cytological methods

Except for experiments using a cytometer, the cells were always handled on a sterile workbench (2.1) with constant laminar flow to prevent contamination. Cell culture media were always pre-warmed before use.

If not stated otherwise the media and growth conditions were:

For HEK293T and HEp-2 cells:

**Dulbecco's modified Eagle's medium (DMEM) supplemented with**

10 %	FBS
1 %	penicillin/streptomycin (Gibco; 10,000 U/ml penicillin, 10,000 mg/ml streptomycin)

For Namalwa.PNT, Namalwa.CSN/70, Ramos, DG75, MAVER-1 and Jeko-1 cells:

**RPMI-1640 supplemented with**

10 %	FBS
1 %	penicillin/streptomycin (Gibco; 10,000 U/ml penicillin, 10,000 mg/ml streptomycin)



For the Jeko-1 cell line:

**RPMI-1640 supplemented with**

20 %	FBS
1 %	penicillin/streptomycin (Gibco; 10,000 U/ml penicillin, 10,000 mg/ml streptomycin)

The cells grew at 37 °C under humidified atmosphere with 5% (v/v) CO<sub>2</sub>. The cell lines were split every two to three days, depending on the cell density. For adherent cell lines (HEK293T and HEp-2), trypsin was used for detachment from the flask or plate. The 10x trypsin solution (PAA Laboratories) was filled up with 9 volumes sterile PBS prior use. The 1x Trypsin was then stored at 4 °C for up to two month.

Suspension cultures were centrifuged and about one-third of the cells were transferred to a new flask.

For Sf9 insect cells:

**Insect-XPRESS™ supplemented with**

10 mg/l	gentamycin (Lonza, 50 mg/ml)
---------	------------------------------

Sf9 cells grew either as adherent culture at 27 °C or as suspension culture at 27 °C with constant shaking at 110 rpm. To split adherent cultures the cells were detached from the flask by vigorous knocking. The minimum cell density for Sf9 cells was 5x10<sup>5</sup> cells/ml.

### 3.4.1 Seeding of eukaryotic cells

Frozen cells were quickly thawed at 37 °C and transferred to pre-warmed cell culture medium. The cell suspension was centrifuged at 100 g for 5 min, the supernatant was discarded and cells were seeded in a 75 m<sup>2</sup> flask with 5 ml medium. As soon as the cells adhered to the flask, the media was changed.

### 3.4.2 Cryopreservation of cells

**Cryopreservation medium for HEK293T, Namalwa.PNT, Namalwa.CSN/70, Ramos, HEp-2, DG75, MAVER-1 and Jeko-1 cell lines:**

45 % (v/v)	DMEM or RPMI-1640 (without supplements)
45 % (v/v)	FBS
10 % (v/v)	DMSO

**Cryopreservation medium for Sf9 cells:**

45 %	Insect-XPRESS (without supplement)
45 %	conditioned* Insect-XPRESS
10 %	DMSO

\* conditioned medium is the centrifuged supernatant of a 2-4 days old Sf9 culture

Cells were counted (3.4.3) and centrifuged at 100 g for 5 min. The supernatant was discarded and the cells were resuspended in the required volume of cryopreservation medium to adjust the cell density per well to  $1 \times 10^7$  cells/ml. Afterwards, the cells were quickly transferred to cryopreservation tubes and frozen using a isopropanol-filled freezing container (Mr. Frosty Freezing Container, Thermo Scientific). The freezing container was placed in the freezer (-80 °C) for 24 h. For long term storage, the cells were transferred into liquid nitrogen.

**3.4.3 Cell counting**

Adherent cells were detached from the flask by vigorous tapping (Sf9) or short incubation with 1x trypsin at 37 °C (HEK293T and HEp-2). The cells were resuspended in medium, 10 µl of the cell suspension were transferred to a new tube and mixed with 90 µl 0.2% (w/v) trypan blue solution (in PBS). Out of this mix, 10 µl were pipetted to a Neubauer improved cell counting chamber. Viable cells in at least four (big) squares ( $1 \text{ mm}^2$ ,  $0.1 \text{ mm}^3$ ) were counted. The average amount of cells per square was calculated and multiplied by 100 to obtain the amount of cells per micro-litre.

**3.4.4 Isolation of peripheral blood mononuclear cells (PBMCs)**

Blood and bone marrow aspirates were diluted 1:1 with sterile PBS in a 50 ml centrifugation tube. The diluted blood was carefully transferred to a 15 ml Ficoll solution (Biochrom AG) in another 50 ml tube. The tube was centrifuged for 20 min at 610 g (2,000 rpm, swing out centrifuge) with disabled brake. Afterwards, the serum (supernatant) was discarded and the grey interphase was transferred to a new 50 ml tube. The tube was filled up with PBS to a total volume of 50 ml. This cell suspension was then centrifuged for 10 min at 345 g and the supernatant was discarded. The pellet was resuspended in 50 ml, 10 µl were used to count the obtained PBMCs (3.4.3), the tube was centrifuged again for 10 min at 345 g and the supernatant was removed.

Eventually, the pellet was resuspended in RPMI-freeze medium with a concentration of  $1 \times 10^7$  cells per ml. The aliquots were and frozen and stored at -80 °C (3.4.2).

### 3.4.5 Eukaryotic production of recombinant proteins

#### 3.4.5.1 In HEK293T cells

##### Transfection of cells

$2 \times 10^5$  HEK293T cells were seeded per well in a six-well plate and were grown overnight to a confluence of more than 70%. The wells were washed with PBS and fresh medium with 10% FBS (but without antibiotics) was added. Afterwards, the transfection mix was prepared:

##### **PEI transfection mix:**

2 $\mu$ g	pBud vector DNA (3.1.13)
ad 200 $\mu$ l	Medium with 10% FBS but without antibiotics
20 $\mu$ l	1 mg/ml polyethylenimine (PEI)

The mix was prepared carefully, incubated for 15 min at room temperature, added to the respective well and incubated for 3 h.

The medium was then discarded, the cells were washed with PBS and new medium (with FBS and P/S) was added. The cells were incubated overnight. Afterwards, the medium was replaced by medium with all supplements and 100  $\mu$ g/ml zeocin to start the positive selection.

##### Selection and monoclonalisation

After transfection, only medium with supplements and zeocin was used to maintain selection pressure. The cells grew for at least one week in the well until more than 70% confluence was reached. They were then transferred to a 75 cm<sup>2</sup> flask and further expanded to two 125 cm<sup>2</sup> flasks. One flask was used to freeze the transfected cells (3.4.2) and the cells of the other flask were monoclonalised.

For monoclonalisation, the cells were detached from the plate with trypsin and counted afterwards (3.4.3). Using multiple steps, the cells were diluted in medium to a final concentration of 10 cells per ml in a total volume of 10 ml. Each well of a 96 well plate (Falcon) was filled with 100  $\mu$ l of this cell suspension and the cells were incubated at 37 °C under humidified atmosphere.

After about one week, the 96-well plate was assessed every day and monoclonal cell populations were marked. When the cells in the wells reached about 80% confluence, the medium was obtained and used for a supernatant ELISA (3.2.9). Only the cells in the three wells with the highest Ig concentration were transferred into 75 cm<sup>2</sup> flasks, further expanded and eventually frozen (3.4.2).

Another supernatant ELISA was performed to predict the sub-cell line with the best Ig expression. These cells were expanded to 12 165 cm<sup>2</sup> cell culture plates for a large scale production.

### Large scale production

While the cells grew in the 165 cm<sup>2</sup> plates, the medium was gradually replaced by serum free ISF-1 medium (without FBS but with penicillin/streptomycin and zeocin), starting from 10% serum free medium. Finally, per plate 25 ml 100% serum-free medium was added and the cells were left in this medium for at least 3 days, to allow the expression of the Ig. Afterwards, the cell culture supernatant was collected, passed through a sterile filter and the expressed protein was purified (3.2.1).

### **3.4.5.2 In Sf9 cells**

#### Generation of baculovirus

Per transfection, 5x10<sup>5</sup> Sf9 insect cells were seeded in 2 ml medium in one well of a 6-well plate. The cells were incubated for about one hour until they were completely attached. Meanwhile, the transfection mix was prepared:

#### **Insect cell transfection:**

250 µl	Insect-XPRESS medium without antibiotic
7.5 µl	TransIT Insect Reagent
7.5 µg	bacmid (3.3.5)

The mix was incubated at room temperature for at least 30 min, added to the cells and incubated for 72 h at 27 °C. The supernatant was then collected and centrifuged at 500 g for 5 min, transferred in a dark centrifugation tube and stored at 4 °C (P1-Stock).

To increase the baculovirus titre, 2.5x10<sup>7</sup> Sf9 cells were seeded in a 175 cm<sup>2</sup> flask. The cells were incubated shortly (20-60 min) until most cells adhered to the flask. Then, 400 µl of the P1-Stock were added to this flask, evenly distributed and the cells were incubated at 27 °C for 72 h.

Afterwards, the cells were detached from the flask (by vigorous tapping), counted and frozen (3.4.3 and 3.4.2) in 500 µl aliquots with a concentration of 1x10<sup>7</sup> cells per ml (BIIC-stock). In addition, two 100 µl aliquots (1x10<sup>7</sup> cells/ml) were frozen for the test expression.

#### Test expression

Sf9 insect cells in 2 ml medium were seeded in all wells of a 6-well plate (1x10<sup>6</sup> cells per well). A 100 µl aliquot of the BIIC-stock was thawed and diluted in 5 ml medium. Different volumes

(between 1  $\mu$ l and 100  $\mu$ l) of this dilution were given to the wells and the infected cells were incubated at 27 °C for 72-96 h.

After this incubation, the medium of each well was collected, centrifuged at 500 g for 5 min and the supernatant was transferred to a new reaction tube. A sufficient amount of denaturing Laemmli loading buffer was added and a Western Blot was performed with 20  $\mu$ l of each supernatant (3.2.7). HPR-labelled anti-human-Fab antibody (AbD Serotec) was used as detection antibody. The virus dilution resulting in the best protein expression was used for the large scale production.

#### Large scale protein production

The Sf9 insect cells were seeded in 300 ml medium in an Erlenmeyer flask with a concentration of  $1.5 \times 10^6$  cells per ml. An appropriate amount of BIIC-stock (determined by test expression) was added to the cell suspension and the cells were shook at 110 rpm for 72 h at 27 °C facilitating the protein expression.

Afterwards, the cells were transferred into centrifugation tubes, centrifuged at 500 g for 5 min at 4 °C and the supernatant was sterile filtered, followed by the purification of the recombinant protein (3.2.1).

### **3.4.6 Immunofluorescence assay**

Unless stated otherwise, all washing steps and dilutions were done with TBS-T (0.1% Tween-20). Coverslips were placed in a 24-well plate and  $1 \times 10^5$  HEp-2 cells were seeded per well. The cells grew overnight until 70-80% confluence was reached. Then, the medium was removed and the cells were washed once with TBS. Two different fixation methods were performed.

#### PFA fixation

For PFA fixation the coverslips were covered with about 300  $\mu$ l of 3.7% PFA (paraformaldehyde) solution and were incubated for 20 min at 37 °C. The PFA was then removed and the slips were washed three times with TBS. To permeabilise the cells, the slips were covered in 0.1% Triton-X100 (in TBS) solution for 15 min.

#### Methanol fixation

Alternatively, the coverslips were covered in pre-cooled (-20 °C) methanol for 20 min at -20 °C. The cells were washed with TBS-T. No further permeabilisation step was required.

### Immune staining

The coverslips were blocked with 5% BSA (in TBS-T) for 1 h. Multiple concentrations of each primary antibody were tested between 10 µg/ml and 200 µg/ml (in 2% BSA). After washing once, the coverslips were placed in a moist chamber and at least 50 µl of the respective primary antibody solutions were transferred onto the coverslip. The chamber with the slips was placed in the fridge (4 °C) overnight. The next morning, all coverslips were washed and placed in a 24-well plate to simplify the subsequent washing steps. Each well was washed three times with at least 400 µl TBS-T. The FITC-labelled anti-human-IgG secondary antibody (1:800, Sigma Aldrich) was diluted in 2% BSA and 200 µl of this solution was transferred to each well. After an incubation for 1 h at room temperature, all wells were washed three times again. Up to four 10 µl drops of mounting medium with DAPI (Vector Laboratories Inc.) were placed on a microscope slide. The coverslips were carefully put “cell-side down” on the prepared slides.

Finally, the coverslips were sealed with nail polish and stored for at least 30 min in the dark until the nail polish dried.

All slides were analysed using a Carl Zeiss fluorescence microscope and the LabQuest (2.9) software.

### **3.4.7 Transduction of Burkitt lymphoma cell lines**

#### Generation of pLeGO vectors

Two pLeGO vectors were generated for the lentiviral transduction of Burkitt lymphoma cell lines. The first one harboured a mouse-derived IgM constant region with a transmembrane domain and a zeocin resistance cassette (Figure 5). This enabled the determination between endogenous and transduced IgM.

The second vector carried the constant light chain gene and a puromycin resistance gene. Similar to the pFBD and pBud vectors, two different variants of the light chain vector for κ- and λ- light chains were designed.

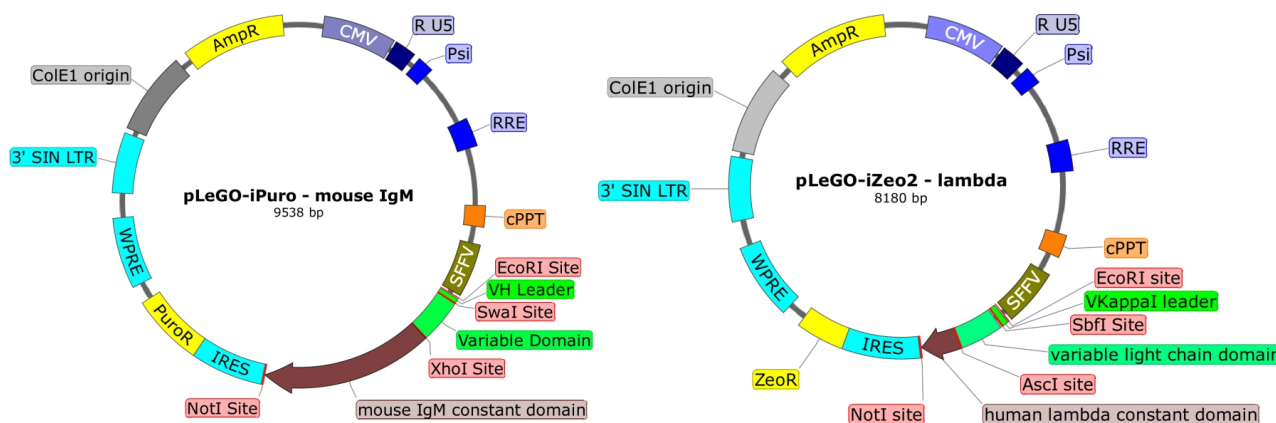


**Figure 5: Maps of the pLeGO vectors used for transduction of lymphoma cell lines.** The respective variable domains were cloned into the vectors, which were used for lentiviral transduction of the cells. The pLeGO-iPURO-mouse IgM vector (left) harboured a murine constant IgM domain and a puromycin resistance cassette for positive selection, whereas pLeGO-iZeo2-lambda vector carried the lambda constant region and a zeocin resistance gene.

The vectors harboured the same respective restriction sites for the insertion of the heavy and light chain variable regions as the pFBD expression vector (3.1.13). The required steps of restriction, ligation and purification as well as the insert amplification were similar to the procedures described above (3.1.6.1, 3.1.10 and 3.1.13).

#### Transduction and selection Ramos cells

The lentiviral transduction was performed by Dr. Kristoffer Riecken (Research Department Cell and Gene Therapy, UKE). The Ramos cells were plated into a 24-well plate at a concentration of 50,000 cells per well in 500  $\mu$ L of RPMI medium. The heavy and light chain harbouring pLeGO vectors were added. Per lentiviral vector, 100  $\mu$ l of supernatant, containing VSV-G pseudotyped viral particles, were used.

Five days after transduction, cells were transferred into a 6-well plate and selection of the double-positive cells (expressing IgH and IgL) was started by adding 1  $\mu$ g/ml puromycin (Sigma Aldrich) and 20  $\mu$ g/ml zeocin (Invitrogen).

The transduced cells grew for up to three weeks until a sufficient cell density was reached. During this time, the medium was changed every two days in order to maintain the selection pressure.

When the transduced cells reached similar growth rate like the untransduced ones, the cells were sorted by FACS (3.4.8).

### 3.4.8 Fluorescence-activated cell sorting (FACS)

#### PBS+Ca<sup>2+</sup> (PBS with Ca<sup>2+</sup>, pyruvate and HEPES):

5 ml	sodium pyruvate (100 mM)	1 mM
12.5 ml	HEPES* (1 M)	25 mM
ad 500 ml	Dulbeccos PBS with calcium and magnesium (Sigma Aldrich)	

\*2-[4-(2-hydroxyethyl)piperazin-1-yl]ethanesulfonic acid

Ramos cells were grown in a 125 cm<sup>2</sup> flask for two days, until a sufficient amount of cells was reached. All cells were collected and centrifuged for 5 min at 150 g. The supernatant was discarded, the pellet was resuspended in PBS+Ca<sup>2+</sup> and a FITC-labelled anti-human-IgM antibody (Dako) was added in a 1:1,000 dilution. From now on, the cells were kept in the dark to prevent bleaching of the fluorochrome. After a 30 min incubation on ice, the cells were washed twice with PBS+Ca<sup>2+</sup>. Afterwards the cells were resuspended in PBS+Ca<sup>2+</sup> and the second PE-labelled anti-human-lambda antibody (Dako) was diluted 1:1,000 in this suspension. Following a 30 min incubation on ice, the cells were washed twice and resuspended in cell culture medium.

The cells were sorted using a FACSAria™ (BD Biosciences) at the “Heinrich-Pette-Institut” (HPI) with the assistance of Arne Düsedau. Transduced Ramos cells were sorted for the presence of a PE-signal and the absence of a FITC-signal. Untransduced cells were selected against both signals.

The sorted cells were collected in the respective medium (with or without puromycin/zeocin), centrifuged (100 g, 5 min) and transferred to a 75 cm<sup>2</sup> flask. Finally, the sorted cells were propagated and frozen (3.4.2) as soon as possible. Sorted cells expressing no human-IgM but mouse-IgM on the cell surface (detected by flow cytometry, 3.4.9) were used for calcium influx-experiments (3.4.10), the far-Western Blot (3.2.8) and a proliferation assay (3.4.11).

### 3.4.9 Flow cytometric cell analysis

The cells were grown until at least 300,000 cells could be acquired. These cells were washed and resuspended in PBS. The staining with labelled antibodies was done as described for the FACS (3.4.8). All cells were labelled with the FITC-labelled anti-human-IgM- (Dako) and the PE-labelled anti-human-lambda-antibodies (Dako). Additionally, another aliquot was labelled with the FITC-labelled anti human-kappa-antibody (Dako).

Transduced cells were also stained with a FITC-labelled anti-mouse-IgM (eBioscience) antibody. The incubation time for each antibody was 30 min and the staining took place on ice in a dark



chamber. Washing was performed with PBS and centrifugation was done at 150 g and room temperature for 5 min.

After the staining was complete, the cells were analysed by a FACSCalibur™ cell analyser (BD Biosciences) with the CellQuest Pro (version 5.2.1, BD Biosciences) and FlowJo software (version 8.7).

### 3.4.10 Calcium influx measurement

The Ca<sup>2+</sup>-Flux protocol was adapted from Schepers et al. (2009)<sup>195</sup>.

Between 2x10<sup>6</sup> and 4x10<sup>6</sup> Ramos cells, expressing a transduced Ig as well as untransduced control cells, were collected, washed with PBS+Ca<sup>2+</sup> and resuspended in 1 ml PBS+Ca<sup>2+</sup> (3.4.8). An aliquot of Fluo-4-AM (Invitrogen) was dissolved in 9.1 µl DMSO and 1 µl of this solution was added to each cell suspension (5 µM Fluo-4-AM per tube). The cells were incubated for 30 min at room temperature in a dark chamber. Afterwards, the tubes were centrifuged for 5 min at 100 g, the supernatant was carefully discarded and the cells were resuspended in 1 ml PBS (without calcium). The cells were centrifuged again (5 min, 100 g), resuspended in 2 ml PBS+Ca<sup>2+</sup> and evenly distributed to up to four FACS tubes. The tubes were filled up with PBS+Ca<sup>2+</sup> to a total volume of 1 ml.

Fluorescence intensity measurements of Fluo-4-loaded cells were performed using a FACS Calibur™ (BD Bioscience) and the BD CellQuest Pro software (version 5.2.1). The signal was measured in the FL1-channel for 180 s.

During stimulation experiments, the baseline signal was measured for 15 s, followed by the rapid addition of either 5 µg/ml SpA (Sigma Aldrich), 2 µg/ml goat-anti-mouse-IgM (eBioscience) or 2 µg/ml goat-anti-human Fab antibody (AbD-Serotec). The Fluo-4 signal was continuously measured.

Analysis was done with the FlowJo software (version 8.7).

### 3.4.11 Proliferation assay

Cells were counted and 50,000 cells per treatment group were given into 5 ml cell culture medium with the respective antigen (5 µg/ml SpA (Sigma Aldrich) or 2 µg/ml anti-mouse-IgM antibody (eBioscience)). The cell density was measured every 24 h for 10 days using the Vi-CELL™ XR cell counter (Beckmann Coulter). The obtained volume per day (500 µl) was replaced with fresh medium supplemented with the 5 µg/ml SpA or 2 µg/ml anti-mouse-IgM antibody.

### **3.5 Institutional approval**

Samples from mantle cell lymphoma patients were anonymised left over tissues from diagnostic procedures. Research on left-over-tissues from lymphoma patients for research on the B cell receptor was approved by the responsible local ethics committee of the Association of Physicians (Ärzttekammer) in Hamburg, Germany.

The Declaration of Helsinki was complied with.

## 4 Results

### 4.1 Analysis of the MCL immunoglobulin sequences

The amplification of the B cell-receptor heavy and light chain variable regions was the crucial step for all further experiments. To avoid cross contaminations between different samples, all PCRs were performed using only a single sample at the same time. Furthermore, at least two independent amplifications, resulting in similar sequences were necessary to verify the appropriate tumour BCR composition. The most successful approach to determine the Ig heavy and light chain sequence repertoire was performed as follows. Isolated RNAs from tumour samples were transcribed into cDNA with oligo(dT)-primer. Afterwards, an oligo-G tail was appended to the cDNA by a terminal transferase (3.1.4). A nested PCR approach was done, using an isotype specific-primer and an oligo-C-primer (BaPpC, 2.6), bearing a specific tail sequence, for the first amplification. The second amplification used another isotype specific-primer within the amplified product as well as a primer (BaP) binding to the tail sequence of the BaPpC primer.

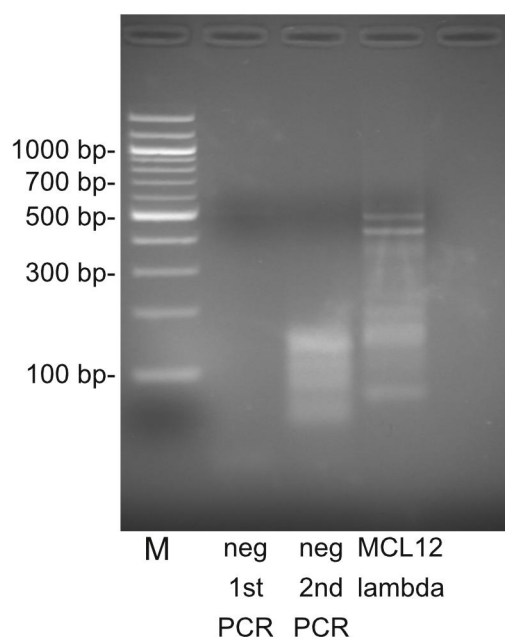


**Figure 6: Exemplary nested-PCR result.** Agarose gel image after a nested PCR, used for the amplification of the variable  $\lambda$ -domain of a MCL lymphoma sample (IGLV). For the first amplification, 100 ng MCL12 cDNA was used as template. Afterwards, 10  $\mu$ l of the first PCR mix was used as template for the second PCR. This nested PCR resulted in two distinct bands between 400 and 500 bp, which were extracted and cloned into a pJet vector for further processing. In addition, the negative control (without DNA) after the first and second PCR is shown. The band between 100 and 200 bp represents unspecific amplification products.

Samples were separated on a 2% (w/v) agarose gel in TAE and stained with ethidium bromide.

M = Marker, Quickload 100 bp DNA-ladder (NEB)

As shown exemplary in Figure 6, the nested PCR often resulted in a distinct band surrounded by unspecific bands or smear. The products with a length between 350 bp and 500 bp were extracted and cloned into a pJet vector (3.1.9). Due to the possibility of unspecific PCR-products, a subsequent colony PCR (cPCR) was necessary to identify subcloned amplification products of the correct size (Figure 7).

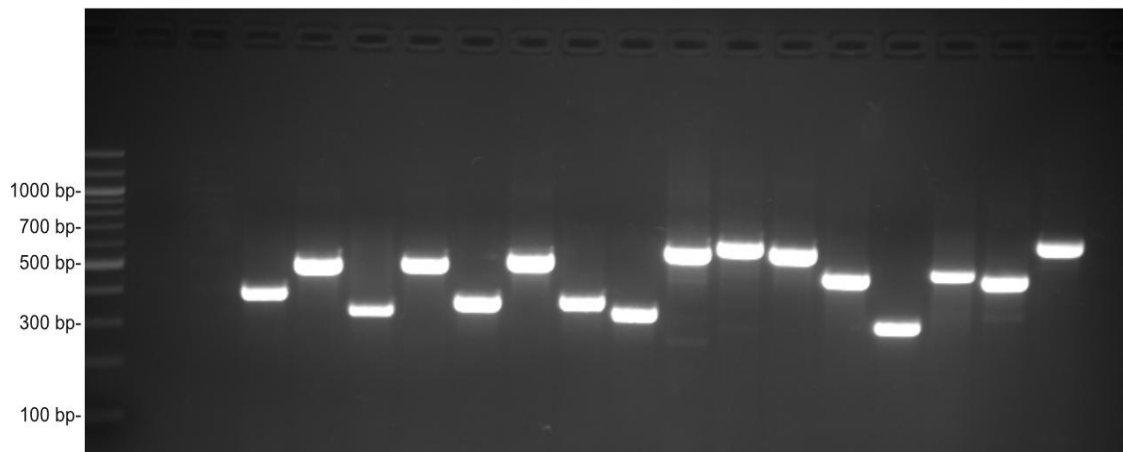


**Figure 7: Result of the colony PCR with subcloned IGLV-amplification products.** Amplificates of the MCL12 IGLV nested PCR (Figure 6) were cloned into a pJet-vector and used for the transformation of XL1-bacteria. The BaP-primer was used as forward and the “lambda nested”-primer was used as reverse prime. At least 8 randomly chosen clones, with insert sizes between 350 bp and 600 bp, were propagated overnight and the plasmids were sequenced. Samples were separated on a 2% (w/v) agarose gel in TAE and stained with ethidium bromide. DNA ladder: Quickload 100 bp DNA-ladder (NEB)

The variable region of an immunoglobulin consists of about 350 bp. Thus, only colonies with a cPCR product larger than 350 bp were amplified overnight and the plasmids were isolated and sequenced subsequently. Using this technique, it was possible to amplify and determine the variable regions of the B cell antigen receptor immunoglobulins from 24 out of 32 different patient samples (Table 4). A sequence was regarded as MCL-derived if at least half of the acquired sequences were identical and present in two independent amplifications. In most cases, only one distinct sequence was acquired per sample.

For two patients (MCL13 and MCL25), a clear determination of a specific tumour light chain was not possible, because neither the amplifications of  $\kappa$ - nor  $\lambda$ -light chains resulted in unique monoclonal sequences. The Ig-light chains of these cases were regarded as polyclonal (Table 4). For the remaining eight RNA-samples neither a specific heavy nor light chain could be affirmed.

**Table 4: Summary of the successful determined variable heavy and light chain sequences of MCL-derived Igs.**

Sample	V-Gen-family	Iso-type	CDR3 of VH	V-region identity in	V-Gen-family	Iso-type	CDR3 of VL	V-region identity in %
MCL4	IGHV1-8	μ	ATALMTSVTGAWRRRTDDY	98,96	IGKV4-1	κ	QQYYSTPLT	99,66
MCL21	IGHV1-8	μ	ARGILTYGYYHYSMDV	98,61	IGKV1-9	κ	QQLNSYPLT	99,28
MCL32	IGHV1-18	μ	ARVGYDFWSGYSESYYYYYMDV	100	IGKV3-15	κ	QQYNNWPLT	99,64
MCL23	IGHV3-9	μ	AKDLGGGTPGAFDI	100	IGKV3-20	κ	QQYGSSRT	100
MCL1	IGHV3-21	μ	<u>ARDRSQLQDLYYHYMDV</u>	<u>99,65</u>	<u>IGLV3-19</u>	<u>λ</u>	<u>NSRDSSGNHLV</u>	<u>99,64</u>
MCL8	IGHV3-21	μ	<u>ARDENDFWSGYKSPNYDY</u>	<u>100</u>	<u>IGLV3-19</u>	<u>λ</u>	<u>NSRDSSGNHRV</u>	<u>100</u>
MCL11	IGHV3-21	μ	<u>ARDENDFWSGYKSPNYDY</u>	<u>100</u>	<u>IGLV3-19</u>	<u>λ</u>	<u>NSRDSSGNHGV</u>	<u>100</u>
MCL20	IGHV3-21	μ	<u>AREDGSSWPVIAVAGTGYGMDV</u>	<u>98,96</u>	<u>IGLV3-19</u>	<u>λ</u>	<u>NSRDNSGNHLV</u>	<u>99,28</u>
MCL28	IGHV3-21	μ	<u>ARDSYGGTPGYYYYYYMDV</u>	<u>97,92</u>	<u>IGLV3-19</u>	<u>λ</u>	<u>NSRDSSGNHLV</u>	<u>100</u>
MCL2	IGHV3-23	μ	AKDGISGSGSEERATYGMDV	96,88	IGKV4-1	κ	QQYYNTPLT	98,99
MCL22	IGHV3-30	μ	ASGRGGGNCGADCYSGMGGSIDY	98,26	IGKV1-5	κ	QQYNSYSLFT	99,28
MCL13	IGHV3-38	μ	AISRLRADY	99,65	polyclonal			
MCL5	IGHV3-49	μ	TRGSSSPSNFDF	97,28	IGKV1-27	κ	QKYNNAPLT	98,57
MCL31	IGHV3-74	μ	ARGGLDSSNLYPFDY	94,79	IGKV4-1	κ	QQYFSSPYT	97,64
MCL16	IGHV4-34	μ	ASRYCTNGVCPENWFDP	99,65	IGLV1-47	λ	AAWDDSLSGLWV	100
MCL19	IGHV4-34	μ	ARGVLDIVVPAAMGAYYFDY	97,89	IGLV3-19	λ	KSRDSSGNHLV	98,57
MCL24	IGHV4-34	μ	ASINNWFDP	100	IGLV1-40	λ	QSYDSSLGSGSV	100
MCL29	IGHV4-34	μ	ATKAGLDYDYDSSGPNWFDP	100	IGLV1-40	λ	QSYDSSLGSPVV	100
MCL25	IGHV4-34	μ	AVGSGGNNWFDP	98,95	polyclonal			
MCL14	IGHV4-39	μ	ARFFSGGVAGISDYGMDV	99,31	IGLV7-43	λ	LLFYGGAQGV	99,65
MCL30	IGHV4-39	μ	ASARYSSSWYFDY	99,31	IGLV1-40	λ	QSYDSSLGSGFAV	99,65
MCL27	IGHV4-59	μ	AKSGYSYGTLYNFDY	99,3	IGKV1-39	κ	QQSYSTPYT	100
MCL12	IGHV5-51	μ	ATTAILYFDY	100	IGLV2-14	λ	SSYTSSLYV	100
MCL18	IGHV5-51	μ	ARRAEGLDY	98,26	IGKV2-28	κ	MQALQTPMYT	99,66

Note: Greyed samples bearing IGHV3 genes. The underlined samples showed a noticeable pairing bias.

#### 4.1.1 The mantle cell lymphoma Ig repertoire

All sequenced tumour-Ig heavy chains belonged to the  $\mu$ -isotype and the ratio of  $\lambda$ - and  $\kappa$ -isotypes showed a minimal preference for  $\lambda$ -light chains. In total, 10 Igs used the  $\kappa$ - and 12 the  $\lambda$ -light chain isotype (two were polyclonal).

Within this cohort of MCL samples, the Ig heavy variable gene (IGHV)-repertoire was strongly biased towards the usage of IGHV3 genes. About 45% (11 out of 24) of the amplified heavy chains belonged to this family (Figure 8).

In addition, one third of the Igs used variable heavy chains of family 4 with IGHV4-34 as the most dominant IGHV4 gene segment (5 out of 8).

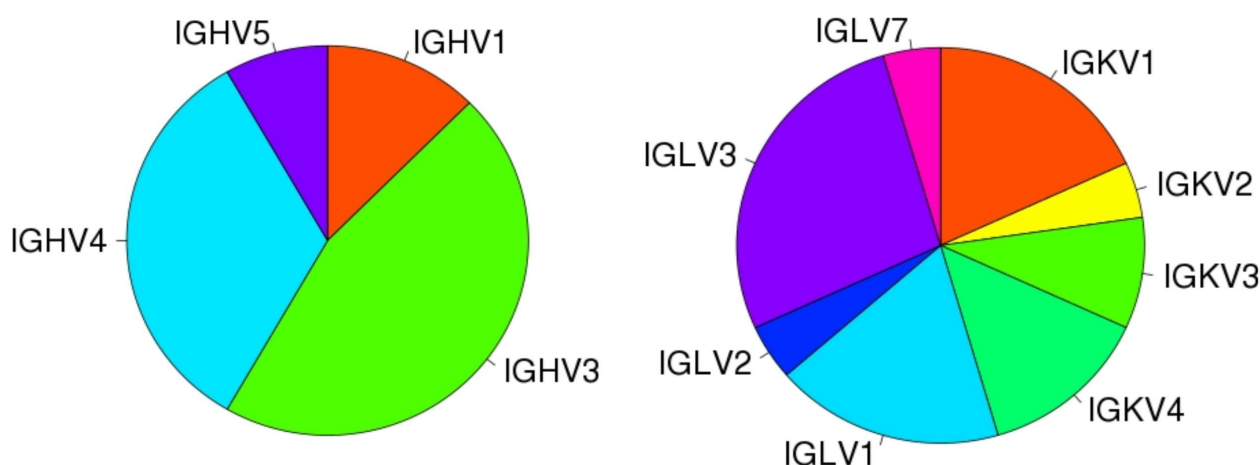


**Figure 8: Distribution of heavy and light chain gene families within the MCL patient cohort.** The BCR repertoire was biased towards the usage of IGHV3 and IGHV4 genes. 19 out of 24 samples expressed a variable heavy chain of one of these two gene families (left). The light chain bias was not as strong as for the heavy chains but more than a quarter (6 out of 22) of the cohort used the IGLV3 genes (right).

Moreover, the pairings of the heavy and light chains were also biased. Within the sub-population harbouring the family 3 heavy chains, 5 out 11 samples showed an association of the IGHV3-21 heavy chain with an IGLV3-19  $\lambda$ -light chain (underlined in Table 4). While only five IGHV3-21 sequences were present in the cohort, IGLV3-19 was sequenced six times and therefore accounted for the most abundant light chain gene, followed by IGKV4-1 and IGLV-1-40 (three samples each). Within the IGHV3-21 subgroup, four Igs presented a CDR3 region of the same length and two Igs were almost identical (MCL8 and MCL11, see Table 5 and Table 6).

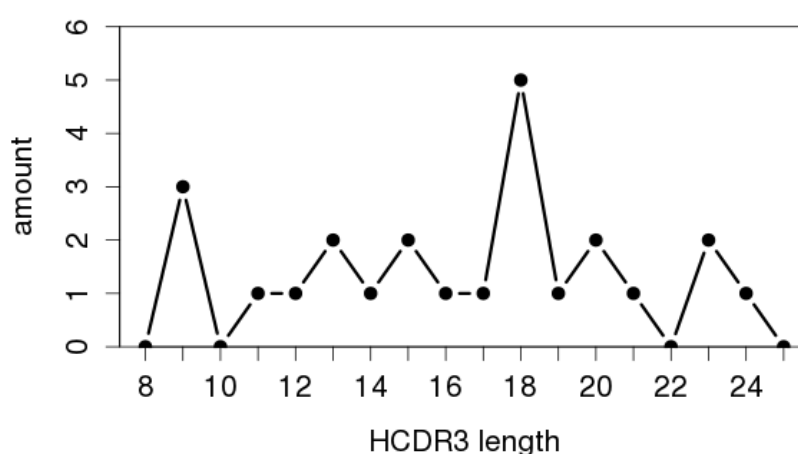
**Table 5: Heavy chain complementarity determining regions (HCDRs) of a strongly biased subgroup.**

<b>Sample</b>	<b>HCDR1</b>	<b>HCDR2</b>	<b>HCDR3</b>
MCL1	GFTFSSYS	ISSSSSYI	ARDRSQLQDLYYHYMDV
MCL8	GFTFSSYS	ISSSSSYI	ARDENDFWSGYKSPNYDY
MCL11	GFTFSSYS	ISSSSSYI	ARDENDFWSGYKSPNYDY
MCL20	GFTFSSYS	ISSSSSYI	AREDGSSWPVIAVAGTGYYGMDV
MCL28	GFTFSSYD	ISSSSSYI	ARDSYGGTPGYYYYYMDV

**Table 6: Light chain complementarity determining regions (LCDRs) of a strongly biased subgroup.**

<b>Sample</b>	<b>LCDR1</b>	<b>LCDR2</b>	<b>LCDR3</b>
MCL1	SLRSYY	GKN	NSRDSSGNHLV
MCL8	SLRSYY	GKN	NSRDSSGNHRV
MCL11	SLRSYY	GKN	NSRDSSGNHGV
MCL20	SLRSYY	GKN	NSRDNSGNHLV
MCL28	SLRSYY	GKN	NSRDSSGNHLV

The heavy chain CDR3-regions (HCDR3) in this subgroup had a length of 18 amino acids (AA) for all but MCL20, which had a 23 AA long HCDR3. However, except for MCL8 and MCL11, the HCDR3-regions differed significantly. In contrast, the LCDR3-regions were almost identical with only a single AA exchange in two samples (MCL8 and MCL11, Table 6). Of note, the mutational load is generally lower in light chains than heavy chains (4.1.2).

**Figure 9: Length distribution of the variable heavy chain CDR3-region in the whole MCL cohort.**

The median HCDR3 length of the whole cohort was 17.5 AA. The shortest HCDR3 was shaped by 9 AA and the longest had 24 AA. Figure 9 summarises the HCDR3 length distribution. Besides the preferred usage of 18 AA long HCDR3 regions in the IGHV3-21 expressing sub-group, no further

preferences were observed for other IGHV families. Especially samples harbouring the IGHV4-34 gene segment showed a high diversity in the HCDR3-lengths ranging from 9 AA (MCL24) to 21 AA (MCL19).

The diversity of the LCDR3-regions was much less pronounced. MCL23 showed the shortest LCDR3, which was formed by 8 AA, whereas the longest LCDR3-regions consisted of 12 AA (MCL16, MCL29, MCL30). The median length of the cohort was 10 AA.

#### 4.1.2 Comparison of the mutational load of NHL-Igs

The mutational load of the MCL-Igs was compared to Igs of CLL and FL samples (Figure 10). For a larger dataset, CLL sequences acquired in this work-group as well as published data by Minden et al.<sup>113</sup> was used.

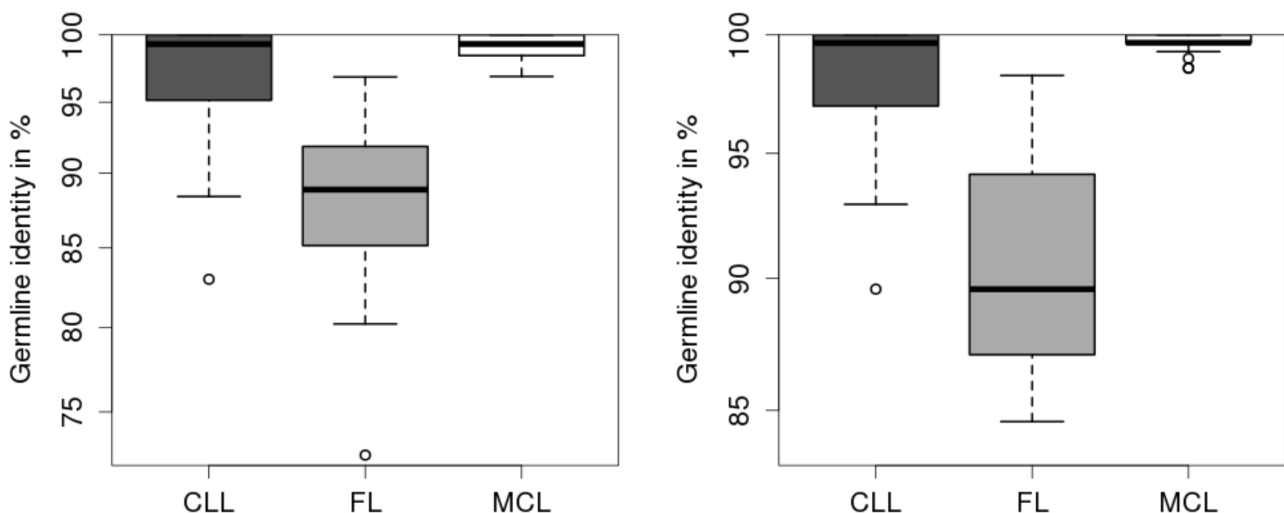


**Figure 10: Boxplots representing the germline identity of the variable Ig sequences from three NHL cohorts.** While the Igs of follicular lymphomas (FL, grey) were highly somatically hypermutated, the majority of MCL (white) and CLL (black) variable regions showed only a minimal mutational load or were unmutated. Heavy chains of all entities (left) showed higher mutational load than their respective light chains (right). CLL and FL sequences were previously acquired in our work-group. In addition, CLL data was supplemented with sequences published by Minden et al.<sup>113</sup>. Mutated and unmutated CLL cases were used and not preselected. Cohort sizes: CLL: 35 FL: 24 MCL: 24 (heavy chains) / 22 (light chains)

As shown in Figure 10, MCL-Igs displayed the lowest mutational load of these three entities. The mean germline identity was 99.12% and 99.62% for heavy and light chains, respectively. Besides bearing fewer mutations than CLL and FL Igs, the MCL-Ig cohort was more homogeneous with only little diversity in the mutational load. Importantly, the CLL cohort was not separated into unmutated and mutated CLL cases. The median of the mutational load of all CLL samples was therefore similar to the one observed in the MCL cohort.



In addition, the location and amount of silent (S) and replacement (R) mutations within the mutated subset of the cohort were analysed. The overall R/S-ratio was 1.26 and 4.0 for the FRs and CDRs, respectively.

### 4.1.3 Next-Generation Sequencing with two samples of the same patient

It was possible to analyse two samples of the same patient (MCL27), which were acquired in an interval of four years. This opportunity was used to analyse these samples using Next-Generation Sequencing (NGS). The much greater output of this technique compared to classical Sanger sequencing (3.1.14) enabled a more detailed insight into the genetic stability and variability of the MCL-Ig genes over time.

*Table 7: IMGT clonotype summary of two MCL samples acquired from a patient in a 4 year interval.*

Sample	Locus	Nb of IMGT clonotypes (AA)	Nb of sequences assigned to IMGT clonotypes (AA)	% of total sequence Nb	Nb of in-frame productive sequences	% of total sequence Nb	Nb of submitted sequences
MCL27 (2008)	IgH	39	4508	80.95	5066	90.97	21280
	IgK	217	6369	91.09	6028	86.21	
	IgL	244	1383	25.7	4971	92.38	
MCL27 (2012)	IgH	42	3665	76.15	4062	84.4	22853
	IgK	267	6412	89.17	5967	82.98	
	IgL	688	3810	47.98	6780	85.39	
	Total	1497	26147	69.01	32874	86.77	44133

As shown in Table 7, the NGS resulted in more than 40,000 sequences with 86.77% in-frame productive sequences. To analyse this large set of data, sequences sharing specific features like equal CDR3 amino acid sequences and similar V(D)J-regions were assigned to specific IMGT clonotypes. For 70% of all sequences, an assignment to an IMGT clonotype was made. Since the IMGT algorithm partly assigned unproductive or out-of-frame sequences to a distinct clonotype, the amount of sequences assigned to the clonotypes was larger than the number of productive sequences for the IgK-locus.

At both points in time, more clonotypes were present at the light chain loci than the heavy chain locus. The amount of clonotypes at the IgH- and IgK-loci was very stable over time, but differed strongly for the IgL-locus.

## Results

The small diversity of IgH-clonotypes demonstrated the restricted usage of few distinct Ig heavy chain sequences.

**Table 8: Exclusive and common CDR3 clonotypes (AA) in the two MCL27 samples.**

Locus	Present in	Nb of IMGT CDR3-clonotypes (AA)	Nb of sequences assigned to IMGT clonotypes (AA)
IgH	2008	16	62
	2012	24	105
	both	1	8006
IgK	2008	137	168
	2012	182	233
	both	73	12380
IgL	2008	215	1087
	2012	669	3700
	both	8	406

Next, all V-region sequences with the same HCDR3 amino acid sequence were merged into CDR3-clonotypes. Table 8 summarises the amount of these clonotypes that were either exclusive or common at both points in time. For the IgH-locus, only a single clonotype is present in both samples but accounts for nearly 98% of all assigned sequences. Despite a higher diversity of  $\kappa$ -light chain clonotypes, about 96% of all sequences at the IgK-locus were present in both samples and a single clonotype accounted for 11,233 out of the 12,380 (~91%) acquired sequences. In contrast, the majority of  $\lambda$ -light chain sequences were exclusive at a specific time and less than 10% of the  $\lambda$ -repertoire remained similar over time.

The very low diversity between these samples showed a genetically stable expression of the MCL-Ig in this patient. It also demonstrated that the heavy chain had a smaller genetic variance than the light chain.

Additionally, the NGS confirmed the results acquired by sanger sequencing as described above (Table 4). With both techniques the same dominant sequences were found, showing the reliability of this method.

#### **4.1.4 Prediction of N-glycosylation in MCL-Igs**

In FL, the BCR Igs are highly glycosylated, which plays a role during tumour development of this NHL entity (1.3.2). Therefore, the NetNglyc software <sup>196</sup> was used to predict the existence of novel or lost N-glycosylation sites in the MCL-Ig sequences. As shown in Table 9, none of the MCL-Igs acquired a different glycosylation pattern compared to their respective germline sequence. Since some germline sequences already harboured motifs for N-glycosylation, up to seven samples might be glycosylated.

**Table 9: Summary of acquired and germline coded glycosylation sites in MCL-derived Igs.**

<b>Sample</b>	<b>V-Gen-family</b>	<b>Predicted glycosylation site</b>	<b>Glycosylation site in germline</b>	<b>V-Gen-family</b>	<b>Predicted glycosylation site</b>	<b>Glycosylation site in germline</b>
MCL4	IGHV1-8	+	+	IGKV4-1	-	-
MCL21	IGHV1-8	+	+	IGKV1-9	-	-
MCL32	IGHV1-18	-	-	IGKV3-15	-	-
MCL23	IGHV3-9	-	-	IGKV3-20	-	-
MCL1	IGHV3-21	-	-	IGLV3-19	-	-
MCL8	IGHV3-21	-	-	IGLV3-19	-	-
MCL11	IGHV3-21	-	-	IGLV3-19	-	-
MCL20	IGHV3-21	-	-	IGLV3-19	-	-
MCL28	IGHV3-21	-	-	IGLV3-19	-	-
MCL2	IGHV3-23	-	-	IGKV4-1	-	-
MCL22	IGHV3-30	-	-	IGKV1-5	-	-
MCL13	IGHV3-38	-	-			
MCL5	IGHV3-49	-	-	IGKV1-27	-	-
MCL31	IGHV3-74	-	-	IGKV4-1	-	-
MCL16	IGHV4-34	+	+	IGLV1-47	-	-
MCL19	IGHV4-34	+	+	IGLV3-19	-	-
MCL24	IGHV4-34	+	+	IGLV1-40	-	-
MCL25	IGHV4-34	+	+	IGLV1-40	-	-
MCL29	IGHV4-34	+	+			
MCL14	IGHV4-39	-	-	IGLV7-43	-	-
MCL30	IGHV4-39	-	-	IGLV1-40	-	-
MCL27	IGHV4-59	-	-	IGKV1-39	-	-
MCL12	IGHV5-51	-	-	IGLV2-14	-	-
MCL18	IGHV5-51	-	-	IGKV2-28	-	-

## 4.2 Characterisation of mantle cell lymphoma-derived Igs

For this study, the MCL material was mostly isolated RNA from tumour samples. However, to analyse the binding abilities and affinities of the tumour Igs, a large amount of purified tumour Ig was required. For that reason, the variable regions of different tumour Igs were cloned into an IgG or Fab expression vector (3.1.13) to produce soluble IgGs or Fabs which had the same antigen binding properties as the original BCR of the primary MCL B cells without the need of having extensive amount of it.

### 4.2.1 Production of recombinant antibodies with two expression systems

In total 11 MCL and 7 FL full length IgGs were produced, using either HEK293T- (FL) or Sf9-insect cells (MCL). Due to the constantly weak expression of FL antibodies, the Bac-to-Bac expression system (3.4.5) was used for the production of MCL antibodies. The amount of antibodies produced and recovered in HEK293T and Sf9 cells, is shown in Table 10.

*Table 10: The total obtained amount of recombinant antibodies after production in HEK293T or Sf9 cells.*

HEK293T production		Sf9 production	
Sample	Yield in $\mu\text{g}$	Sample	Yield in $\mu\text{g}$
FL4	214*	MCL2	2142
FL6	65*	MCL4	587
FL8	456*	MCL5	1455
FL10	2199	MCL11	4903
FL11	592*	MCL12	3116
FL101	980	MCL18	6988
MCL2	926	MCL19	2286
		MCL22	6339
		MCL23	8289
		MCL24	3952
		MCL27	965
Average yield	776	Average yield	~ 3729

*Note: For each production 300 ml media was used. \*average yield of two independent productions*

The average yield of the Ig productions using the baculovirus expression system was greatly increased and the reliability of different productions was improved. MCL2 was produced in Sf9 and

HEK293T cells, thus allowing a direct comparison. In fact, the yield doubled by using the baculovirus expression system. However, individual differences between distinct productions remained. Nevertheless, the overall higher yield and concentration achieved with the Bac-to-Bac expression system qualified it as the standard expression system for all MCL-derived Ig productions. It opened up the opportunity for a greater variety of downstream experiments without the need of repeated time and cost intensive productions.

Due to the absence of glycosylation sites in most of the MCL-BCRs (4.1.4), the varying glycosylation abilities of insect cells compared to human cell lines were probably not an issue but must be taken into account for up to four antibodies (MCL4, MCL19, MCL24, MCL27).

### **4.2.2 Epitope identification with random peptide phage display**

Phage Display library screenings were used to determine specific epitopes of the produced antibodies and therefore the lymphoma BCRs. The selections were performed with four different libraries ( $X_{12^-}$ ,  $X_{18^-}$  and  $\beta$ -sheet-Fuse55-libraries<sup>194</sup> as well as the Ph.D.<sup>TM</sup>-12 Phage Display Library Kit(NEB)). All libraries shared a random peptide insert, which was attached to the pIII protein of a M13 phage. Multiple selection rounds were needed to enrich specific epitope mimics and with the beginning of the second round, all selections were performed with a double pre-incubation step against polyclonal human-IgG (Intratect®) to deplete unspecifically binding phages (3.2.13). In addition, the preselected phages were split and incubated either with the polyclonal human-IgG or the target antibody. The ratio between the colonies acquired by the incubation with the target antibody and the polyclonal human IgG was defined as the enrichment. All selections were repeated for 4 rounds if at least a five-fold enrichment was observed at round 3 or earlier. If no enrichment was seen, the selection was restarted at round one. Two selections without enrichment were regarded as negative.

As shown in Table 11, only few phages could be enriched in the majority of cases and no enrichment was seen using the  $\beta$ -sheet- or  $X_{18^-}$ -Fuse libraries. Furthermore, the observed enrichments were weak for the MCL4 and MCL22 antibodies. Only one selection with MCL18 achieved a very strong enrichment using the Ph. D.<sup>TM</sup>-12 library.

After a successful phage enrichment, randomly chosen phage clones were amplified and tested for a specific binding to the antibody used for selection but not to polyclonal IgG. The peptide sequences of the specific binders were identified (3.2.13.6) and screened for motifs present in multiple enriched peptides. The acquired sequences are shown in Table 11 and shared sequence motifs are marked with different colours.

Table 11 Selected phages with potential motifs after 4 selection rounds.

Sample	Enrichment	Library	Selected Phage peptide sequence	Times sequenced
MCL2	-	-	n.e.	
MCL4	12.5x	X <sub>12</sub> -Fuse5	NCMMVKPTLIVC	6x
MCL5	-	-	n.e.	
MCL11	-	-	n.e.	
MCL12	-	-	n.e.	
MCL18	1100x	Ph.D. <sup>TM</sup> -12 (NEB)	WKGQYVSNIPLL YSGDPKWRWLPQ YDLKWEYVVKPP DNKWQHVINYSL	1x 1x 2x 1x
MCL19	-	-	n.e.	
MCL22	17x	X <sub>12</sub> -Fuse5	SLFYTACNPKVC CNHKCAELVTSA	5x 4x
MCL23	-	-	n.e.	
MCL24	-	-	n.e.	
MCL27	-	-	n.e.	

Note: Marked amino acids belonged to a motif found in at least two phage peptides, n.e. = no enrichment.

Selections with low enrichment yielded only a few enriched peptides. During the MCL4 selection, just a single peptide was enriched that bound specifically to the MCL4-antibody. In case of the MCL22 selection, two phage peptides were enriched, which shared a motif with “CNxK” as consensus sequence.

The most varying peptide sequences were enriched using the MCL18-antibody for selection. Four different specifically binding peptides were acquired. The comparison of these peptide sequences resulted in “DxKWQYVxNxPL” as a potential consensus sequence.

All enriched peptide sequences as well as the motifs were aligned with known proteins of human and bacterial origin using BLAST (2.9) but no definite proteins were found.

### 4.2.3 Affinity and cross-reactivity of selected epitope mimics

Only a few MCL-derived antibodies showed an enrichment during phage display selections (4.2.2). To estimate the affinity of the respective immunoglobulins to the selected phages, an ELISA for each sample was performed. Therefore, enriched phages were diluted in the range of  $1 \times 10^6$  to  $1 \times 10^{10}$  phages per ml and incubated with the coated immunoglobulins (Figure 11, 3.2.9).

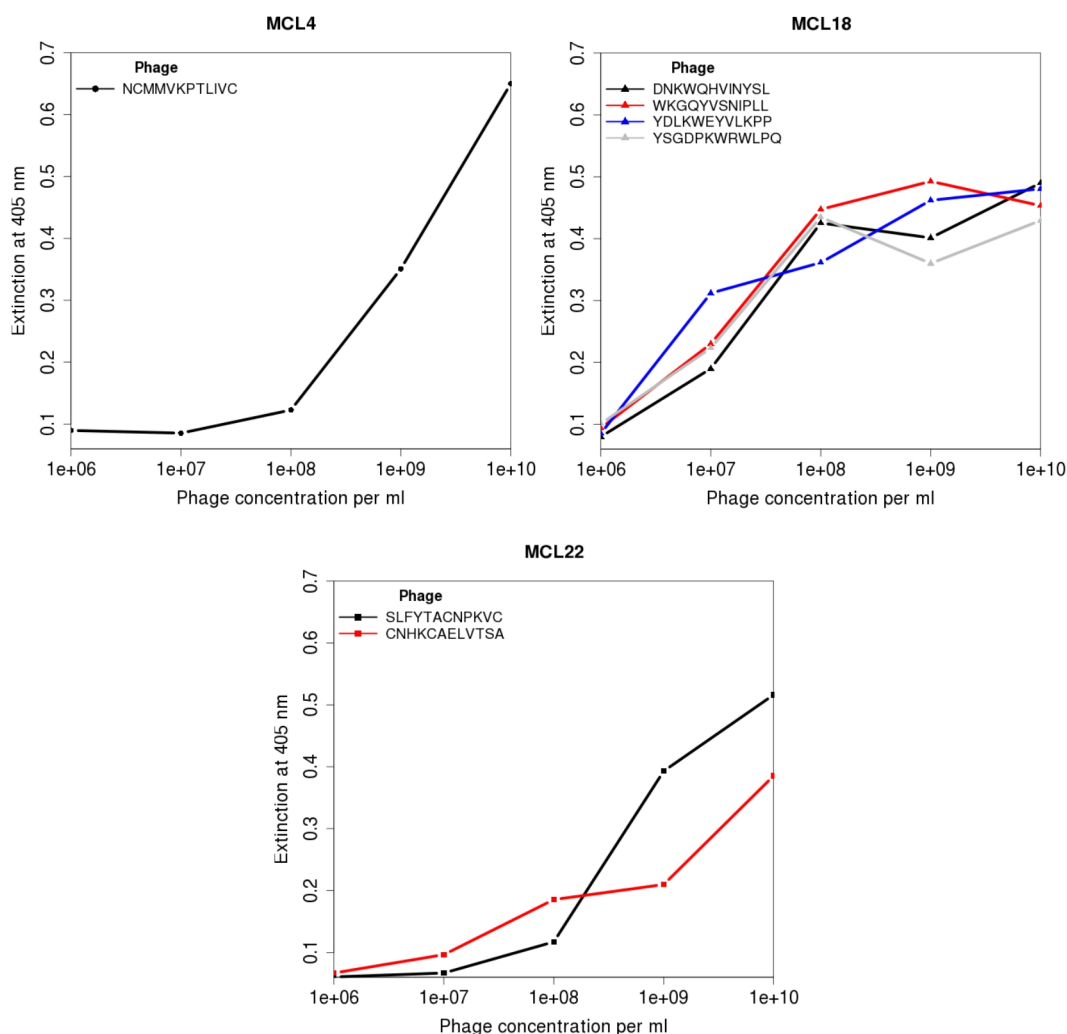


**Figure 11: Anti-phage-ELISA with enriched phages at multiple dilutions.** The three immunoglobulins, which successfully enriched phages during phage display, were coated and incubated with multiple dilutions of the respective monoclonal phages. Bound phages were detected using an HRP-labelled anti-M13-antibody and an ABTS containing citrate buffer as substrate. The extinction at 405 nm was measured as readout.  $n=3$

Phages acquired by selection with MCL4 (Figure 11, A) were bound only weakly by the MCL4-Ig. The signal intensity was low at high phage dilutions (less than  $1 \times 10^8$  phages per ml) and increased from  $1 \times 10^8$  phages per ml onwards. Also, phages captured by the selection with MCL22 showed weak signals at phage concentrations less than  $1 \times 10^8$  phages per ml. The extinction increased more



linear for the “CNHKCAELVTSA”-carrying phage, but showed a very steep increase for the “SLFYTACNPKVC”-carrying phage. The weak signal intensity at low phage concentrations as well as the absence of a clear saturation even at very high phage concentrations indicated a low affinity of the immunoglobulins to their respective enriched phages.

In contrast, the MCL18-derived Ig displayed a very high affinity to all four phages which were enriched by random peptide phage library screening. The ELISA revealed a strong extinction even at low phage concentrations of  $1 \times 10^7$  phages per ml. Furthermore, the extinction increased for all tested phages almost similarly and reached a plateau between  $1 \times 10^8$  and  $1 \times 10^9$  phages per ml. This observation might indicate a saturation of the coated immunoglobulin and a high affinity against all enriched phages. It is important to note, that the measured extinction between different ELISAs is not comparable. That means, a higher extinction value, as observed in the MCL4 ELISA, not necessarily represents more bound phages.

The differences of the binding affinities seen with the anti-phage ELISA were also represented by the achieved enrichments after four selection rounds (Table 11). While MCL4 and MCL22 showed only minimal enrichments and weak affinities, a very strong enrichment and a high affinity was observed with MCL18 during phage display and ELISA, respectively.

Next, all selected phages were checked for cross-reactivity against other MCL-derived IgGs, because some of the antibodies might share similar epitopes. (3.2.9). Each monoclonal antibody was incubated with either  $2 \times 10^9$  phages per ml for the weak binding phages or  $2 \times 10^8$  phages per ml for the phages derived from the selection with MCL18 IgGs.

As shown in Figure 12, only very little cross-reactivity was observed. Phages, enriched via selection with MCL18-derived IgG, bound exclusively to the MCL18-Ig.

Phages acquired by selection against either MCL4- or MCL22-Igs were also mostly specific to their respective Ig. However, especially the MCL11-Ig, but to a lesser extend also the MCL19- and MCL27-Igs, showed elevated signals with the “NCMMVKPTLIVC” peptide-carrying phage (selected against MCL4, (Figure 12A). Furthermore, the MCL4- and MCL11-derived Igs showed increased extinctions when incubated with “SLFYTACNPKVC” peptide phages (Figure 12C).

All phages were enriched on mutated Igs with a germline identity between 98 and 99%. The unspecifically binding MCL11, however, was completely unmutated (Table 4).

In conclusion, by random peptide phage library screenings on MCL-derived Igs only a few selections showed enrichment. A strong enrichment was only seen with the MCL18-Ig and only this Ig showed high affinities to the selected phages. In addition, despite MCL4- and MCL11-Igs none of the MCL-derived Igs showed notable cross-reactivity with any of the selected phages.

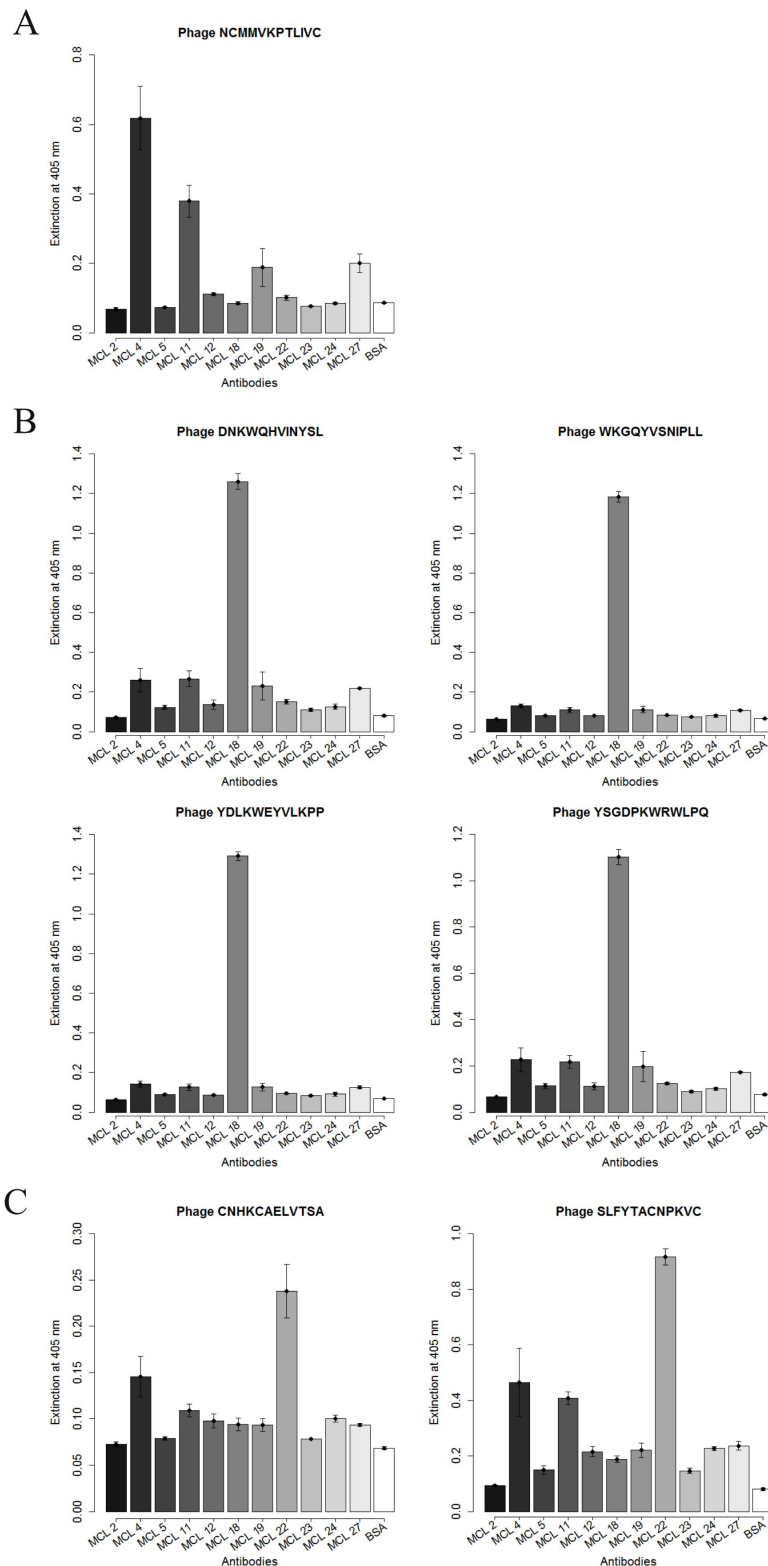


**Figure 12: Cross-reactivity ELISA of enriched phages.** Either  $2 \times 10^8$  (B) or  $2 \times 10^9$  (A and C) phages per ml, acquired during phage panning with MCL4, MCL18 and MCL22, were incubated with coated recombinant MCL-Igs to evaluate potential cross-reactivity and epitope sharing. A: Phage selected with the MCL4-Ig. B: Phages enriched during panning with the MCL18-Ig. C: Phages enriched in the selection with MCL22-Ig. Note that all phages strongly bound to the Igs which were used for initial selection. An HRP-labelled anti-M13-antibody and an ABTS containing citrate buffer was used for detection. The extinction at 405 nm was measured as readout.  $n=4$

#### 4.2.4 Dynamic light scattering measurement of MCL-Igs

The poor enrichments during phage display selections raised the question whether the antibodies recognise a specific motif within the immunoglobulin itself. Such a phenomenon has already been described for some CLL samples (1.3.2) and would lead to an occupied antigen binding site. As a result, no phages could be bound by these Igs. Self-reactive antibodies would form large aggregates, since each Ig would be able to bind two further immunoglobulins.

Dynamic light scattering (DLS, 3.2.12) was used to determine the hydrodynamic radii of the proteins in purified antibody solutions. The concentration of all Igs was adjusted to 1 mg/ml and a co-incubation of the MCL11- or MCL19-Ig with an anti-human-IgG antibody served as positive control for aggregation.

Figure 13 summarises the acquired results as a heatmap. All solutions had a homogeneous constitution and the hydrodynamic radii of the proteins, calculated by the Spectro software, were mostly in a range between 5-10 nm. Using this software, it was further possible to calculate the molecular weight of a hypothetical spherical molecule with the given hydrodynamic radius. A protein with a hydrodynamic radius of about 5.3 nm would have a molecular weight of about 150 kDa in this setting. An IgG molecule, however, is a more Y-shaped molecule (1.2.2.1) and the size was therefore mostly overestimated. Studies measured a hydrodynamic radius of 11 nm for IgG molecules but this value depends on temperature, protein concentration and buffer composition<sup>197,198</sup>. Although the radii differed slightly between the samples, only MCL11 showed a notable variance of the hydrodynamic radius with little more than 11 nm in average.

Finally, two antibodies (MCL11 and MCL19) were mixed with a stoichiometric equal amount of anti-IgG antibody to estimate the size of oligomeric Igs. The hydrodynamic radii of these mixtures strongly increased and were more than three times larger than the monomeric Ig solutions alone. Moreover, the estimated particle size of the cross-linked Igs is much larger than the hydrodynamic radius seen with the pure MCL11-Ig solution.

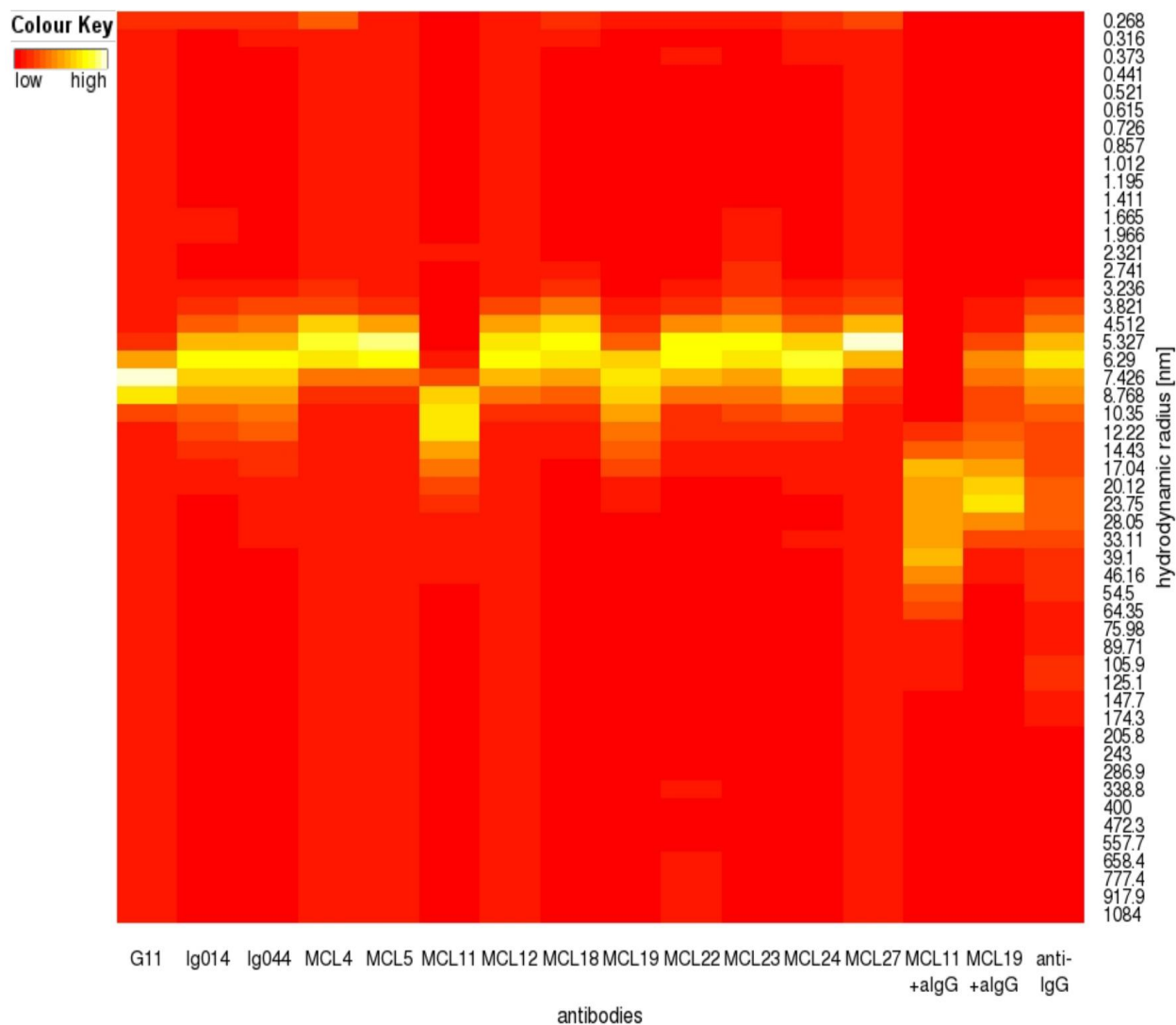


**Figure 13: Heatmap of calculated hydrodynamic radii of MCL-derived Igs in solution determined by dynamic light scattering measurements.** The hydrodynamic radii were calculated by the spectro software, applying the Stokes-Einstein equation. All monoclonal antibody solutions showed hydrodynamic radii between 5 and 12 nm. The concentration of the all Igs was 1 mg/ml. As positive control, 1 mg/ml recombinant MCL-derived IgGs were mixed with 1 mg/ml anti-human-IgG antibody solution. These co-incubations led to a strong increase of the calculated hydrodynamic radii. The dynamic intensity shifts of the scattered light were detected with a spectroSize 300 instrument. The G11 Ig was a FL-derived IgG. Ig014 and Ig044 were CLL-derived.

#### 4.2.5 HEp-2 cell immunofluorescence assays

The HEp-2 cell line is a human cervix carcinoma cell line which is probably derived from the HeLa cell line. It features a large nucleus and it is often used for the detection of anti-nuclear antibodies<sup>199,200</sup>. It was shown that multiple CLL-derived Igs bind distinctive patterns within HEp-2 cells<sup>109</sup>. Therefore, HEp-2 cells were fixed and used for an immunofluorescence assay with the recombinant MCL-derived antibodies to check if these Igs showed similar properties (3.4.6). Since different fixation methods might expose different antigens and therefore influence the staining patterns, the cells were fixed either with 3.7% para-formaldehyde followed by permeabilisation with Triton X-100, or with methanol (3.4.6).

Only 3 out of 11 recombinant MCL antibodies successfully stained methanol-fixed HEp-2 cells (Figure 14). Moreover, the intensity and staining patterns differed between these Igs. Using a MCL2-derived Ig as primary antibody revealed a very strong FITC-signal and a filament like pattern. In contrast, MCL12- and MCL22-derived Igs as primary antibodies resulted in less intense signals and a more diffuse cytoplasmatic staining pattern.

Furthermore, the incubation with MCL2- and MCL12-derived antibodies resulted in large and very bright spots in all experiments. A reduction of the antibody concentrations did not result in a significant reduction of these artificial background spots.

Using PFA instead of methanol as a fixation agent revealed slightly different staining patterns (Figure 15). MCL2-derived Ig still showed a strong signal but the filamentous staining was less intense and more diffuse with a shift towards a more cytoplasmatic appearance. A staining with MCL22-derived Ig resulted in high fluorescence intensity with a very similar specificity compared to the methanol fixations. Moreover, the MCL22-Ig also stained the nuclei of some PFA-fixed cells. However, it remained unclear whether this antibody bound an antigen inside the nucleus, at the nuclear membrane or whether the signal was artificial.

In addition, the MCL11 Ig reacted only with PFA-fixed cells. That might indicate, that the antibody bound an antigen which was only accessible when PFA was used as a fixation agent. In contrast, the MCL12 signal is much weaker on PFA-fixed compared to methanol-fixed cells.

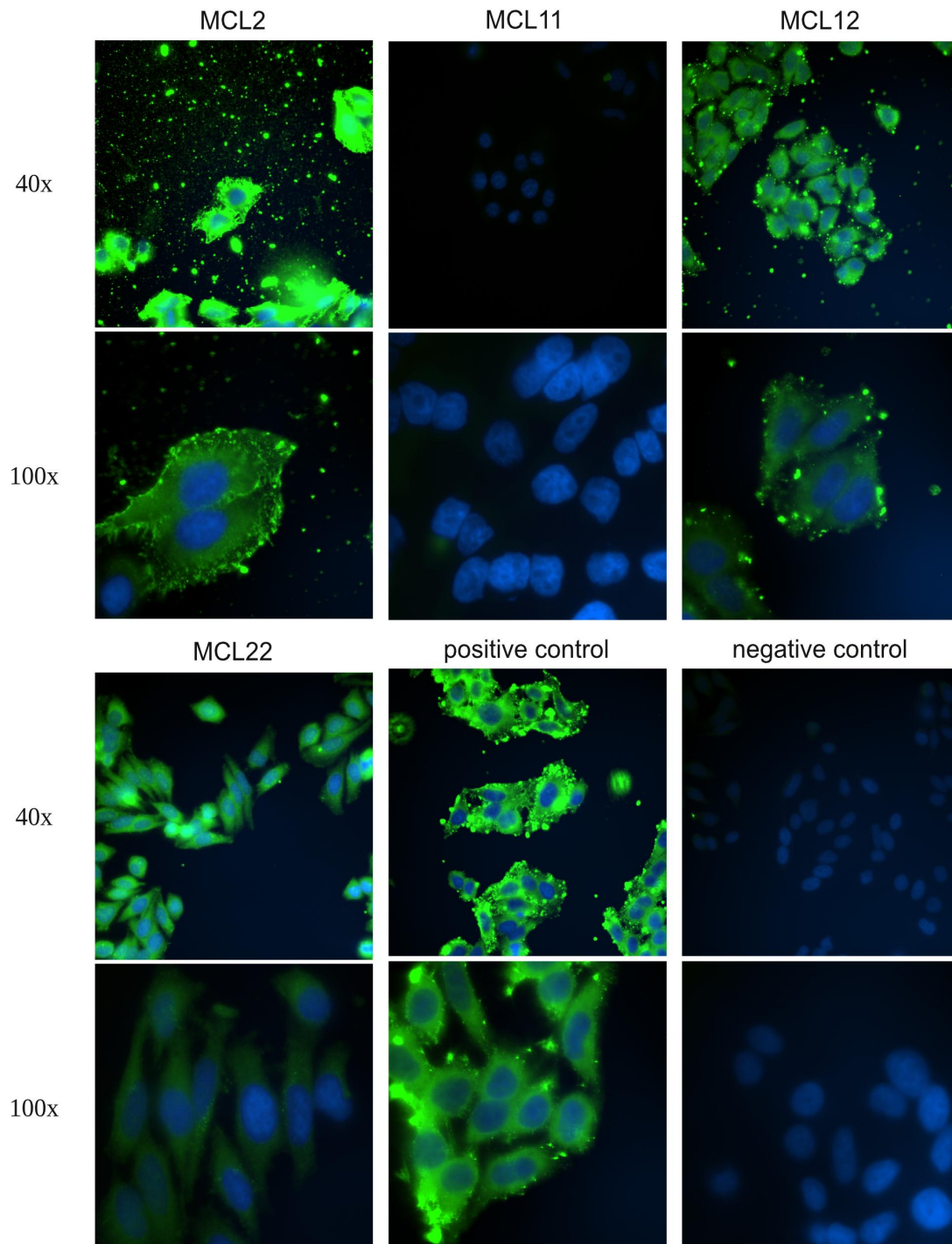


**Figure 14: Immunofluorescence assay of recombinant MCL-Ig antibodies with methanol-fixed HEp-2 cells.** Fixed HEp-2 cells were incubated with 50  $\mu\text{g/ml}$  of MCL-derived antibodies overnight. A FITC-labelled anti-human IgG antibody was used for detection of bound Igs and the nucleus was co-stained with DAPI (blue). The figure shows the Igs which reacted with HEp-2 cells at two different magnifications. Additionally, the staining with MCL11-Ig is shown, since it stained PFA-fixed HEp-2 cells (Figure 15). The exposure time was similar in all experiments (40x: 50 ms; 100x: 100 ms). While incubation with the MCL2-Ig resulted in a strong signal and a filament-like pattern, MCL12- and MCL22-Igs showed a more diffuse cytoplasmic staining. All assays with MCL2- and MCL12-Igs showed strong background signals with multiple very bright but artificial spots. The vimentin-specific CLL-derived Ig044 antibody served as positive control. The anti-CD20 antibody Rituximab was used as negative control and showed no signal.

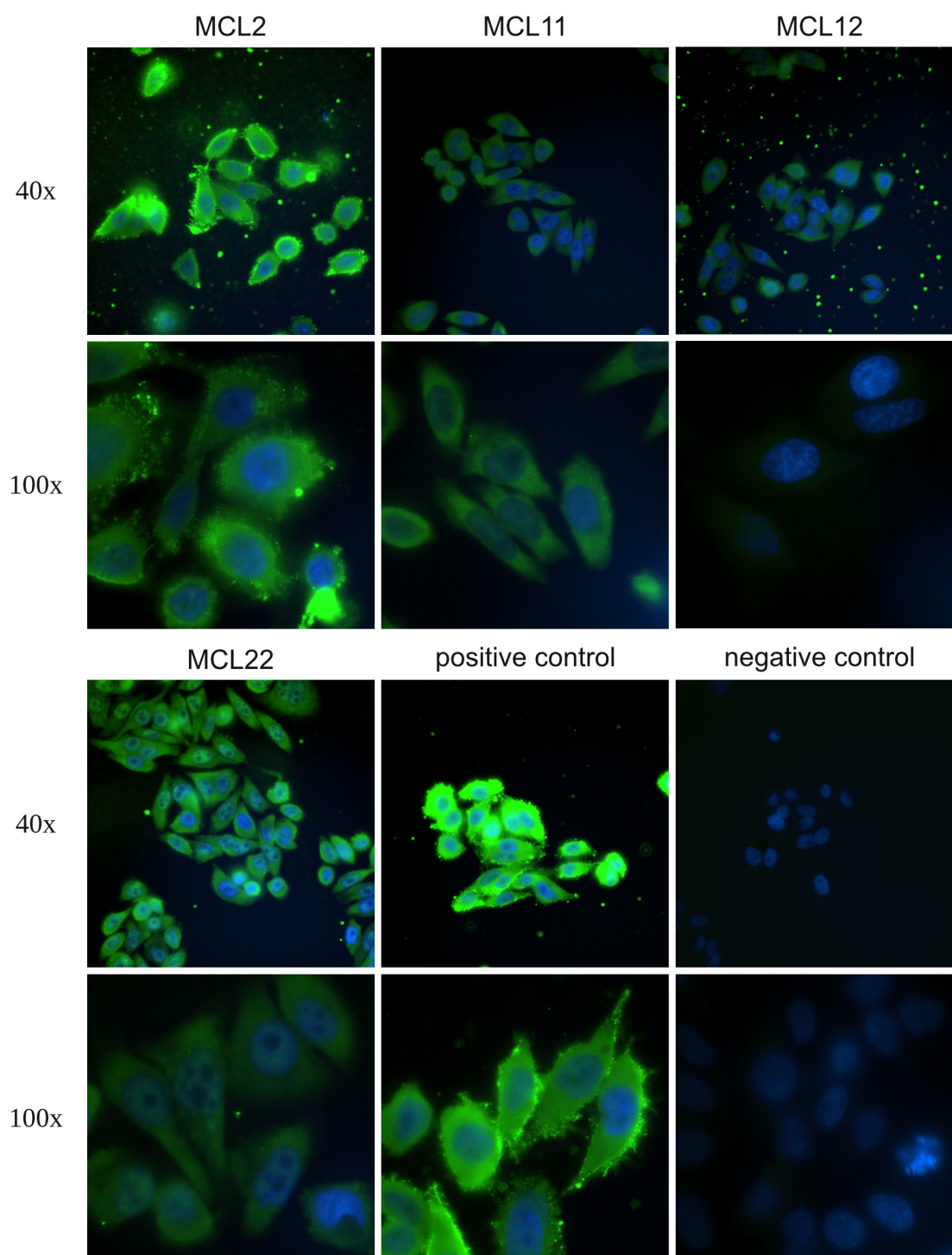


**Figure 15: Immunofluorescence assay of MCL-derived Igs with PFA-fixed HEp-2 cells.** HEp-2 cells were fixed with 3.7% PFA and permeabilised using 0.5% Triton-X100. Afterwards, the cells were incubated with 50  $\mu\text{g/ml}$  recombinant MCL-derived Igs overnight. The bound antibodies were detected with a FITC-labelled anti-human IgG antibody and DAPI was used to stain the nucleus. Only Igs which reacted with the cells are shown. The exposure time was kept similar for all samples to allow better comparison (40x: 50 ms; 100x: 100 ms). Incubation with the MCL2-Ig resulted in a slightly weaker filamentous pattern compared to methanol-fixed cells. In contrast, the MCL11-Ig showed a signal which was not seen in methanol-fixed cells. As already seen with PFA-fixed cells, staining with MCL2- or MCL12-Igs produced bright artificial spots on the coverslips. The vimentin-specific CLL-derived Ig044 antibody served as positive control. The anti-CD20 antibody Rituximab was used as negative control and showed no signal.

#### 4.2.6 Western Blot with HEp-2 cell lysates

The immunofluorescence assays revealed possible autoantigens presented by HEp-2 cells. Thus, protein lysates of these cells were generated and used for Western Blots (3.2.3 and 3.2.7). All recombinant Igs were used, independently of the immunofluorescence assay results. Since every antibody may have different binding affinities, different concentrations were used to check whether the Ig bind in the Western Blot. All recombinant Igs showed a very unspecific binding pattern as demonstrated with the MCL19 and MCL24 blot (Figure 16C).

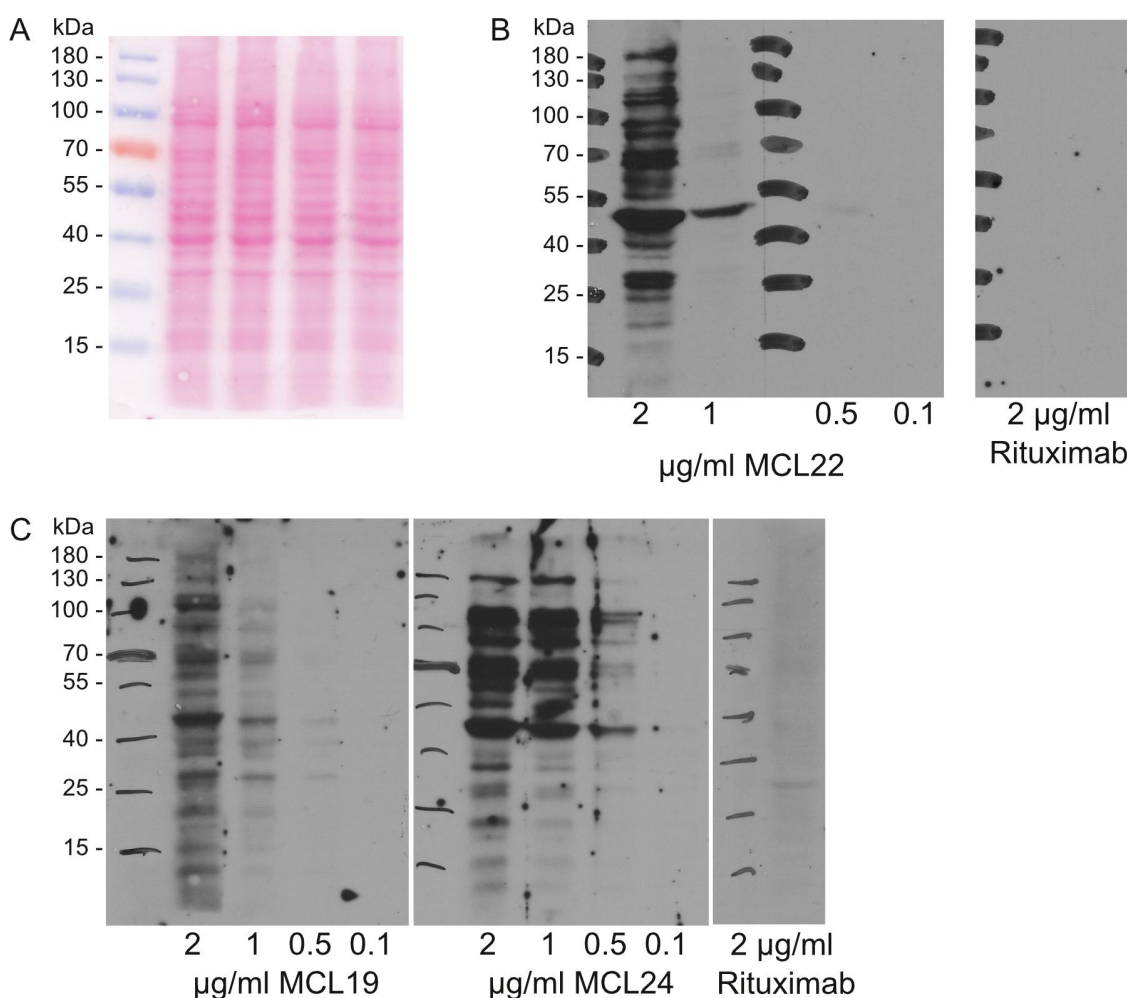


**Figure 16: Western Blots with different concentrations of MCL-derived Igs on HEp-2 cell lysates.** Per lane, 10 µg HEp-2 RIPA lysate was separated by SDS-PAGE on a 10% gel and blotted onto a PVDF-membrane. A: Ponceau S staining of the PVDF membrane used for the incubation with MCL19 Ig (C) before blocking with 5% (m/v) skim-milk. B and C: Different concentrations of the depicted MCL-derived Igs were incubated at 4 °C overnight. All MCL-derived Igs bound completely unspecifically at high concentrations. Only the MCL22-Ig showed a specific band below 55 kDa at a concentration of 1 µg/ml. An HRP-labelled anti-human-Fab antibody (1:5,000; AbD Serotec) was used as secondary antibody. The anti-CD20 antibody Rituximab served as negative control. Marker: PageRuler™ Prestained Protein Ladder (Thermo Fisher Scientific)



Although distinct bands were visible, none of them seemed to be specific and all of them disappeared with decreasing Ig concentrations. Only the MCL22-Ig showed a slightly different behaviour. It also showed an unspecific binding pattern at high concentrations. However, at 1  $\mu\text{g/ml}$  most of the unspecific bands disappeared and only one band below 55 kDa remained (Figure 16B). This band was also the most prominent one at higher antibody concentrations, although also multiple other bands were visible. Moreover, as seen in Figure 16A, the bound protein was not the most abundant one in the lysate. Nevertheless, the signal was lost at concentrations below 0.5  $\mu\text{g/ml}$ . MCL 19 and MCL24 also bound to this protein but the signal constantly decreased with the surrounding bands.

#### 4.2.7 Immunoprecipitation using MCL-derived Igs

Immunoprecipitations (IPs) were performed with different protein lysates, derived from cell lines, human bone marrow, or murine lymph nodes (3.2.10). All MCL-derived Igs were bound to protein A-dynabeads® and incubated with up to 500  $\mu\text{g}$  of lysates at 4 °C overnight.

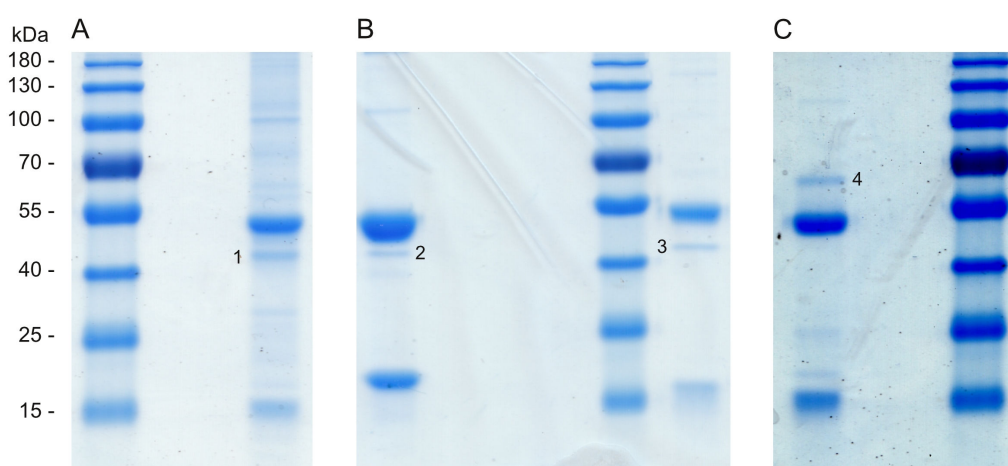


**Figure 17: Precipitated proteins after an immunoprecipitation with MCL-Igs on RIPA protein lysates.** A) IP with MCL22-Ig on HEp-2 cell lysate. B) IP of MCL22- (left lane) and MCL12-Igs (right lane) on SK-BR3 cell lysate C) IP with MCL12-Ig on murine lymph node lysate. Cells or tissues were lysed with RIPA buffer. Four  $\mu\text{g}$  of the respective Igs were loaded to 50  $\mu\text{l}$  Protein A-Dynabeads® and incubated with 500  $\mu\text{g}$  protein lysates overnight. The precipitated proteins were separated on 10% SDS-polyacrylamide gels and stained with colloidal coomassie. The numbered bands were extracted from the gel and analysed by mass spectrometry. Marker: PageRuler™ Prestained Protein Ladder (Thermo Fisher Scientific)

The IPs showed strong bands at ~50 and 25 kDa. These bands represented the heavy (~50 kDa) and light (~25 kDa) chains of the immunoglobulin.

Besides this, only MCL12- and MCL22-derived Igs precipitated further proteins.

Although some of the MCL-derived Igs showed strong signals in the immunofluorescence assay (Figure 14 and Figure 15) and highly unspecific binding patterns in the Western Blot (Figure 16),

only the MCL22-Ig precipitated a protein in HEp-2 cell lysate (Figure 17A, 1). Since the MCL22 precipitated a band at a similar height as seen in the Western Blot (4.2.6), the band was extracted for mass spectrometric analysis (3.2.11) and identified as  $\beta$ -actin (4.2.8). Because  $\beta$ -actin is expressed by multiple different cell lines, another IP using protein lysate of the SK-BR3 adenocarcinoma cell line was performed. It confirmed the precipitation of the specific band above 40 kDa with the MCL22-derived Ig. With SK-BR3 lysate, also the MCL12-Ig precipitated a protein at a similar height (Figure 17B, 2 and 3). These protein bands were extracted and analysed by mass spectrometry, as well (4.2.8).

In addition, the MCL12-Ig precipitated a further protein from murine lymph node lysate (Figure 17C, 4) with a molecular weight between 55 and 70 kDa, which was also identified by mass spectrometry (4.2.8).

#### 4.2.8 Mass spectrometry analysis of precipitated proteins

The identification of the precipitated proteins (4.2.7) was accomplished by mass spectrometry (MS). Processing of the protein bands cut out from electrophoresis gels, the MS analysis, as well as the peptide alignments were performed at the Core Facility Mass Spectrometric Proteomics of the University Medical Centre Hamburg-Eppendorf.

Multiple proteins were matched with the obtained peptides. The analysis of the bands extracted after the IPs with MCL22- and MCL12-Igs on HEp-2 and SK-BR3 lysates, revealed  $\beta$ -actin as the most probable precipitated protein. It had the highest score and the most matched peptides (Table 12 and Table 13).

**Table 12: Proteins identified by mass spectrometric analysis of the obtained protein band after IP with an MCL22-Ig on HEp-2 cell lysate (Band 1, Figure 17A).**

Name	Species	Score	Matched peptides	Molecular weight
Actin, cytoplasmic 1	Homo sapiens	443	16	41.7
POTE ankyrin domain family member E	Homo sapiens	133	6	121.3
Beta-actin-like protein 2	Mus musculus	126	8	42

**Table 13: Proteins identified by mass spectrometric analysis of a band obtained with an IP of the MCL12 Ig on SK-BR-3 cell lysate (Band 3, Figure 17B).**

Name	Species	Score	Matched peptides	Molecular weight
Actin, cytoplasmic 1	Homo sapiens	406	29	41.7
Ig gamma-1 chain C region	Homo sapiens	258	8	36.1
POTE ankyrin domain family member E	Homo sapiens	151	11	121.3

The C-terminus of the POTE ankyrin domain family member E belongs to the actin family. Due to this sequence homology, the peptides were also matched by the algorithm. Nevertheless, the molecular weight (~121 kDa) did not fit to the electrophoretic migration pattern of the precipitated protein.

The  $\beta$ -actin-like protein 2 was also present in the MCL22 precipitation but with a lower score. However, like for the POTE ankyrin domain family member E, the match most likely resulted from the sequence similarities with  $\beta$ -actin. In addition, HEP-2 is a human cell line and the matched protein belonged to mice.

Finally, the identified Ig gamma-1 chain C region-protein is a methodological artefact resulting from the antibody used for precipitation.

Therefore, only  $\beta$ -actin remained as a possible newly identified MCL antigen.

The MCL12 Ig also precipitated a specific band from murine lymph node lysate, which was identified as the NADP-dependent malic enzyme (Table 14).

**Table 14: Proteins identified by mass spectrometric analysis after an IP with the MCL12-Ig on lymph node protein lysates of FVB/N mice (Band 4, Figure 17C)**

Name	Species	Score	Matched peptides	Molecular weight
NADP-dependent malic enzyme	Mus musculus	156.61	23	63.9
Keratin, type II cytoskeletal 1	Homo sapiens	77.59	19	66
Keratin, type II cytoskeletal 5	Mus musculus	13.45	3	61.7

Despite great effort to avoid contaminations, human keratin was detected in the analysed sample, a common contaminant in MS. Even though the molecular weight would fit to the precipitated protein it was regarded as artificial.

Since the precipitated NADP-dependent malic enzyme derived from mice, it was checked if the human protein could be precipitated as well. An IP with a human cell line SK-BR3, expressing the

malic enzyme, was performed (4.2.7) but the enzyme could not be precipitated after multiple IPs (Figure 17B).

It remains elusive why the NADP-dependent malic enzyme was specifically bound by the MCL12 Ig in murine lymph node lysates but not in human cell lines.

#### 4.2.9 Vimentin binding capabilities of MCL-Igs

The binding of vimentin was described for multiple CLL-derived Igs (1.3.2). To check if that might also be the case for some MCL-derived Igs, recombinant vimentin was used for Western Blots. The Ig014-Ig, a CLL-derived Ig, was used as a positive control, as it was demonstrated earlier that it binds vimentin <sup>112</sup>.

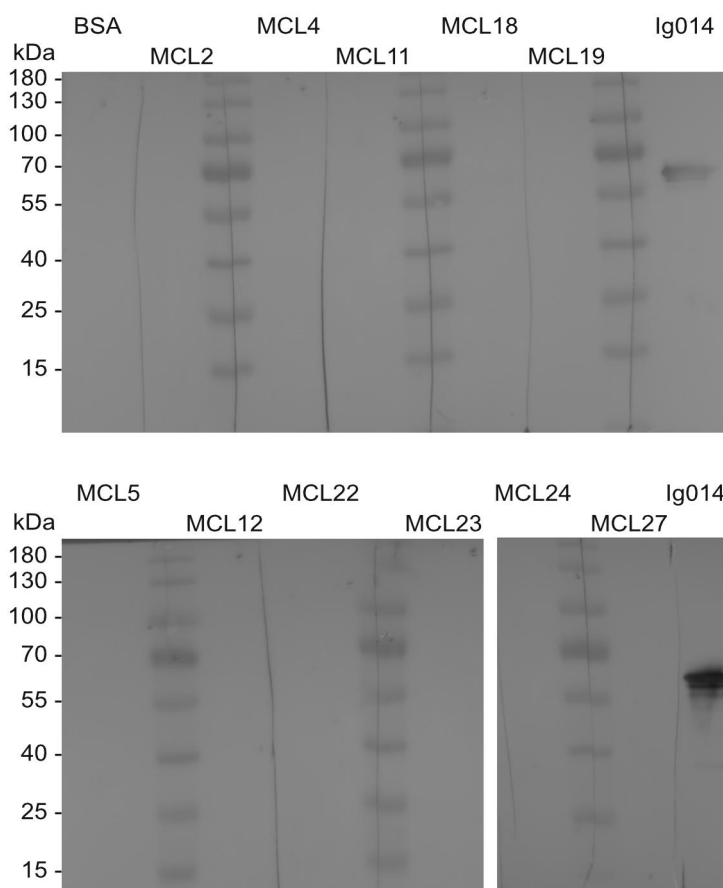


**Figure 18: Anti-vimentin Western Blot with MCL-derived Igs.** Per lane, 1 µg purified vimentin (Sigma-Aldrich) was separated on a 12% SDS-polyacrylamide gel and blotted onto a PVDF-membrane. The membrane was incubated with 1 µg/ml of the indicated immunoglobulins overnight. An HRP-labelled anti-human-Fab antibody (AbD Serotec, 1:5,000) was used to detect bound Igs.

The vimentin-specific binding, CLL-derived Ig014 antibody was used as positive control.

As shown in Figure 18, none of the MCL-derived Igs bound to vimentin. Only the Ig014 antibody displayed a distinct signal for vimentin. This is confirmatory, since most Igs did not stain vimentin-expressing HEp-2-cells during immunofluorescence assays (4.2.5).

### 4.3 SpA as a potential superantigen for MCL BCRs

The outlined experiments showed only limited cross-reactivity between different MCL-Iggs and only a few precipitated a protein. For that reason, superantigens were taken into account as antigens able to interact with a great amount of different BCRs.

#### 4.3.1 The SpA binding motif

The *Staphylococcus aureus* Protein A (SpA) is a superantigen that binds a specific motif in the variable region of immunoglobulin heavy chains (1.4.1). This motif is only present in IGHV3-genes and the light chains are not involved in the interaction. Table 15 summarises the SpA binding motif and the presence of this motif in IGHV3-expressing MCL-, CLL- and FL-samples.

**Table 15: Representation of SpA binding motif in lymphoma Igs expressing IGHV3-genes.**

Sample	SpA-motif	G	S	R/K	K/I/T	Y	K	G	R	T	S	Q	N/G	S
	IGHV-Gene segment	HFR1			HCDR2	HFR3								
		16	18	20	65	67	72	74	75	77	79	90	92	93
MCL23	IGHV3-9	G	S	R	I	Y	K	G	R	T	S	Q	N	S
MCL1	IGHV3-21	G	S	R	I	Y	K	G	R	T	S	Q	N	S
MCL8	IGHV3-21	G	S	R	I	Y	K	G	R	T	S	Q	N	S
MCL11	IGHV3-21	G	S	R	I	Y	K	G	R	T	S	Q	N	S
MCL20	IGHV3-21	G	S	R	I	Y	K	G	R	T	S	Q	N	S
MCL28	IGHV3-21	G	S	R	I	Y	K	G	R	T	S	Q	N	S
MCL2	IGHV3-23	G	S	R	T	Y	K	G	R	T	S	Q	N	S
MCL10	IGHV3-23	G	S	R	T	Y	K	G	R	T	S	Q	N	S
MCL22	IGHV3-30	G	S	R	K	Y	K	G	R	T	S	Q	N	S
MCL13	IGHV3-48	G	S	R	I	Y	K	G	R	T	S	Q	N	S
MCL5	IGHV3-49	G	S	R	T	Y	K	G	R	T	S	Q	N	S
MCL31	IGHV3-74	G	S	R	T	Y	K	G	R	T	S	Q	N	S
FL6	IGHV3-11	G	S	R	T	Y	K	G	R	T	S	Q	N	S
FL10	IGHV3-11	G	S	R	T	Y	<b>E</b>	G	R	<b>F</b>	S	Q	N	<b>N</b>
FL8	IGHV3-11	G	S	R	T	Y	K	G	R	T	S	Q	N	S
FL101	IGHV3-15	G	S	R	T	Y	<b>R</b>	G	R	T	S	<b>H</b>	<b>S</b>	<b>N</b>
FL11	IGHV3-23	G	S	R	T	Y	K	G	R	<b>S</b>	S	<b>H</b>	N	<b>R</b>
FL5	IGHV3-53	G	S	R	T	Y	K	G	R	T	S	Q	N	<b>T</b>
CLL149	IGHV3-7	G	S	R	K	F	K	G	R	<b>S</b>	S	Q	N	S
CLL172	IGHV3-7	G	<b>T</b>	R	K	Y	<b>R</b>	G	R	T	S	Q	N	S
CLL024	IGHV3-9	G	S	R	I	Y	K	G	R	T	S	Q	N	S
CLL83	IGHV3-21	G	S	R	<b>M</b>	Y	K	G	R	T	S	Q	N	S
CLL173	IGHV3-23	G	<b>A</b>	R	T	Y	<b>E</b>	G	R	T	S	Q	N	S
CLL003	IGHV3-30	G	S	R	K	Y	K	G	R	T	S	Q	N	S
CLL145	IGHV3-30	G	S	R	K	Y	K	G	R	T	S	Q	N	S

Note: A black background highlights deviations from the SpA binding motif.

All MCL samples, expressing an IGHV3-gene, showed no deviations from this motif. In contrast, four out of six follicular lymphoma (FL) and four out of seven chronic lymphocytic leukaemia (CLL) Igs contained at least one mutation in the motif. While CLL derived Igs had only one or two mutations, FL Igs showed up to four amino acid exchanges at these specific positions.

### 4.3.2 Binding of SpA by NHL-derived Fab fragments

Next, an anti-SpA ELISA was performed (3.2.9) to check if the presence of the SpA motif in the lymphoma Igs also leads to a detectable Ig binding. Due to the high affinity of SpA to the IgG constant region, it became necessary to produce Fab fragments of the lymphoma Igs (3.4.5). In total, six MCL-, one FL- and two CLL-derived Fabs were selectively chosen on the basis of presence or absence of the SpA motif and produced. For the detection of bound Fabs, a goat-anti-Fab antibody was used. SpA has only a very weak affinity to goat antibodies, which limited the background intensity of the secondary antibody.

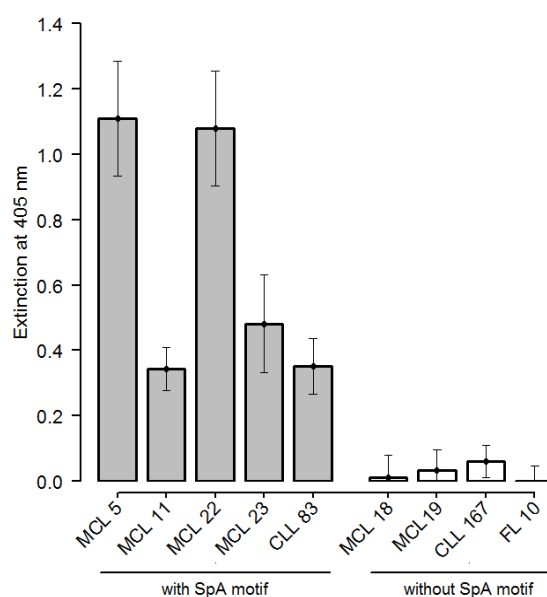


**Figure 19: Anti-SpA ELISA with Fab fragments.** Recombinantly expressed, lymphoma-derived Fab fragments were incubated with coated SpA and detected with a HRP-labelled goat-anti-human-Fab antibody. The extinction at 405 nm was measured and the background signal (acquired by incubation with the secondary antibody only) was subtracted. Only Fabs with the motif bound to SpA, whereas motif-negative Fabs showed no signal. Of Note, the CLL83-Ig had a single mutation in the SpA motif and was regarded as motif positive, whereas FL10 with three mutations was regarded as motif negative.  $n=5$

All MCL-derived Fab fragments harbouring the motif bound to the immobilised SpA. The Fabs without the motif did not show a signal (Figure 19). The CLL83 Fab had only a single amino acid exchange within the motif (as shown in Table 15) but still bound to SpA, whereas FL10 had several mutations, completely lacked the ability to bind SpA, and was therefore regarded as motif-negative.

The MCL5 and MCL22 Fabs showed a much stronger signal than the other motif-positive Fabs for an unknown reason.

## 4.4 Generation of a model system for the analysis of BCR activation

To facilitate a downstream signalling, two BCR molecules must cross-link to enable intracellular phosphorylation and B cell proliferation (1.2.5). These cross-linking capabilities cannot be easily examined using soluble Igs or Fab fragments.

Due to the lack of primary cells from mantle cell lymphoma patients, it was necessary to establish a method as a surrogate for primary B cells. Two vectors were designed carrying a heavy or light chain constant region and the respective variable regions of selected lymphoma BCRs (3.4.7).

Since the formation of the BCR complex and the downstream signalling pathway requires multiple proteins, B cell-derived cell lines were chosen, which should already express the proteins necessary for the downstream signalling. Therefore, three different Burkitt lymphoma cell lines were used (Namalwa.CSN/70, DG75 and Ramos) to establish this system.

All cell lines were provided by Dr. Niklas Engels (University of Göttingen) and were supposed to be negative for endogenous BCR expression. However, prior the transduction, the cell lines were stained with a FITC-labelled anti-human-IgM antibody to verify the absence of surface-IgM (Figure 20).

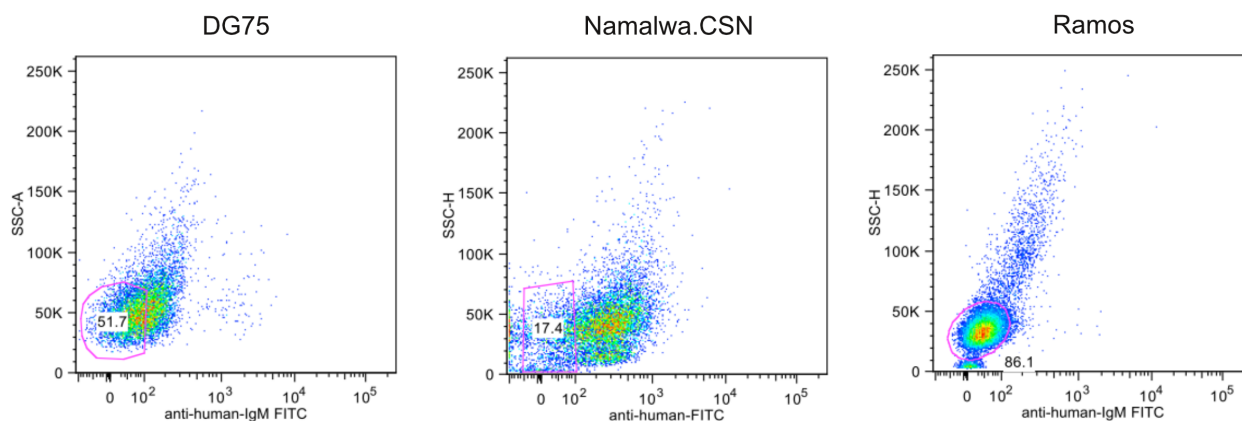


**Figure 20: Fluorescence activated cell sorting of different Burkitt lymphoma B cell lines.** Cells were stained with a FITC-labelled anti-human-IgM antibody and sorted against the presence of the FITC signal (violet boxes). The numbers indicate the percentage of the sorted cells against the whole population.

Figure 20 shows that all cell lines still expressed endogenous IgM, but the amount differed strongly. Namalwa.CSN/70 cells had an expression of surface-IgM in the majority of cells. In DG75 cells about half of the cells were IgM-negative but some cells showed a strong FITC signal. The Ramos cells were the most homogeneous population with only few cells expressing the endogenous human



IgM. To ensure that only IgM-negative cells were used for following experiments, all cell lines were sorted for IgM-negativity (indicated by the gates in Figure 20).

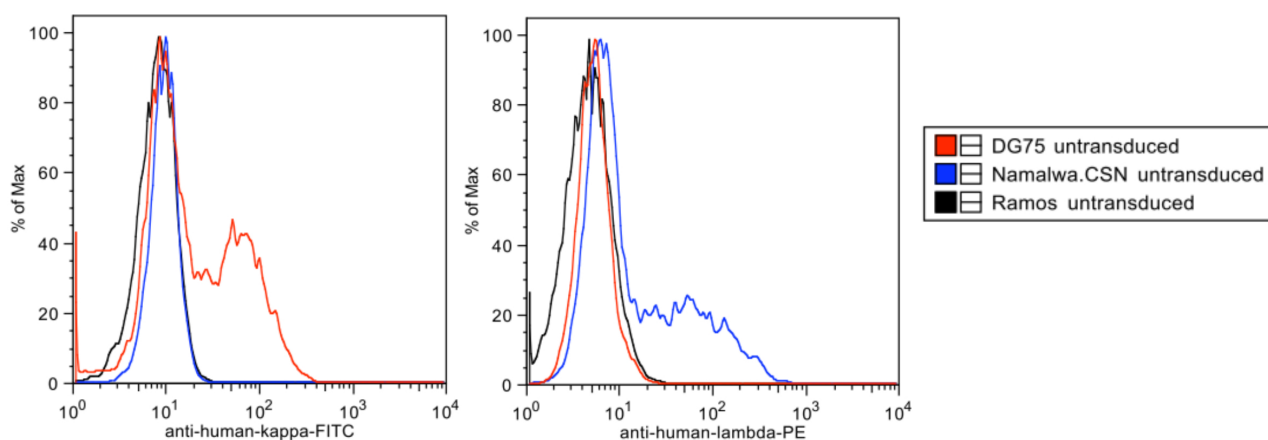


**Figure 21: Flow cytometric analysis of human Ig light chain expression in lymphoma cell lines, sorted for Ig negativity.** The sorted DG75, Namalwa.CSN/70 and Ramos cell lines were stained with a FITC-labelled anti-human-kappa (left) or PE-labelled anti-human-lambda (right) antibody. A substantial proportion of DG75 (red) and Namalwa.CSN/70 cells (blue) still expressed their respective endogenous light chain (Namalwa.CSN/70:  $\lambda$ ; DG75:  $\kappa$ ). In contrast, sorted Ramos cells (black) showed no expression of their endogenous  $\lambda$ -light chains.

One week after the FACS, the sorted cells were analysed by flow cytometry (Figure 21) but only the Ramos cells showed no endogenous human-Ig light chain expression. In DG75 and Namalwa.CSN/70 cells, a substantial proportion of cells retained a human light chain molecule on the cell surface. Since light chains must be associated with a membrane-bound heavy chain to be bound on the cell surface, this also indicated the expression of an endogenous heavy chain.

As a consequence, subsequent experiments were performed with Ramos cells.

Finally, the absence of endogenous human-IgM and human-IgG in the sorted Ramos cells was checked by Western Blot and as shown in Figure 22 no IgM or IgG signal was observed.

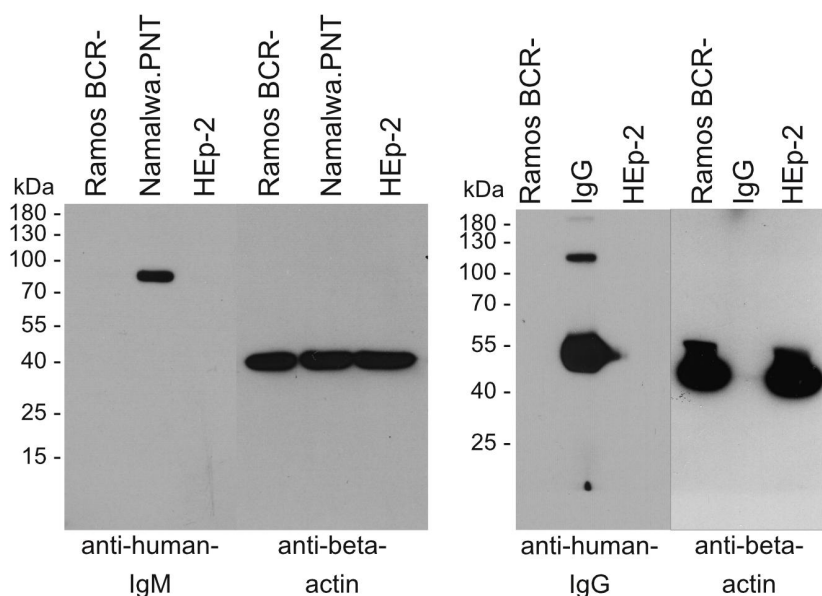


**Figure 22: Western Blot analysis of sorted BCR-negative Ramos cells.** RIPA protein lysate of sorted Ramos cells was separated by SDS-PAGE on a 10% gel, blotted to a PVDF membrane and stained with an anti-human-IgM (left) or anti-human-IgG (right) antibody. No signal for residual expression of endogenous immunoglobulins was detected. HEp-2 cells served as negative control. Human BCR-positive Namalwa.PNT cells and recombinant IgGs served as positive control for the anti-human-IgM or anti-human-IgG blot, respectively.  $\beta$ -actin was used as loading control.

#### 4.4.1 Establishment of the surface immunoglobulin expression

Having obtained a B cell line without endogenous surface IgM expression, the sorted cells were lentivirally transduced with the heavy or the light chain of selected MCL-derived Igs (MCL11 and MCL19) (3.4.7). The heavy chain constant region of the transduced Igs was murine, which enabled a clear differentiation between (potential) endogenous and transgenic immunoglobulins. The light chain constant regions were human. Minden et al. <sup>113</sup> had demonstrated, that such a chimeric IgM did not impair the assembly and signalling capacity of the BCR.

After transduction, the cells grew for at least two weeks with 40  $\mu$ g/ml zeocin and 1  $\mu$ g/ml puromycin treatment as selection marker.

The successfully transduced cells were sorted again for the presence of a human-lambda light chain and the absence of human surface-IgM (Figure 23).

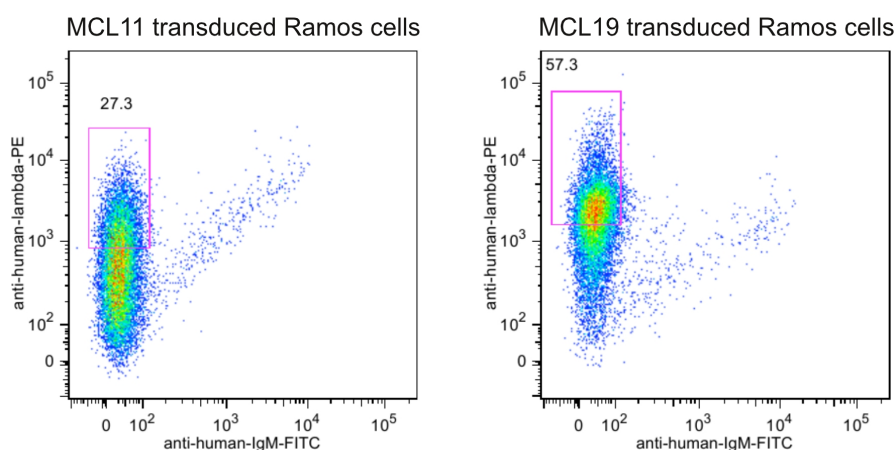


**Figure 23: Fluorescence activated cell sorting of transduced Ramos B cell lines.** Cells, which were transduced with a MCL11 (left) or MCL19 (right) Ig, were co-stained with a FITC-labelled anti-human-IgM antibody and a PE-labelled anti-human-lambda antibody. The transduced Ig heavy chain was mouse-derived. Therefore, only cells with a strong PE- but no FITC-signal were collected (gates). The numbers indicate the percentage of sorted cells to the whole population. A notably amount of cells showed an expression of human-IgM, although only BCR negative cells were used for transduction. Moreover, cells, which were transduced with the MCL19-derived Ig, showed a much stronger PE signal compared to the ones transduced with a MCL11-derived Ig.

Although only BCR-negative Ramos cells were used for the transduction, a small proportion of cells showed the expression of a human-IgM after the transduction and was sorted out.

The re-sorted cells were then stained with an anti-human-IgM, an anti-mouse-IgM and an anti-human-lambda antibody (Figure 24).

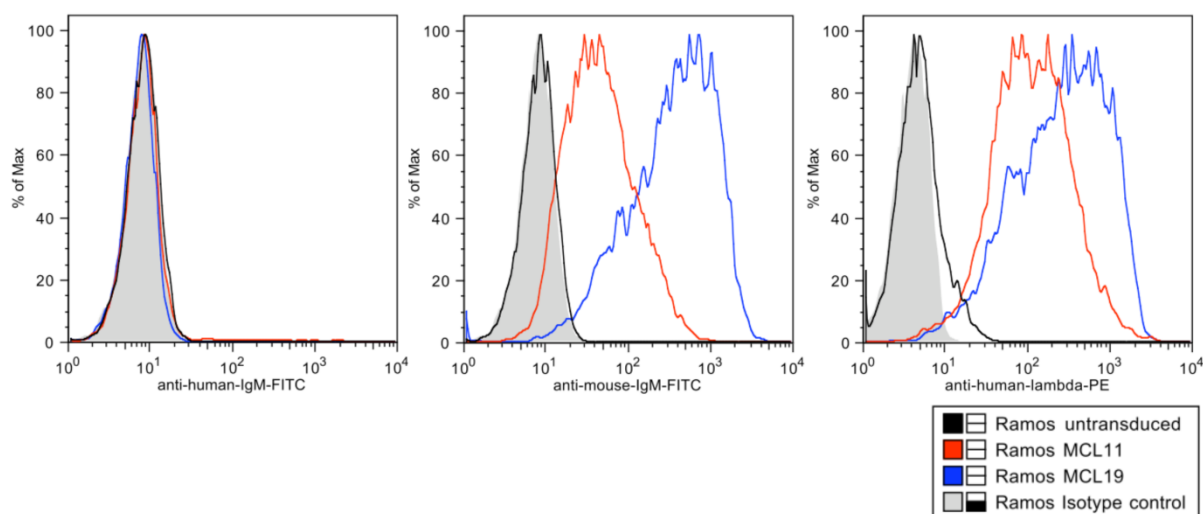


**Figure 24: Flow cytometric analysis of Ramos cells transduced with recombinant Igs.** Ramos cells, which were transduced with a chimeric IgM, harbouring the variable domains of an MCL-derived Ig, were stained with a FITC-labelled anti-human IgM (left), a FITC-labelled anti-mouse-IgM (center) or a PE-labelled anti-human-lambda antibody (right). Since the transduced IgM harboured a murine constant IgM domain, endogenous and transduced IgM could be distinguished. Untransduced Ramos cells (black) showed no signals, whereas cells transduced with MCL11- (red) or MCL19-Igs (blue) showed a signal with the anti-mouse-IgM and anti-human-lambda antibodies. Note the very different expression rates of the transduced IgM.

As shown in Figure 24, both transductions led to an expression of surface Igs harbouring a murine  $\mu$ -heavy chain and a human  $\lambda$ -light chain. In addition, no human-IgM was present on the cell surface.

As already seen in the context of the cell sorting (Figure 23), the expression of the transduced Ig differed strongly. The FITC signal was almost ten times higher in MCL19-transduced cells compared to the MCL11-Ramos cells. Nevertheless, both established cell lines were used for subsequent experiments.

#### 4.4.2 $\text{Ca}^{2+}$ -Flux assay of transduced and untransduced Ramos cells

During activation of the BCR downstream signalling cascade,  $\text{Ca}^{2+}$  is released into the cytoplasm of the B cell (1.2.5). Thus, the  $\text{Ca}^{2+}$ -release can be measured by  $\text{Ca}^{2+}$  chelators, like Fluo-4, and act as a second messenger for BCR cross-linking.

A  $\text{Ca}^{2+}$ -influx assay was performed (3.4.10) using the transduced Ramos cells (4.4.1) to investigate whether the introduced BCR were able to activate the cells (Figure 25).

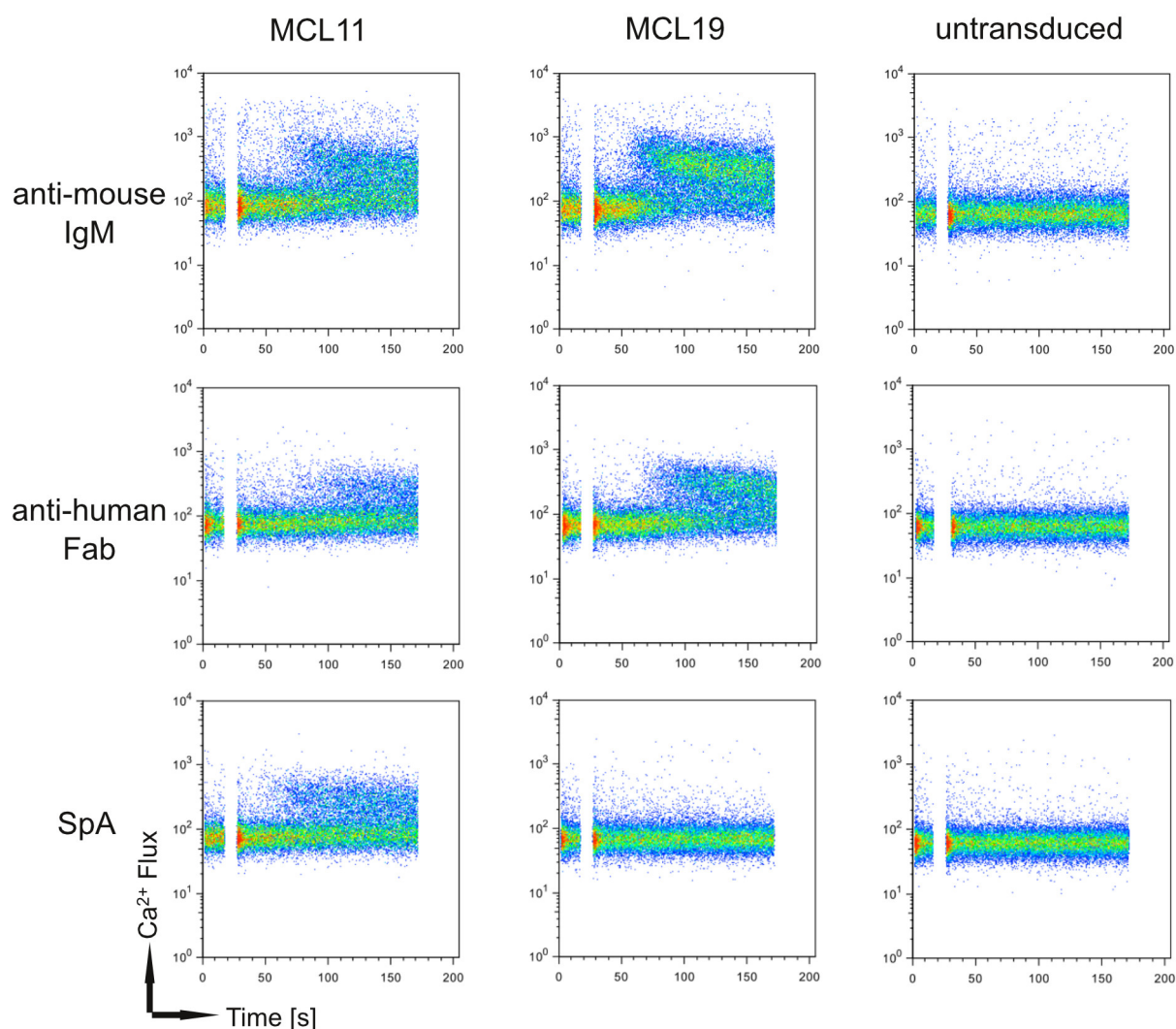


**Figure 25:  $Ca^{2+}$ -mobilisation assay of Ramos cells expressing MCL-derived membrane bound immunoglobulins.** The Fluo-4 signal intensity shift after addition of  $2\ \mu\text{g/ml}$  anti-mouse-IgM-antibody (upper row),  $2\ \mu\text{g/ml}$  anti-human-Fab antibody or  $5\ \mu\text{g/ml}$  SpA (lower row) within 180 seconds is shown in this figure. The baseline signal was measured for 15 seconds and the gap indicates the time of addition. Both transduced cell lines showed a  $Ca^{2+}$ -influx after IgM cross-linking with the anti-mouse-IgM and anti-human-Fab antibodies, whereas only MCL11-transduced cells showed an altered  $Ca^{2+}$ -level after addition of SpA.

Ramos cells expressing transduced Igs showed an increased Fluo-4 signal intensity following the addition of  $2\ \mu\text{g/ml}$  anti-mouse-IgM antibody (Figure 25, top row). This demonstrated that the introduced chimeric BCRs were properly assembled and able to activate the downstream signalling cascade. Untransduced cells could not be activated by the incubation with anti-mouse-IgM antibody. Moreover, stimulation with an anti-human-Fab antibody also showed signal-alterations exclusively in transduced cells (Figure 25, middle row), indicating that no residual endogenous human BCR was present on the cell surface of sorted untransduced Ramos cells. Since the

transduced Igs harboured a human variable region as well as a human light chain, they could be induced by the anti-human Fab-antibody.

Finally, cells expressing the MCL11-derived BCR exhibited a strong increase of  $\text{Ca}^{2+}$ -flux during incubation with SpA (Figure 25, bottom row). In contrast, neither the cells transduced with the SpA-motif-negative MCL19-derived Ig nor untransduced cells showed an alteration of intracellular calcium levels.

#### 4.4.3 $\text{Ca}^{2+}$ -Flux assay of mantle cell lymphoma cell lines

To verify the capability of SpA inducing the BCR signalling cascade in MCL, the  $\text{Ca}^{2+}$ -Flux assay was performed with the MCL cell lines MAVER-1 and Jeko-1 (Figure 26). According to Pighi et al.<sup>201</sup> MAVER-1 cells express the unmutated IGHV3-9 gene and therefore harbour the SpA motif. Jeko-1 cells, in turn, express the IGHV2-70 gene and thus do not harbour the motif.

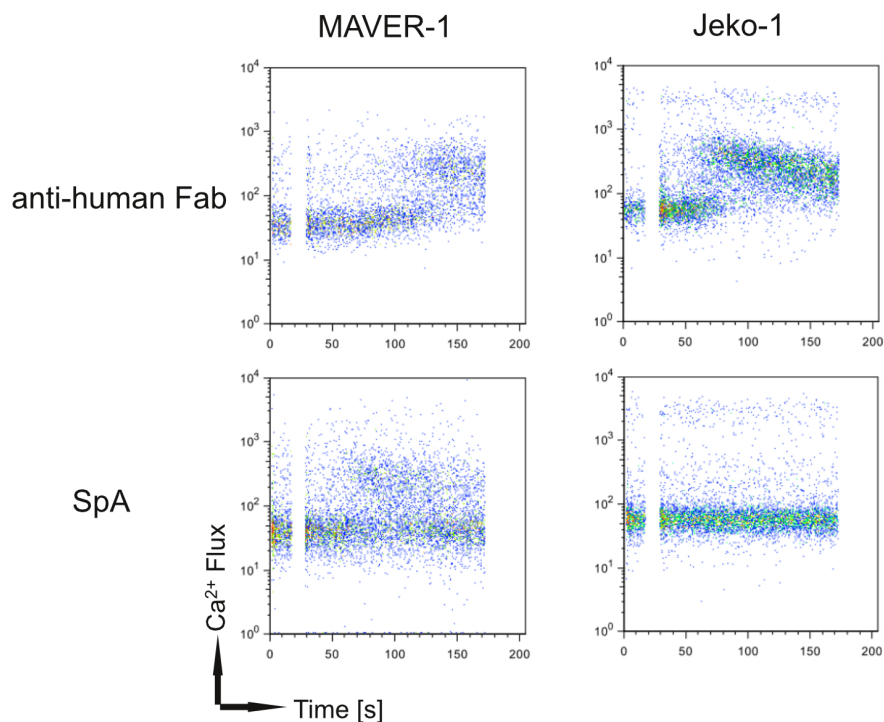


**Figure 26:  $\text{Ca}^{2+}$ -mobilisation assay of MAVER-1 and Jeko-1 MCL cells.** The shift of the Fluo-4 signal intensity after addition of either 2  $\mu\text{g/ml}$  anti-human-Fab antibody (upper row) or 5  $\mu\text{g/ml}$  SpA (lower row) within 180 seconds is depicted in this figure. The baseline signal was measured for 15 seconds. The gap indicates the time of addition. Both cell lines showed a cell activation after incubation with the anti-human-Fab antibody. While MAVER-1 cells expressed an unmutated IGHV3-9 gene and thus presented the SpA motif, Jeko-1 cells expressed the IGHV2-70 gene and did not harbour the motif. Consequently, only MAVER-1 cells showed an  $\text{Ca}^{2+}$ -flux after treatment with SpA.

As demonstrated in Figure 26, both cell lines showed an increased fluorescence signal when incubated with the anti-human-Fab antibody, whereas SpA treatment led to a fluorescence intensity shift only in MAVER-1 cells.

#### 4.4.4 Far Western Blot analysis of induced Ramos cells

Besides using  $\text{Ca}^{2+}$  as a second messenger, the phosphorylation of BCR pathway downstream molecules was analysed with a far-Western Blot. This technique allows visualisation of phosphorylated proteins by using SH2-domains as phosphoproboscopes. Unlike Western Blots utilising specific antibodies against distinct phosphorylation sites, multiple phosphorylated proteins can be screened at once<sup>202</sup>. For this study, the cell lysates were probed with the GRB2- and the SHP2-SH2 domains.

The far-Western Blots resulted in multiple bands on both Blots. Most of these bands had the same intensity in the treated and untreated cells. Using GRP2 as a probe, one band above 160 kDa showed different signal intensities (Figure 27A, black box). The intensity of this band increased in cells, which were treated with anti-mouse-IgM or anti-human-Fab antibody and harboured a BCR on the surface (MCL11 and MCL19) compared to untransduced cells. In addition, the phosphorylation pattern after incubation with SpA in cells expressing the MCL11-derived Ig was similar to the pattern seen in the anti-antibody treated cells. In contrast, cells, which were transduced with the MCL19 Ig did not show an altered phosphorylation pattern after SpA treatment. The SHP2-Blot revealed a protein slightly below 160 kDa, which was alternatively phosphorylated (Figure 27B). However, in MCL11-transduced cells the signal difference is only minimal with a very little increase for all treated cells, including SpA treatment, compared to the untreated ones. In the MCL19 Ramos cells this difference was very strong but only for the group incubated with an anti-mouse-IgM antibody. These cells also showed a strong increase in the phosphorylation of a protein between 40 and 50 kDa.

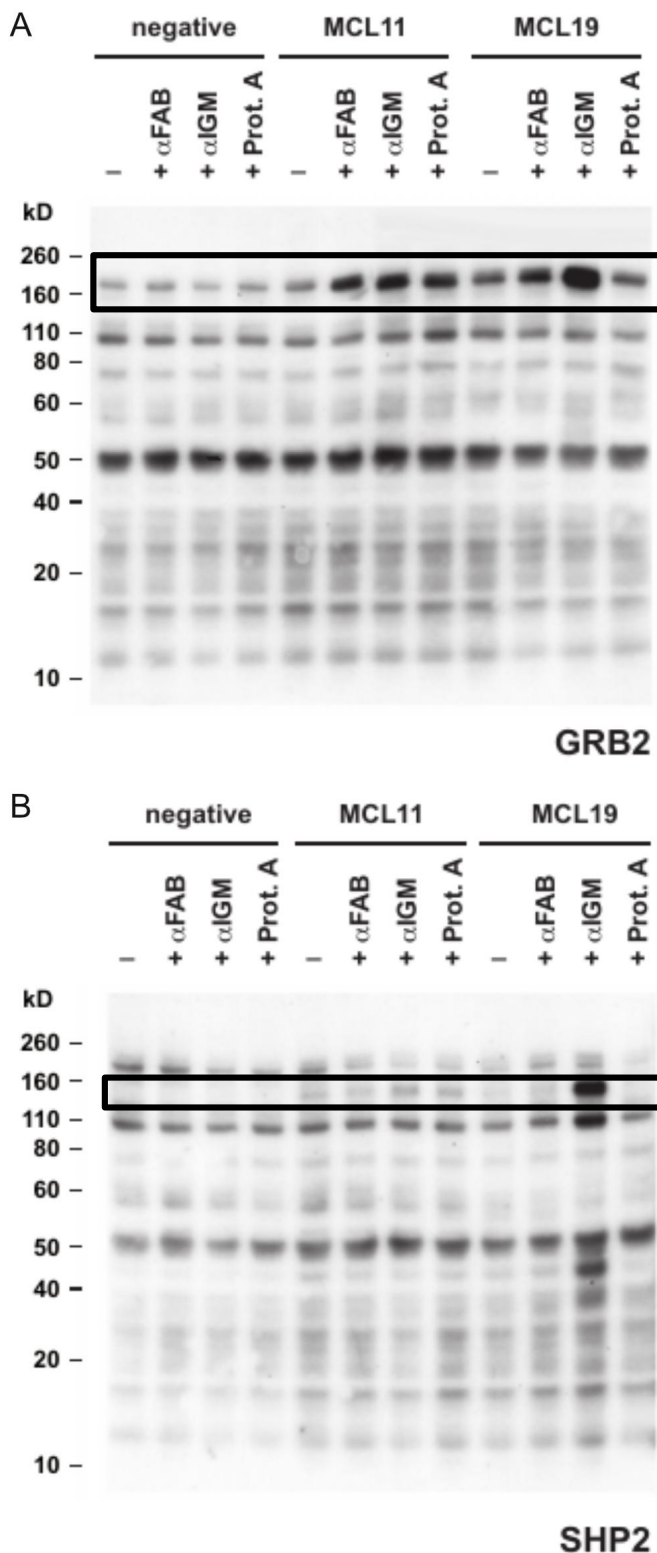


**Figure 27: Far-Western Blot to detect altered phosphorylation patterns in stimulated and unstimulated Ramos cells.** Ramos cells, which expressed an MCL-derived IgM as well as untransduced BCR-negative Ramos cells were incubated for 2 h with an anti-human-Fab antibody, an anti-mouse-IgM antibody or the staphylococcal protein A (SpA). The cells were lysed and the lysates were separated by SDS-PAGE. Phosphorylation was probed either with the GRB2- (A) or SHP2-SH2 domain (B).

With the GRB2-phosphoprobe (upper blot), MCL11-expressing Ramos cells, stimulated with SpA, anti-human-Fab and anti-mouse-IgM, showed a stronger band above 160 kDa compared to untreated cells (box). This band was also altered in MCL19-Ramos cells incubated with anti-human-Fab or anti-mouse-IgM, but did not increase in SpA treated cells.

Using SHP2 as a phosphoprobe (lower blot) a band below 160 kDa showed different intensities in treated and untreated cells. However, these differences are much weaker in the MCL11-transduced cells compared to the ones observed with the GRB2 probe. This band was very strong in The MCL19-Ramos cells, incubated with the anti-mouse-IgM antibody, but was nearly invisible in the other treatment groups.



#### 4.4.5 Proliferation assay of stimulated Ramos cells

To check whether the alterations in the protein phosphorylation also result in different cell behaviour, the transduced cells were incubated for 10 days with 5  $\mu\text{g/ml}$  SpA or 2  $\mu\text{g/ml}$  anti-mouse-IgM. The cell count was determined every day (3.4.11).

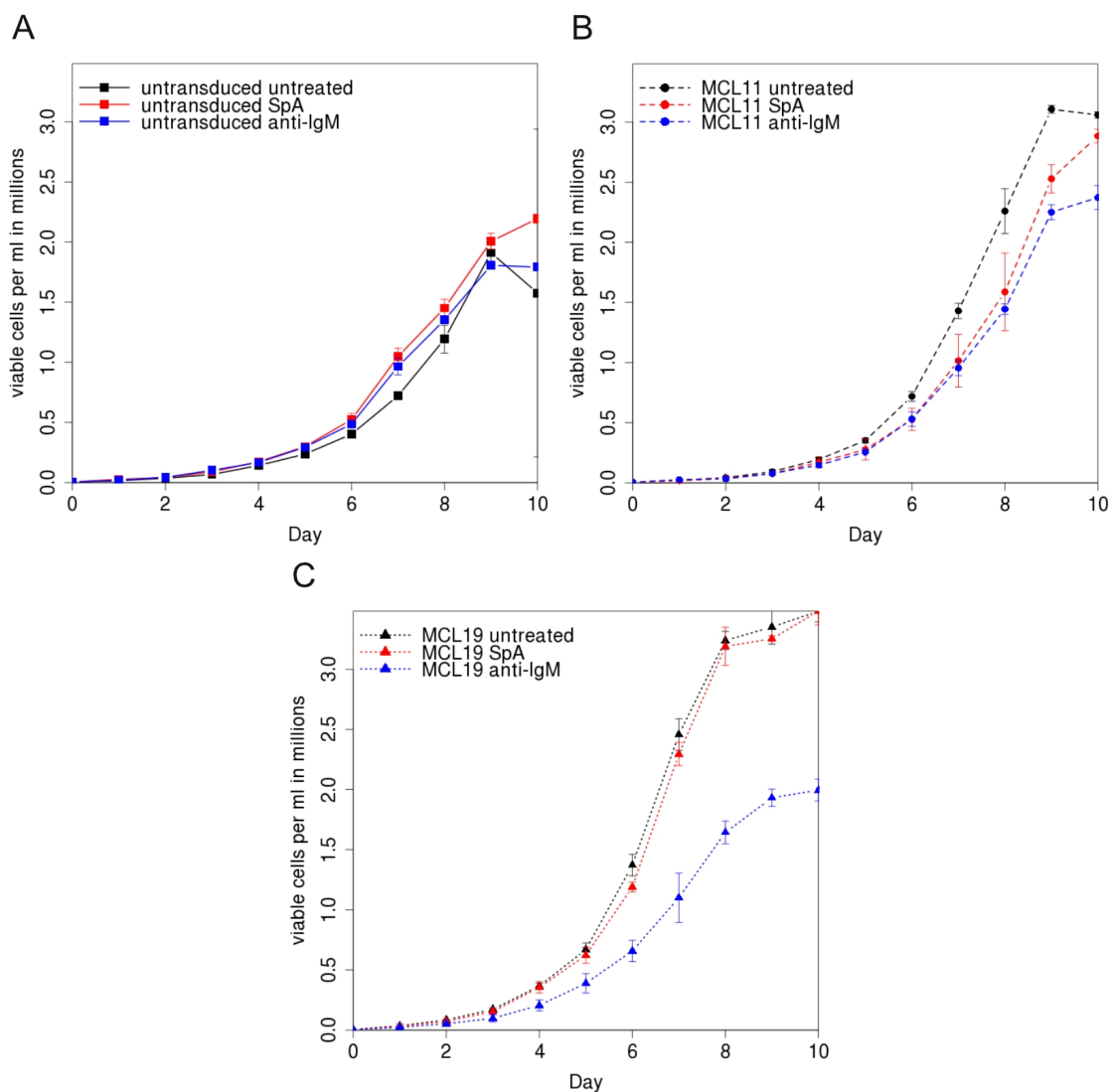


**Figure 28: Proliferation of transduced and untransduced Ramos cells.** Untransduced Ramos cells (A) as well as Ramos cells expressing a MCL11- (B) or MCL19-derived Ig (C) were either treated with anti-mouse-IgM antibody (blue) or SpA (red) or left untreated (black). At start, 50,000 cells were seeded in 5 ml medium (+/- supplements) and the obtained volume per measurement (500  $\mu\text{l}$ ) was always replaced with fresh medium (+/- supplements). The viability and the amount of cells was determined every day for ten days. Triplicates were used for each treatment group.

Figure 28 summarises the cell proliferation of the different groups over time. Ramos cells expressing the MCL11-IgM had a growth delay if an anti-mouse-IgM antibody or SpA was

## Results

---

supplemented to the medium. In contrast, the MCL19-IgM altered the cell behaviour only after stimulation with the anti-mouse-IgM antibody and was not affected by SpA treatment.

The untransduced Ramos cells did not react to any of the treatments. However, they grew slower than the untreated groups of the transduced cells.

Again, this result demonstrated the ability of SpA to induce the BCR and the downstream signalling cascade. Nevertheless, the BCR activation in this cell system did not lead towards a growth stimulation but an inhibition.

## 5 Discussion

### 5.1 The Ig repertoire of mantle cell lymphoma

The B cell receptor is a functional key molecule of B cells. Since it is also expressed in most and functional in many B cell neoplasias (1.3.2), it is likely that that the BCR is salient to lymphoma cell survival at least at some point of lymphomagenesis and disease progression. In fact, the blockage of this pathway showed promising therapeutic effects, partially beyond any therapeutic strength observed before, in chronic lymphocytic leukaemia and mantle cell lymphoma<sup>164–166,203–205</sup>. Nevertheless, the role of the BCR in lymphoma is not completely understood and it is unknown which antigens are bound and potentially stimulate tumour cell growth in individual patient cases. Analysis of the BCR Ig repertoire can give valuable information about the developmental stage of the B cell at the supposed time of malignant transformation. Despite the fact that MCL is a rare disease, it was possible to acquire 32 MCL samples for this study. The crucial step for all downstream experiments was the identification of the Ig sequence of the malignant B cells (4.1.1). It was possible to determine the variable heavy chain Ig sequence of 24 out of 32 investigated samples. Moreover, for all but two samples the associated Ig light chain was determined, as well. In these two cases, multiple light chain sequences were identified for the  $\kappa$ - and  $\lambda$ -isotype. Since no unequivocal monoclonal sequence was found, the light chains of these patients were regarded as polyclonal. This observation raised the possibility that malignant transformation of a clone occurred before the rearrangement of the light chain, i.e. before the transition from pre-B to B cell. However, whether the observed polyclonality was a technical artefact or a special property of these two patient samples remained elusive.

#### 5.1.1 MCL-derived Igs were only minimally mutated

In line with previous results, the Igs of MCL BCRs were only minimally mutated<sup>138,149</sup>. It was demonstrated in CLL that tumours with minimally mutated Igs have a poor prognosis. A threshold of 2% deviation from the germline identity effectively separates mutated and unmutated CLLs<sup>206,107</sup>. Due to the prognostic value of this threshold in CLL, multiple studies used it for characterisation of other NHL-entities, as well. Applying the 2% cut-off to the cohort of the study presented here, 79% of all cases had unmutated and only 21% had mutated Igs. Earlier studies with larger cohorts showed a similar result with 20-29% of all MCL samples having Igs with less than 98% germline homology<sup>145,147,149,207</sup>. However, the relevance of the 2% threshold as a prognostic factor in MCL

remains questionable and does not seem to be applicable<sup>146,148,208</sup>. For that reason, it might be better to further separate the cohort into the three subgroups, completely unmutated (100% germline identity (GI)), minimally/borderline mutated (99.9–97% GI) and hypermutated (<97% GI) as proposed by Hadzidimitriou et al.<sup>149</sup>. Separating the cohort in these subgroups, one out of four Igs were unmutated and only two samples were hypermutated (~8%). The majority of cases (~67%) presented a minimally or borderline mutational pattern. Comparable results were published in a much larger cohort (29.5% unmutated; 56.7% minimally/borderline; 13.8% hypermutated)<sup>149</sup>.

It was often suggested that an antigenic selection could be determined by analysing silent and replacement mutations in the FRs and CDRs of an Ig<sup>149,209,210</sup>. Since the FRs are responsible for the stability of the antibody whereas the CDRs determine the specificity, somatic hypermutation should introduce more R mutations in the CDRs<sup>210</sup>. In the cohort presented here, the R/S ratios were 1.26 and 4.0 for the FRs and CDRs, respectively. Hadzidimitriou et al. published similar results with overall R/S-ratios of 1.75 for the FRs and 3.69 for the CDRs. Such an increased introduction of R mutations in the CDRs compared to the FRs could be regarded as a result of antigen-driven BCR maturation<sup>211</sup>.

However, due to a bias in codon usage, CDRs generally seem to be more susceptible to R than S mutations<sup>210</sup>. Especially in the light of the very low mutation rate of MCL-Igs, this may introduce a bias towards a probable antigenic contact even if it is absent<sup>210</sup>. As a consequence, the “simple statistical analysis of the distribution pattern of somatic mutations in a clone cannot be utilized as a reliable tool to state whether or not an antibody is a product of antigen-driven selection”<sup>210</sup>.

Considering the limitations in the analysis of R/S-ratios, it was calculated only for the purpose of comparison with a previous publication from Hadzidimitriou et al.<sup>149</sup>.

### **5.1.2 Mantle cell lymphoma B cells showed a biased IGHV expression**

A biased usage of BCR genes is an evidence for antigen involvement during tumour development<sup>93</sup>. For MCL, a strong bias in immunoglobulin gene usage was described in multiple studies. They revealed four heavy chain genes (IGHV3-21, IGHV4-34, IGHV1-8 and IGHV3-23) in about half of all cases<sup>135,145–149,207</sup>. These findings were confirmed in the study described here, although IGHV3-21 was slightly under-represented. Moreover, comparisons with the gene distribution in naïve B cells and other B cell malignancies have shown major differences in the usage of Ig heavy chain genes in MCL<sup>212,149</sup>. These results not only indicate an antigenic drive but also highlight the possibility for a limited set of antigens that may be involved in the pathogenesis of the disease.

The knowledge of the expressed light chain genes and the pairing of heavy and light chains is limited in MCL. In this study, a slight bias towards the usage of the  $\lambda$ -light chain was observed (ratio  $\lambda/\kappa$ : 1.2:1). This is in line with observations in earlier studies, which also demonstrated a preferred use of  $\lambda$ -light chains in MCL<sup>123</sup>. However, the ratio observed in the study presented here, was lower than the  $\lambda/\kappa$ -ratios published by Bertoni et al.<sup>213</sup> (5:1) or Schraders et al.<sup>148</sup> (1.8:1). Given the relatively small cohort size in our study, these differences most likely result from statistical deviations.

Importantly, a strong bias in the heavy and light chain pairings was observed. All samples expressing the IGHV3-21 gene exclusively used the IGLV3-19 gene for the light chains. This finding was also observed earlier and appears to display a special subgroup of MCL<sup>146,149</sup>. It was further shown that the IGHV3-21-positive subgroup had a better prognosis than the rest of the cohort<sup>146</sup>. Interestingly, the restricted usage of heavy and light chain genes in such a large proportion of patients strongly indicates an antigen involvement in the pathogenesis of this subset and MCL in general. Of note, the IGHV3-21 gene was also overrepresented in CLL cohorts and also exhibited a restricted pairing with lambda light chains but was associated with a shorter overall survival<sup>214</sup>.

The lack of strong hypermutation in MCL samples supports the idea that MCL cells might derive from pre-germinal centre cells (1.3.3). Nevertheless, this does not necessarily mean the absence of any antigenic-drive during tumour development. The highly biased Ig repertoire points towards the need of distinct Ig sequences for tumour growth and development. These sequences might be preferentially preserved to serve that purpose. In addition, somatic hypermutation did not need to occur in the germinal centre and it is therefore possible that the mutated MCL BCRs underwent extrafollicular affinity maturation often seen against bacterial antigens<sup>215,216</sup>.

To conclude, the biased IGHV usage and SHM status of the cohort in this study is in line with results published before and can be seen as representative for further analysis.

### 5.1.3 MCL-Igs acquired no novel glycosylation sites

In follicular lymphoma, acquisition of novel N-glycosylation sites in the variable regions, especially the CDRs of the Ig heavy chains, was observed and revealed a new potential mechanism for BCR activation<sup>116,117,217</sup>. These added mannose-rich glycans may create “a functional bridge between human follicular lymphoma and the microenvironment”<sup>118</sup>.

Furthermore, bacterial lectins can bind to these glycosylated BCRs, inducing  $\text{Ca}^{2+}$ -influx and activation of the B cell<sup>119</sup>. In CLL, the frequencies of introduction of novel N-glycosylation sites were similar to those seen in normal B cells (8-9%)<sup>116</sup>. The MCL cohort in the study presented here,

however, showed no novel sites for N-glycosylation. Due to the minimal mutational load in most MCL cases, only the germline-coded sites remained. Since the small size of the cohort might hide alterations of acquired or lost N-glycosylation sites, published sequences of the four most abundant Ig heavy chains by Hadzidimitriou et al.<sup>149</sup> were analysed. Out of all published sequences (in total 241), only six (2%) presented novel N-glycosylation sites. Importantly, IGHV1-8 and IGHV4-34 genes harbour such sites in the germline. These sites were mostly preserved in the IGHV4-34 genes, but 9 out of 36 IGHV1-8 bearing Igs lost them during maturation. As these introduction frequencies are below the rate in normal B cells, it is possible that a glycosylation site might interfere with the BCR signalling in at least a subgroup of MCL and is suppressed. Moreover, a tumour promoting effect of lectins as seen in FL samples is unlikely in MCL.

### 5.1.4 The MCL-Ig did not mutate over time

Within this study, it was possible to perform next generation sequencing (NGS) for two samples of the same patient, obtained in the years 2008 and 2012. The Ig sequences in this MCL patient were highly conserved over that time period. Despite being only a single observation and probably not generalisable, it gave valuable insights about the genetic stability of the Igs in MCL. To date, only little is known about ongoing mutations in the Igs after lymphomagenesis. In FL, the IGHV genes usually underwent ongoing somatic mutation in all patients<sup>218</sup>. These results are in great contrast to the findings of highly conserved Ig sequences presented here for MCL samples. However, the molecular pathogenesis of FL differs significantly compared to MCL and the FL Igs are always highly mutated<sup>93,94</sup>.

A genetic stability over such a long period of time might indicate that the B cell consistently depends on the BCR during MCL progression and further highlight this molecule as a valuable research object.

Moreover, the NGS demonstrated that only one heavy chain clonotype was present at both points in time, whereas 73  $\kappa$ -clonotypes were present in both samples. This opens up the questions why only the IGHV was restricted to a specific clonotype.

A possible biological explanation may be that only the heavy chain promotes the tumour growth. As a result, the light chain would have no selection pressure and also cells with mutated light chains could survive and proliferate. Since the clonotypes are separated by the amino acid sequence of the CDR3, any non-conservative mutation in this region created a new clonotype. Nevertheless, also the mutational rate of the MCL light chains remained very low over time. Almost 90% (11233 of 12380) of the shared sequences derived from a single clonotype, suggesting that only few cells have acquired mutations during lymphoma development. These few mutations might not cause such a

strong disadvantage for the respective B cells to disappear completely. As a result, also B cells with slightly altered Ig light chains survived besides the dominant clone within the analysed time period. Importantly, the Ig repertoire at the IgL locus changed strongly within the four years. Since the lambda light chain is not involved in tumour development, this is expected and might represent the continual renewal of the healthy B cell repertoire.

To verify the observations of this study, further samples must be analysed with high-throughput methods like NGS to make general conclusions. Nevertheless, if these results could be confirmed in future studies it has the potential to greatly improve our knowledge of the MCL development.

## 5.2 Identification of antigens and epitopes in NHL

After successful determination of the Ig sequences, the next step in this work was to explore the binding properties of the MCL-derived Igs. Due to the limited amount of primary material and the large demand of monoclonal Igs for the subsequent experiments, multiple Igs were produced as recombinant IgGs.

### 5.2.1 Three MCL-Igs enriched epitope mimics during phage display selection

Phage Display screenings were performed to enrich specific phage-bound peptides mimicking the epitopes of the Igs. Selections with CLL-derived Igs have demonstrated previously that this method is suitable to screen for unidentified epitopes<sup>114,219</sup>. It was also shown in our group that CLL Igs, polyreactive against multiple selective phage peptides, had a poor prognosis and thus highlighting a potential clinical relevance<sup>220</sup>. Performing phage display using MCL-derived Igs, however, had only limited success. Enrichment of phages against polyclonal IgGs, used for depletion of unspecific binders, was only achieved in three out of eleven cases (MCL4, MCL18 and MCL22, 4.2.2). While the MCL18-Ig showed a very strong enrichment after four selection rounds, only minimal enrichments were achieved using the MCL4- and MCL22-derived antibodies. Furthermore, in one case (MCL4) only a single peptide sequence was acquired and therefore no consensus peptide motif could be determined.

The selection with MCL22 enriched two different phage peptides. These peptides displayed a potential consensus motif “CNxK”. It has been demonstrated with IgEs that even very short peptides may be sufficient as a linear epitope for the Ig binding sites<sup>221</sup>. However, the binding affinity of the phage-associated peptides differed strongly. The “CNHKCAELVTSA”-peptide was bound only weakly by the Ig, whereas the MCL22-derived Ig had a much bigger affinity to the

“SLFYTACNPKVC”-peptide. A single mutation in the motif like the substitution of proline (P) with histidine (H) might heavily affect the binding affinity of the Ig against these peptides. However, it is further likely that the short consensus motif did not represent the whole epitope of the Ig. Thus, the residual amino-acids of the peptide also influenced the binding strength. This implies that the “SLFYTACNPKVC”-peptide mimics the epitope in a better way than the “CNHKCAELVTSA”-peptide.

Interestingly, two cysteines were present in all three enriched peptide sequences of the MCL4- and MCL22-selections. This is especially remarkably because selections with a specifically designed library harbouring two cysteines in a fixed position ( $\beta$ -sheet library) did not yield any enrichments. The different amount of amino acids between the cysteines in the  $\beta$ -sheet library (6 AAs) compared to the selected peptides (3/4 AAs) might indicate that the steric properties of the  $\beta$ -sheet library cannot mimic the required epitopes of these Igs in a sufficient way. Nevertheless, it remains elusive whether this observation has any significance or is only an artificial coincidence.

The immunoglobulin MCL18 with the greatest phage enrichment yielded the most diverse peptide sequences. In total, four different peptide sequences were acquired. The affinity of the MCL18-Ig to these peptides was very high and showed, in contrast to all other selected phages, a clear saturation in the anti-phage ELISA. In addition, all peptides were bound with a very similar affinity. The four selected sequences displayed “DxKWQYVxNxPL” as a probable consensus sequence.

As already outlined, it was demonstrated that multiple CLL samples shared epitopes<sup>220</sup>. Due to the biased Ig repertoire, this might be the case in MCL as well<sup>149</sup>. However, the observed cross-reactivities of the selected phages in this study were only minimal. The MCL11-Ig showed a minor reactivity with the phage enriched by MCL4. In addition, MCL11 as well as MCL4 bound to the “SLFYTACNPKVC”-phage, enriched by MCL22. This is remarkable since MCL4 and MCL11 harboured different heavy chains and light chain isotypes (Table 4). Furthermore, although the CDR3-length was equal (18 AAs) the actual CDR3-sequences showed no similarities. Finally, also MCL22 differed from MCL4 and MCL11 with a 24 AAs long CDR3-region.

Taken together, only MCL4 and MCL11 showed a slight cross-reactivity in epitope binding, but most of the tested MCL-Igs did not seem to bind the epitopes selected by phage display.

Unfortunately, a BLAST alignment to identify sequence homology of the peptide sequences or motifs did not yield any potential antigen<sup>222</sup>. This was expected as the search for such short sequences mostly results in a vast amount of output sequences. Even if the search is limited to only human proteins, it did not result in a distinct protein. Without any further evidences narrowing



down the search parameter, this approach will, in general, not lead to a distinct antigen in the setting used here.

One of the major drawbacks of that technique is the selection for a more or less linear epitope. Besides linear epitopes, a conformational epitope can be formed by amino acids which are far away from each other in the amino acid sequence but close together in the tertiary structure of the protein<sup>221</sup>. A selected phage peptide might be able to mimic the steric and electrochemical properties of the tertiary structure in a linear peptide but it will be nearly impossible to track down the real epitope out of such a sequence.

Using immunoprecipitation,  $\beta$ -actin was identified as a potential antigen for the MCL22 Ig (5.2.3). Even if the motif search is limited to this protein it was still impossible to determine a clear epitope since multiple parts of the protein sequence matched with short parts of the phage peptide sequences.

In addition, the limited size and diversity of any phage library must be taken into account. Thus, not every possible peptide is present in a phage library and a few peptides might be over-represented. As a result, even if an Ig strongly binds an epitope, it cannot be enriched if it is not in the library. Finally, Igs might not enrich a peptide for technical reasons. This includes peptides washed away from low affinity antibodies or being captured by the antibody used for negative selection and the propagation of unrelated and unspecific binders<sup>223</sup>.

Therefore, selections with the MCL-derived Igs which did not enrich any phages, does not necessarily demonstrate the absence of a distinct antigen for these Igs. Instead, it might be indicative for a low affinity of these antibodies or a superantigen, capable of binding to the polyclonal IgGs used for depletion of unspecific phages.

## **5.2.2 Most MCL-Igs did not bind to HEp-2 cell expressed auto-antigens**

Besides the phage panning, other protein-based approaches were performed to characterise the binding abilities of MCL-derived Igs and to identify potential antigens. Due to similarities of the MCL and CLL pathogenesis, it was decided to perform experiments made with CLL samples, using the MCL-Igs. It was shown that unmutated-CLL (UM-CLL) Igs are polyreactive and bind to auto-antigens presented by HEp-2 cells<sup>109</sup>. Since the cell-fixation procedure might cover some antigens or epitopes, two different fixation agents (methanol and PFA) were used to minimise the probability for false negative results. In total, 4 out of 11 (~36%) MCL-Igs showed a reaction with HEp-2 cells. This is in line with previously published results using HEp2-cell lysate<sup>224</sup>. In contrast, about 89.6%

of UM-CLL and 56.7% of M-CLL Igs bind to antigens presented in HEp-2 cells<sup>109</sup>. Nevertheless, the observed rate in MCL is still higher than the HEp-2 reactivity observed in naïve B cells (~20%) and is comparable with the auto-reactivity rate of immature B cells (~40%)<sup>109,225</sup>.

The staining patterns varied between the reactive Igs. MCL2 showed a very filamentous pattern while MCL11, MCL12 and MCL22 stained the cytoplasm in a more diffuse manner. Only one Ig (MCL22 on PFA-fixed cells) showed a potential binding in the nucleus. Nevertheless, it mostly stained the cytoplasm and therefore none of the MCL-Igs was regarded as true anti-nuclear antibody (ANA) which are often correlated with auto-immune diseases like systemic lupus erythematosus<sup>226</sup>. Interestingly, MCL11 showed a signal only with PFA-fixed cells and created no signal when the cells were fixed with methanol. MCL12, in turn, showed much weaker signals in PFA-fixed cells. This might indicate different antigens recognised by these Igs or at least different epitopes with more or less favourable accessibility depending on the fixation method.

Importantly, all antibodies harboured heavy and light chains of different families. Moreover, the CDR3-regions were quite heterogeneous. The CDR3-length and the amount of positively charged amino acids were often correlated with auto-reactive behaviour<sup>225</sup>. In line with that observation, MCL2 and MCL22 indeed harboured long CDR3-regions (20 and 24 amino acids, respectively). However, the CDR3-length of MCL11 was intermediate (18 AAs) and only 11 amino acids formed the CDR3-region of the MCL12-Ig. In addition, the antibody showing the strongest signal, MCL2, had two positive charges in the CDR3, as well as MCL11 (MCL22: one, MCL12: none). Thus, the information of sequence analysis is not sufficient to detect auto-reactive antibodies and molecular biological evidences must be included.

Unfortunately, the MCL2- and MCL12-derived Igs persistently produced large artificial spots on the coverslips. It was not possible to minimise these artefacts using reduced antibody concentration or wash them away with more stringent washing steps. The reason for that behaviour is not clear and might either come from aggregates formed by the primary antibodies or, less likely, antigens which were released from the cells and were fixed on the cover slip.

In conclusion, only a small proportion of MCL-BCRs seemed to be reactive against antigens presented by HEp-2 cells and the (auto-)antigens might differ between these patients. Interestingly, only one (MCL22) of the antibodies staining the cells also enriched specific phages during phage display. Moreover, the Ig with the best enrichment during phage library screenings (MCL18) did not react with HEp2-cells. That might indicate a distinct epitope not expressed in HEp2-cells.

### 5.2.3 Cytoskeletal proteins are potential antigens for MCL-Igs

As a next step, it was tried to identify the antigens, expressed by HEp-2 cells and bound by some of the MCL-Igs. Therefore, cell lysates were prepared to perform Western Blots (WB) and immunoprecipitations (IP). Although not all recombinant Igs showed reactivity in the immunofluorescence assays, every produced antibody was tested on the WB. In general, most MCL-derived Igs showed a very unspecific behaviour, binding multiple protein in the lysate. This unspecific reactivity was independent of a positive signal during the immunofluorescence assay. In contrast, the CD20-specific antibody Rituximab, did not show this polyreactivity. To minimise the unspecific binding properties, a serial dilution was performed for every Ig. In most cases, an increase of the dilution of the primary antibody resulted in a decreased signal, which eventually vanished upon applying low antibody concentrations.

MCL22 also showed an unspecific binding at high concentrations. At an intermediate concentration, however, only a single band remained between 40 and 55 kDa, a pattern not seen with other antibodies. A subsequent IP with HEp2 and SK-BR3 cell lysates, followed by mass spectrometric analysis, revealed  $\beta$ -actin as the bound protein. It was already observed that mutated  $\beta$ -actin might be involved in the pathogenesis of DLBCL<sup>227</sup>. Moreover, during B cell activation it plays an important role supporting the signal transduction into the cell. Shortly after the antigen binding by the BCR, the cortical actin network depolymerises to enable interaction with other BCRs<sup>228</sup>. Afterwards, actin reassembles at the formed BCR microclusters, leading to polarisation and expanding of the B cell in order to increase the contact area with the antigen surface<sup>228,229</sup>. However, all of these processes take place within the cell and usually no extracellular actin is presented to initially activate the B cell.

A potential antigenic source of  $\beta$ -actin might derive from activated platelets<sup>230,231</sup>. It was shown that incubation of platelets with thrombin leads to an increased amount of surface actin<sup>230,231</sup>. Since platelets are formed in the bone marrow and persistently flow through the bloodstream, it is possible that MCL (progenitor) B cells come into contact with surface actin<sup>232</sup>. Such mechanism would allow an ongoing activation of the B cell, which could lead towards tumour development.

A similar pathogenic process was described in other NHLs, mainly CLL, for other proteins forming the cytoskeleton<sup>233</sup>. A well-investigated cytoskeletal auto-antigen is vimentin, a structural protein forming intermediate filaments<sup>234</sup>. It was long thought to be an exclusively intracellular protein but it was shown that it is also secreted as a result of inflammatory signals<sup>235</sup>. Vimentin was found to be a potential auto-antigen in CLL as well as other NHLs including MCL<sup>112,224,233</sup>. However, in contrast

to the published data and the CLL-derived Ig014 and Ig044 used here, none of the MCL-derived Igs in the cohort of this study bound vimentin in WB (4.2.9).

Nevertheless, at least a subset of MCL-BCRs might be activated by proteins of the cytoskeleton. Regarding the very filamentous immunofluorescence staining of MCL2, it is possible that also this Ig binds to a cytoskeletal or associated protein. The reason why MCL2 and MCL11 did not precipitate an antigen, although they reacted in the immunofluorescence assay, remains unclear. However, it could be possible, that the concentration of the potential antigen was too low in the RIPA lysate or that the antigen could not be isolated with the RIPA buffer. Since the lymphoma Igs probably had low affinities for their respective epitope, the high detergent concentration in the RIPA buffer may also have impaired the precipitation abilities of those Igs.

### **5.2.4 The NADP-dependent malic enzyme is a potential antigen recognised by MCL B cell receptors**

Besides HEp2-cell lysates also other lysates were used to find novel antigens of the MCL-Igs. Using murine lymph node lysates, MCL12 precipitated a protein with a molecular weight between 54 and 70 kDa (4.2.7). This protein was identified as the NADP-dependent malic enzyme, a protein which generates NADPH for the fatty acid biosynthesis<sup>236</sup>. Due to the high similarity between the human and the murine variant, it was regarded as a potential antigen. According to the Human Protein Atlas ([www.proteinatlas.org](http://www.proteinatlas.org)) the human metastatic breast adenocarcinoma cell line SK-BR3 should express this protein<sup>237,238</sup>. However, none of the performed IPs precipitated the NADP-dependent malic enzyme. Moreover, MCL12 as well as MCL22 precipitated  $\beta$ -actin from this cell lysate. It remains unknown why the NADP-dependent malic enzyme was obtained from murine lymph node lysate but not from human cell line lysates.

### **5.2.5 MCL-Igs did not recognise themselves**

Studies with CLL-BCRs demonstrated a potential activation of the BCR by “antigen-independent cell autonomous signalling”<sup>113</sup>. In these cases, the Igs bind to an endogenous epitope within the BCR itself<sup>114</sup>. As a result, the CLL progenitor B cell becomes chronically activated, which finally leads to tumour development. While self-recognition plays a major role in the pathogenesis of CLL, experiments with MCL BCRs showed no cell autonomous signalling<sup>113</sup>. Nevertheless, the produced recombinant MCL-Igs were tested whether they might bind themselves.

In order to answer this question, it was measured whether recombinant antibodies in solution are bound to each other. Since every Ig has two antigen binding sites, a self-reactive antibody could recruit two other Igs, leading towards the formation of large aggregates. To detect these aggregated

proteins in solution, dynamic light scattering measurements were performed. This technique measures the fluctuation of the scattered light intensity, which allows the calculation of the translational diffusion coefficient<sup>193</sup>. Applying the Stokes-Einstein equation, the particle size of a hypothetical spherical protein could be calculated<sup>193</sup>.

A spherical protein of about 150 kDa should have a hydrodynamic radius of about 6 nm at room temperature in water and nearly all MCL-IgG were in line with the expectations. MCL11, however, showed a slightly increased hydrodynamic radius. Since antibodies are not spherical, this might be an overestimation but still showed a deviation of the patterns observed with the other IgG. Nevertheless, cross-linking of the IgG with an anti-human-IgG antibody led to much larger aggregates with radii over 20 nm. As a result, self-recognition of the IgG can be excluded for all but one MCL-BCR.

Interestingly, also the CLL-derived IgG showed no self-aggregation in this setting. This either indicate that these IgG does not recognise themselves, that soluble IgG not completely met the steric needs which are present on the cell surface or further molecules on the cell membrane are required for aggregation. Another possibility is that the CLL-IgG recognise an epitope in the constant region instead of an epitope in the variable regions. Since all recombinant IgG harboured the IgG isotype but all MCL- and also some CLL-BCRs were constituted of IgM, it might limit the significance of the DLS results. Nevertheless, under the given circumstances, the DLS experiment indicated no self recognition for the tested antibodies.

The reason for the different scatter behaviour of MCL11 remains elusive and could indicate a weak self-binding IgG. However, cells harbouring the variable regions of this IgG on the cell surface were not persistently activated and remained inducible by anti-Fab-antibodies (5.5). This, in turn, contradicts the possibility of self-recognition, since the cells would be either permanently activated or would downregulate the signalling molecules, rendering the cell unresponsive.

### **5.2.6 Possible high throughput methods for antigen detection**

The identification of a new antigen for a given antibody is a challenging process. Limited knowledge about a potential source of the searched proteins and an unknown affinity of the individual IgG makes predictions of valuable antigen sources very difficult. In this study, phage display screenings and the comparison with other NHLs with known antigens were used to narrow down the nearly unlimited field of antigens. Nevertheless, only in two out of eleven cases, potential antigens were identified and only three phage display selections returned specific phages. As outlined before, phage display techniques have some major drawbacks if used as a tool for identification of a distinct unknown antigen (5.2.1). In addition, immunofluorescence assays,

Western Blots and immunoprecipitations are very time demanding techniques and often do not result in the identification of a specific protein.

To address some of the disadvantages, protein microarrays could be used <sup>239</sup>. This technique enables the screening of an antibody against a large amount of proteins within a much shorter time period and higher sensitivity <sup>239,240</sup>. Besides a faster screening, it would also be possible to quickly determine potential cross-reactivity of the tested antibodies <sup>240</sup>. Using Igs, derived from primary lymphoma of the central nervous system (PCNSL) patients, microarrays have already been used successfully to determine specific antigens of PCNSL-Igs <sup>241</sup>. It is likely that this technique could also lead to the detection of (auto-)antigens in other NHL-entities like MCL.

Unfortunately, due to the high price of microarrays, it was not possible to make use of it and screen the MCL-Igs. Further studies, however, should take advantage of this promising high-throughput technique.

### **5.3 Bacterial superantigens bind to MCL-Igs**

The poor phage enrichments and the difficulties in identifying potential antigens led to the consideration whether superantigens might be involved during MCL pathogenesis. Superantigens are special antigens, which are bound by the Igs independently from the CDRs (1.4) <sup>173</sup>. The minimally mutated or unmutated BCR-repertoire and the overuse of IGHV3-genes pointed towards the staphylococcal protein A (SpA) as a possible MCL superantigen (1.4.1).

SpA has a clearly characterised binding site within the framework region of IGHV3 harbouring Igs <sup>180</sup>. Thus, MCL-Igs in the cohort, harbouring these heavy chains were screened for the presence of the motif and it was shown that all of them presented it without deviations (4.3.1). In contrast, 4 out of 6 (66%) FL- and 4 out of 7 (57%) CLL-samples harbouring IGHV3-genes, had at least one mutation within the SpA-motif.

Since the cohort size might be too small to allow general conclusions, sequences published by Hadzidimitriou et al. <sup>149</sup> were also screened for the presence of the unmutated motif. This dataset included only the mutated IGHV3-21 and IGHV3-23 genes, which accounted for 127 sequences in total. Within this cohort, 31 sequences (24.4%) had at least one mutation in the motif. It was demonstrated that a single mutation within the motif did not result in a complete lack of binding with the only exception of mutations which would result in electrostatic repulsion (like a K65E-mutation) <sup>174</sup>. Taken this observation into account, only 9 out of 127 (7%) samples might have lost the ability to bind SpA. In turn, this highlighted that the great majority of MCL-Igs, even the mutated ones, preserved the SpA-binding motif. Moreover, about 40% of the IGHV3-21 and 17%

of the IGHV3-23 sequences were completely unmutated and therefore also harboured the SpA motif. Including the unmutated cases, less than 5% of the published IGHV3-21 and IGHV3-23 sequences might have lost the ability to bind SpA.

To confirm that the presence of this motif results in the binding of SpA, an ELISA was performed. A total of 9 representative Fabs with and without the motif were generated to circumvent the high affinity of SpA to the F<sub>C</sub> domain of IgGs. As expected, all Fabs harbouring the motif bound to SpA and the single mutation in the CLL83-Ig did not interfere with the binding. In contrast, FL10, bearing three mutations within the motif, was completely non-reactive and therefore regarded as motif-negative.

Having established that all IGHV3 MCL-Igs in the cohort were able to interact with SpA, the next step was to check if SpA is able to cross-link BCRs on the cell surface. Due to the lack of primary material, it became necessary to establish a cell system capable of expressing a functional BCR (see 5.5). The variable regions of two samples (MCL11 and MCL19) were cloned into a vector and transduced into BCR-negative Ramos cells. The Ca<sup>2+</sup>-influx into the cells was used as readout system for B cell activation and thus for the BCR cross-linking.

When treated with SpA, only cells transduced with the motif-positive MCL11-Ig were activated, while cells harbouring the motif-negative MCL19 Ig did not react upon stimulation. This proved that SpA not only binds to the susceptible Igs but also can cross-link the BCRs and, as a consequence, is able to alter the behaviour of a B cell.

Finally, to confirm that the observed cell activation after SpA treatment also occur in MCL-derived cells, the MCL cell lines MAVER-1 and Jeko-1 were used for Ca<sup>2+</sup>-flux experiments. It had been shown previously, that MAVER-1 cells express the unmutated IGHV3-9 gene and therefore present the SpA motif<sup>201</sup>. On the other hand, Jeko-1 cells express the unmutated IGHV2-70 gene and do not harbour the motif<sup>201</sup>. In both cell lines, the addition of an anti-human-Fab antibody, resulted in increase of the intracellular Ca<sup>2+</sup>-level, which indicated the induction of the cells via the BCR. Furthermore, only the MAVER-1 cell line showed an alteration of the Ca<sup>2+</sup>-level after treatment with SpA. This experiment demonstrated two things. First, SpA is able to activate IGHV3-expressing MCL-derived cell lines, which indicates a potential involvement of SpA during tumour development. Second, the established Ramos-based cell system can be used as a versatile tool to analyse the activation of specific BCRs without the need of distinct cell lines or primary material expressing the particular Ig.

It is important to note that the binding of SpA to the framework region did not interfere with the antigen binding site of the Ig<sup>174</sup>. For that reason, it remains possible that a (lymphoma) B cell is

activated by SpA although the Ig has a high (or low) affinity for a different antigen bound by the paratope. Therefore, the demonstrated protein precipitations and positive auto-antigen staining with HEp-2 cells are not contradictory to the proposed superantigenic stimulation.

*In vivo* experiments already demonstrated that (i.p administered) SpA quickly navigates to lymphoid sites in mice and is bound by B cells <sup>242</sup>. It was further shown that stimulating human blood cells with SpA *in vitro* resulted in a strongly biased IgM repertoire, with only IGHV3-expressing B cells proliferating <sup>176</sup>. In contrast, B cell stimulation with SpA in mice led to a loss of IGHV3-expressing B cells, possibly due to overconsumption of cytokines and the lack of secondary signals <sup>242</sup>. Taken into account that a MCL progenitor B cell must have acquired multiple mutations before it became a cancer cell, it is conceivable that this cell could have overcome the lack of signals from the surroundings and is therefore able to proliferate.

As outlined above, up to 50% of healthy individuals are temporarily colonised with *Staphylococcus aureus* (1.4.1) <sup>171</sup>. Therefore, it is a plausible scenario that at least the IGHV3 harbouring subset of MCL patients may have faced an *S. aureus* infection. Since the development of a B cell neoplasia is a multi-step process this infection must probably take place at a critical point in time during B cell development to affect the mutated cell. However, whether a persistent colonisation is necessary or if a single SpA contact might be sufficient to induce the disease, cannot be answered at this point. In this study, it was not possible to investigate whether the MCL patients were colonised by *S. aureus* or not. Future studies, however, should also test for an ongoing infection with this pathogen in the patient.

### 5.4 MCL-Igs might be susceptible for further superantigens

Besides the binding site for SpA, further superantigen binding sites were found in MCL-Igs. For instance, carbohydrate I/i, present on red blood cells, binds to a hydrophobic patch within the framework region 1 of the IGHV4-34 heavy chains <sup>243</sup>. All five samples in this study expressing this gene were positive for the binding motif. The analysis of the much larger cohort published by Hadzidimitriou et al. <sup>149</sup>, as done for the SpA motif, revealed that 77 out of 78 (98.7%) Igs presented this motif. More remarkably, this dataset only included samples with mutated sequences accounting for 67.8% of all IGHV4-34 sequences in the cohort. The remaining 32.2% must also contain this motif since it is germline-coded.

Taken together, 66.67% of the Igs in the MCL cohort presented here expressed either an IGHV3- or the IGHV4-34-gene (Hadzidimitriou et al. cohort: 66.17%). Most of them preserved the binding capability to bind to SpA or carbohydrate I/i, respectively. If this observation can be confirmed by



further data, about two thirds of all MCL cases could be associated with exo- and endogenous superantigens.

Protein L (PpL), produced by *Peptostreptococcus magnus*, is an antigen targeting the specific families (IGKV1, IGKV3 and IGKV4) of the  $\kappa$ - but not  $\lambda$ -light chains<sup>180</sup>. In this cohort, 36.4% (in total 8) of the MCL samples carrying these light chains, with 5 out of these 8 also harbouring the SpA motif. The SpA and PpL binding sites are far away from each other and a simultaneous binding of both superantigens would be sterically possible<sup>180</sup>. However, as described above, in this study as well as in previous studies the  $\lambda/\kappa$ -ratio in MCL was biased towards the  $\lambda$ -isotype<sup>123,148,213</sup>. Therefore, PpL might be involved only in a small subset compared to SpA.

To date, pathogen infections can be linked to some cancers. A prominent example is the association between human papillomavirus (HPV) infection and cervix carcinoma<sup>244</sup>. Furthermore, in mucosa-associated lymphoid tissue (MALT) lymphoma, *Helicobacter pylori* colonisation plays an important role in pathogenesis<sup>245</sup>. It was shown that a complete eradication of this pathogen sometimes led to a complete remission of this cancer<sup>245,246</sup>. These remarkable findings suggest a chance for cancer prevention or treatment by the identification and elimination of cancer causing pathogen.

The results presented in this study indicate the possibility of an involvement of an external pathogen in lymphoma development. Nevertheless, further evidence for a link between superantigen recognition and lymphoma pathogenesis in MCL must be found. Thus, future studies have to evaluate if superantigens are present during lymphoma progression and if the elimination of them results in a more favourable course of the disease.

## 5.5 Development of a cellular readout system for BCR activation

The activation of the BCR signalling cascade requires the cross-linking of two separate BCR complexes. For that reason, not every molecule is capable to induce intracellular signalling (1.2.5). Using recombinant antibodies is a helpful tool to identify potential antigens since large amounts can be produced and they are easy to handle. However, using a cellular readout system, effectively demonstrating an ongoing B cell activation, would be useful to prove the functional antigenic potential of a specific antigen. Therefore, one part of this project was the development of a cellular system expressing an inducible BCR with the Ig variable regions of MCL patient samples. This would widen the experimental possibilities without the need for a large supply of primary tissue, especially for rare diseases like MCL. It also enables the opportunity to discover unusual activation mechanisms as shown for the self-activation in CLL<sup>113,115</sup>.

### 5.5.1 Ramos cells could be activated by a transduced IgM

Since the BCR signalling highly depends on the coordinated action of multiple proteins, it was decided to use a B cell line already expressing these proteins. The Burkitt lymphoma-derived cell lines DG75, Namalwa.CSN/70, and Ramos were repeatedly sorted against surface Ig expression but only Ramos cells remained negative for surface IgM after sorting.

To distinguish between endogenous and transduced IgM the introduced IgM consisted of a murine constant region. Previous work had already demonstrated that the combination of murine constant regions and human variable regions did not interfere with the binding and activation ability of such chimeric BCRs<sup>113,115</sup>. The cells were lentivirally transduced, to achieve high gene transfer efficiency.

To establish the system, the Ig sequences of two MCL (MCL11, MCL19) samples were used. With stably transduced B cells bearing the chimeric BCR on the surface, it was proven that the introduced BCR is inducible. This was measured by Ca<sup>2+</sup>-influx as readout<sup>84,195</sup>. The cross-linking of two Igs by an anti-human-Fab antibody finally led to a strong increase of the intracellular Ca<sup>2+</sup>-level, which demonstrated a functioning signalling of the transduced IgM. In contrast, untransduced cells showed no reaction upon anti-Fab stimulation, further demonstrating the complete removal of endogenous surface Igs.

Using this new technique, it was further possible to confirm SpA as a superantigen able to activate B cells harbouring susceptible BCRs (5.3). Finally, this system also helped to falsify a potential self-recognition of the MCL11-Ig (5.2.5).

### 5.5.2 Induction of the introduced BCR altered the cell behaviour

The activation of the BCR signalling cascade requires multiple phosphorylation steps to alter the cell behaviour. Instead of using site-specific anti-phosphotyrosine antibodies, it was chosen to use SH2-profiling to characterise the phosphorylation state after BCR cross-linking<sup>202,247</sup>. This technique uses Src Homology 2 (SH2)-domains to recognise phosphorylated motifs<sup>247</sup>. Thus, it allows to globally analyse altered phosphorylation patterns even without sufficient knowledge about the affected pathways and the need for specific antibodies<sup>247</sup>.

As expected, the phosphorylation patterns differed between activated and non-activated B cells. With both used phosphoproboscopes (GRB2 and SHP2), one specific band showed a stronger signal in activated cells compared to untreated or untransduced ones. This band was above 160 kDa for the GRB2 probe and below 160 kDa for the SHP2 probe. Interestingly, treating the cells with an anti-mouse-IgM seemed to have a much larger impact on the phosphorylation of the respective proteins

than a treatment with an anti-human-Fab antibody. This became especially apparent during activation of the MCL19-transduced Ramos cells. Probed with the SHP2-domain, a single band had a very strong intensity only present in the anti-mouse-IgM treated cells. The same band was also slightly stronger in MCL11-transduced cells treated with anti-human-IgM as well as SpA. However, it remained elusive why the incubation with an anti-human-Fab-antibody altered the phosphorylation pattern detected by GRB2 but not by SHP2.

Importantly, the phospho-proteome analysis was performed after 2 h of stimulation. This demonstrates a long lasting effect following the BCR activation with a potential alteration in cell behaviour. Finally, it also provided an additional prove that SpA activates the B cells in a similar manner as cross-linking by an anti-IgM antibody and thus as a classical antigen does.

Nevertheless, the disadvantage of the SH2-profiling is the lack of information which proteins are actually phosphorylated<sup>247</sup>. Since the transduced protein was an IgM which most likely resulted in the assembly of a BCR, the phosphorylated proteins were probably part of the BCR signalling cascade. However, a subsequent analysis using antibodies or mass spectrometry should be performed in future studies to unravel the involved pathways and proteins.

Finally, it was tried to enhance the proliferation of the transduced cells by supplementing either an antibody able to cross-link the BCRs or using SpA as an antigen. In contrast to an *in vitro* study demonstrating the proliferation of IGHV3 harbouring B cells, no additional cytokines (besides FBS) or T cells were provided to aid the cell proliferation after incubation with SpA<sup>176</sup>. The observation of cell growth over 10 days revealed that cells induced by an anti-mouse-IgM antibody grew much slower than untreated cells. In addition, treated with SpA for 10 days, MCL11-Ramos cells proliferated in the same way as MCL11-cells activated by the anti-mouse-IgM antibody. In contrast, cells transduced with the MCL19-Ig and treated with SpA showed no proliferation delay compared to untreated cells. Although it was expected that the activation of the BCR signalling pathway lead to an accelerated proliferation of the cells, the results of the proliferation assay are consistent with the other SpA experiments. It clearly showed that only the MCL11-derived Ig was affected by SpA. One reason for the observed decrease of the proliferation rate might be the shortage of obligatory signals and cytokines which become necessary following the activation. Furthermore, the observation is in line with studies performed in CLL and other lymphoma cell lines<sup>248-250</sup>. These publications demonstrated a growth inhibition after the sole activation of the IgM signalling cascade but not the IgD pathway<sup>248-250</sup>. The Ramos cells used here are only transduced with an IgM. Therefore, a similar inhibition is likely in this setup. However, a more recent paper claimed that sustained anti-IgM stimulation with immobilised anti-IgM-antibodies promotes survival while

soluble antibodies induce apoptosis<sup>251,252</sup>. Since the Ramos cells were only treated with a soluble antibody or antigen this might also be a possible explanation. Further experiments must check for differences if the cells were either incubated with soluble or immobilised antigens.

Nevertheless, the Ramos cell system established in this study may provide a valuable new tool for the analysis of BCR activation without the need of primary material. It might further enable the analysis of intracellular reactions to a given antigen as well as observations over of longer period of time compared to primary cells.

## 5.6 Conclusion and Outlook

This study aimed to provide additional insights to the pathogenesis of mantle cell lymphoma and to find novel antigens of the MCL-B cell receptors. The results of the study confirmed previously published findings which showed a heavily biased BCR-repertoire, indicating an antigen-driven tumourigenesis of this disease<sup>138,146,149,150</sup>. Moreover, this study showed the genetic stability of the MCL-derived immunoglobulin over a long period of time. Since this result was based only on a single patient, additional research is necessary to determine whether the observed absence of ongoing Ig-mutations is typical for MCL. For that reason, future studies should acquire multiple patient samples at different points in time and investigate potential changes of the MCL-Ig over a longer period of time. Next-Generation Sequencing seems to be a suitable tool to analyse the Ig-repertoire changes in large detail and scale.

In addition, this study proposed the staphylococcal protein A as a potential superantigen for a large proportion of MCL samples. It was demonstrated that SpA is able to activate the susceptible B cells. As a consequence, the results indicate that an infection with *Staphylococcus aureus* might trigger or promote the development of MCL. Since mouse models of MCL are scarce, it is actually planned to administer SpA to a murine Burkitt lymphoma model<sup>253</sup>. If the lymphoma Ig-repertoire in the SpA-treated mice develop a bias towards the IGHV3-gene-usage as well, this experiment would provide further support for the involvement of SpA in the lymphoma genesis. However, additional research will be necessary to investigate if a persistent colonisation is required for the malignant transformation, or if a temporary *S. aureus* infection might be sufficient. Moreover, future studies should examine whether MCL patients are colonised by *S. aureus* or had an *S. aureus* infection in the past. In addition, it should be evaluated whether SpA is present in the tumour tissue and if infected MCL patient benefit from an eradication of *S. aureus*.

Since SpA activates exclusively IGHV3-expressing B cells, only half of the MCL-cohort might be affected by an *S. aureus* infection. However, it was shown that the over-represented IGHV4-34-

expressing MCL subgroup presented a superantigen binding motif, as well. Thus, it is possible that a superantigen recognition might represent a general mechanism in the MCL tumourigenesis and should be investigated in further detail. Moreover, also other Non-Hodgkin lymphoma, like the chronic lymphocytic leukaemia, showed biased Ig-repertoires<sup>108</sup>. A possible superantigen involvement should be elucidated in these entities, as well. This could foster our knowledge about differences and similarities in the development of the different NHL entities.

Finally, the present study has also shown that some MCL-Igs bind auto-antigens expressed by HEp-2 cells. The NADP-dependent malic enzyme and  $\beta$ -actin were identified as potential antigens for at least a few MCL-Igs. As a next step, these Igs should be transduced into the BCR-negative Ramos cells to examine if the identified antigens are able to activate the respective MCL-B cells. Since superantigen binding does not impair the antigen-binding site<sup>173</sup>, a CDR-dependent binding of antigens would not contradict the theory of a superantigen involvement during MCL development. However, it highlights the necessity to further investigate at which critical point in time a CDR-independent B cell activation is needed and if the absence of this stimulus might be compensated by the binding of auto-antigens in later stages.

To conclude, the data presented in this study indicate a significant role of superantigens in MCL and may provide the basis to gain further insights to the genesis and progression of this largely incurable disease.

## 6 References

1. Akira, S., Uematsu, S. & Takeuchi, O. Pathogen Recognition and Innate Immunity. *Cell* **124**, 783–801 (2006).
2. Martin, S. F. Adaptation in the innate immune system and heterologous innate immunity. *Cell. Mol. Life Sci. CMLS* **71**, 4115–4130 (2014).
3. Janeway, C. A. & Medzhitov, R. Innate immune recognition. *Annu. Rev. Immunol.* **20**, 197–216 (2002).
4. Gordon, S. Pattern Recognition Receptors: Doubling Up for the Innate Immune Response. *Cell* **111**, 927–930 (2002).
5. Portou, M. J., Baker, D., Abraham, D. & Tsui, J. The innate immune system, toll-like receptors and dermal wound healing: A review. *Vascul. Pharmacol.* **71**, 31–36 (2015).
6. Mancini, R. J., Stutts, L., Ryu, K. A., Tom, J. K. & Esser-Kahn, A. P. Directing the immune system with chemical compounds. *ACS Chem. Biol.* **9**, 1075–1085 (2014).
7. Cooper, M. D. & Alder, M. N. The Evolution of Adaptive Immune Systems. *Cell* **124**, 815–822 (2006).
8. Cooper, M. D., Peterson, R. D. A. & Good, R. A. Delineation of the Thymic and Bursal Lymphoid Systems in the Chicken. *Nature* **205**, 143–146 (1965).
9. Hirano, M., Das, S., Guo, P. & Cooper, M. D. The evolution of adaptive immunity in vertebrates. *Adv. Immunol.* **109**, 125–157 (2011).
10. den Haan, J. M. M., Arens, R. & van Zelm, M. C. The activation of the adaptive immune system: Cross-talk between antigen-presenting cells, T cells and B cells. *Immunol. Lett.* **162**, 103–112 (2014).
11. Alberts, B. *et al.* *Molecular Biology of the Cell*. (Garland Science, 2002).
12. Hardy, R. R. & Hayakawa, K. B cell development pathways. *Annu. Rev. Immunol.* **19**, 595–621 (2001).
13. Adolfsson, J. *et al.* Upregulation of Flt3 Expression within the Bone Marrow Lin<sup>−</sup>Sca1<sup>+</sup>c-kit<sup>+</sup> Stem Cell Compartment Is Accompanied by Loss of Self-Renewal Capacity. *Immunity* **15**, 659–669 (2001).
14. Pelayo, R., Welner, R. S., Nagai, Y. & Kincade, P. W. Life before the pre-B cell receptor checkpoint: Specification and commitment of primitive lymphoid progenitors in adult bone marrow. *Semin. Immunol.* **18**, 2–11 (2006).
15. Akashi, K., Traver, D., Miyamoto, T. & Weissman, I. L. A clonogenic common myeloid progenitor that gives rise to all myeloid lineages. *Nature* **404**, 193–197 (2000).
16. Tudor, K.-S. R. S., Payne, K. J., Yamashita, Y. & Kincade, P. W. Functional Assessment of Precursors from Murine Bone Marrow Suggests a Sequence of Early B Lineage

- Differentiation Events. *Immunity* **12**, 335–345 (2000).
17. Igarashi, H., Gregory, S. C., Yokota, T., Sakaguchi, N. & Kincade, P. W. Transcription from the RAG1 Locus Marks the Earliest Lymphocyte Progenitors in Bone Marrow. *Immunity* **17**, 117–130 (2002).
  18. Allman, D., Li, J. & Hardy, R. R. Commitment to the B lymphoid lineage occurs before DH-JH recombination. *J. Exp. Med.* **189**, 735–740 (1999).
  19. Ogawa, M., ten Boekel, E. & Melchers, F. Identification of CD19(-)B220(+)c-Kit(+)Flt3/Flk-2(+)cells as early B lymphoid precursors before pre-B-I cells in juvenile mouse bone marrow. *Int. Immunol.* **12**, 313–324 (2000).
  20. Ochiai, K. *et al.* A self-reinforcing regulatory network triggered by limiting IL-7 activates pre-BCR signaling and differentiation. *Nat. Immunol.* **13**, 300–307 (2012).
  21. Reth, M. Antigen receptors on B lymphocytes. *Annu. Rev. Immunol.* **10**, 97–121 (1992).
  22. Ubelhart, R. *et al.* N-linked glycosylation selectively regulates autonomous precursor BCR function. *Nat. Immunol.* **11**, 759–765 (2010).
  23. Karasuyama, H., Kudo, A. & Melchers, F. The proteins encoded by the VpreB and lambda 5 pre-B cell-specific genes can associate with each other and with mu heavy chain. *J. Exp. Med.* **172**, 969–972 (1990).
  24. Karasuyama, H., Rolink, A. & Melchers, F. A complex of glycoproteins is associated with VpreB/lambda 5 surrogate light chain on the surface of mu heavy chain-negative early precursor B cell lines. *J. Exp. Med.* **178**, 469–478 (1993).
  25. Herzog, S. & Jumaa, H. Self-recognition and clonal selection: autoreactivity drives the generation of B cells. *Curr. Opin. Immunol.* **24**, 166–172 (2012).
  26. Hardy, R. R. & Hayakawa, K. Positive and negative selection of natural autoreactive B cells. *Adv. Exp. Med. Biol.* **750**, 227–238 (2012).
  27. MacLennan, I. C. M. Germinal Centers. *Annu. Rev. Immunol.* **12**, 117–139 (1994).
  28. Melchers, F. Checkpoints that control B cell development. *J. Clin. Invest.* **125**, 2203–2210 (2015).
  29. Nieuwenhuis, P. & Opstelten, D. Functional anatomy of germinal centers. *Am. J. Anat.* **170**, 421–435 (1984).
  30. Schwickert, T. A. *et al.* In vivo imaging of germinal centres reveals a dynamic open structure. *Nature* **446**, 83–87 (2007).
  31. Cyster, J. G. *et al.* Follicular stromal cells and lymphocyte homing to follicles. *Immunol. Rev.* **176**, 181–193 (2000).
  32. Victora, G. D. & Nussenzweig, M. C. Germinal Centers. *Annu. Rev. Immunol.* **30**, 429–457 (2012).
  33. Basso, K. *et al.* Integrated biochemical and computational approach identifies BCL6 direct

## References

---

- target genes controlling multiple pathways in normal germinal center B cells. *Blood* **115**, 975–984 (2010).
34. Schroeder, H. W. & Cavacini, L. Structure and Function of Immunoglobulins. *J. Allergy Clin. Immunol.* **125**, S41–S52 (2010).
  35. Gray, D. Immunological memory. *Annu. Rev. Immunol.* **11**, 49–77 (1993).
  36. Shapiro-Shelef, M. & Calame, K. Regulation of plasma-cell development. *Nat. Rev. Immunol.* **5**, 230–242 (2005).
  37. McHeyzer-Williams, M. G. B cells as effectors. *Curr. Opin. Immunol.* **15**, 354–361 (2003).
  38. Dal Porto, J. M. *et al.* B cell antigen receptor signaling 101. *Mol. Immunol.* **41**, 599–613 (2004).
  39. Williams, A. F. & Barclay, A. N. The immunoglobulin superfamily--domains for cell surface recognition. *Annu. Rev. Immunol.* **6**, 381–405 (1988).
  40. Honjo, T. Immunoglobulin genes. *Annu. Rev. Immunol.* **1**, 499–528 (1983).
  41. Chang, T. W., Wu, P. C., Hsu, C. L. & Hung, A. F. in (ed. Immunology, B.-A. in) **93**, 63–119 (Academic Press, 2007).
  42. Stavnezer, J. & Schrader, C. E. Ig heavy chain class switch recombination: mechanism and regulation. *J. Immunol. Baltim. Md 1950* **193**, 5370–5378 (2014).
  43. Al-Lazikani, B., Lesk, A. M. & Chothia, C. Standard conformations for the canonical structures of immunoglobulins. *J. Mol. Biol.* **273**, 927–948 (1997).
  44. Berg, J. M., Tymoczko, J. L. & Stryer, L. *Stryer Biochemie*. (Spektrum Akademischer Verlag, 2009).
  45. Hombach, J., Tsubata, T., Leclercq, L., Stappert, H. & Reth, M. Molecular components of the B-cell antigen receptor complex of the IgM class. *Nature* **343**, 760–762 (1990).
  46. Siegers, G. M. *et al.* Identification of disulfide bonds in the Ig-alpha/Ig-beta component of the B cell antigen receptor using the Drosophila S2 cell reconstitution system. *Int. Immunol.* **18**, 1385–1396 (2006).
  47. Flaswinkel, H. & Reth, M. Dual role of the tyrosine activation motif of the Ig-alpha protein during signal transduction via the B cell antigen receptor. *EMBO J.* **13**, 83–89 (1994).
  48. Malu, S., Malshetty, V., Francis, D. & Cortes, P. Role of non-homologous end joining in V(D)J recombination. *Immunol. Res.* **54**, 233–246 (2012).
  49. Consortium, I. H. G. S. Finishing the euchromatic sequence of the human genome. *Nature* **431**, 931–945 (2004).
  50. Tonegawa, S. Somatic generation of antibody diversity. *Nature* **302**, 575–581 (1983).
  51. Bassing, C. H., Swat, W. & Alt, F. W. The Mechanism and Regulation of Chromosomal V(D)J Recombination. *Cell* **109**, S45–S55 (2002).



52. Tinguely, A. *et al.* Cross Talk between Immunoglobulin Heavy-Chain Transcription and RNA Surveillance during B Cell Development. *Mol. Cell. Biol.* **32**, 107–117 (2012).
53. Lam, K.-P., Kühn, R. & Rajewsky, K. In Vivo Ablation of Surface Immunoglobulin on Mature B Cells by Inducible Gene Targeting Results in Rapid Cell Death. *Cell* **90**, 1073–1083 (1997).
54. Rajewsky, K. Clonal selection and learning in the antibody system. *Nature* **381**, 751–758 (1996).
55. Muramatsu, M., Nagaoka, H., Shinkura, R., Begum, N. A. & Honjo, T. Discovery of activation-induced cytidine deaminase, the engraver of antibody memory. *Adv. Immunol.* **94**, 1–36 (2007).
56. Maul, R. W. *et al.* Uracil residues dependent on the deaminase AID in immunoglobulin gene variable and switch regions. *Nat. Immunol.* **12**, 70–76 (2011).
57. Saribasak, H. & Gearhart, P. J. Does DNA repair occur during somatic hypermutation? *Semin. Immunol.* **24**, 287–292 (2012).
58. Neuberger, M. S. Antibody diversification by somatic mutation: from Burnet onwards. *Immunol. Cell Biol.* **86**, 124–132 (2008).
59. Cohn, M. *et al.* Reflections on the clonal-selection theory. *Nat. Rev. Immunol.* **7**, 823–830 (2007).
60. Nemazee, D. & Weigert, M. Revising B cell receptors. *J. Exp. Med.* **191**, 1813–1817 (2000).
61. Rolink, A., Grawunder, U., Haasner, D., Strasser, A. & Melchers, F. Immature surface Ig<sup>+</sup> B cells can continue to rearrange kappa and lambda L chain gene loci. *J. Exp. Med.* **178**, 1263–1270 (1993).
62. Wilson, P. C. *et al.* Receptor Revision of Immunoglobulin Heavy Chain Variable Region Genes in Normal Human B Lymphocytes. *J. Exp. Med.* **191**, 1881–1894 (2000).
63. Singer, S. J. & Nicolson, G. L. The fluid mosaic model of the structure of cell membranes. *Science* **175**, 720–731 (1972).
64. Woodruff, M. F., Reid, B. & James, K. Effect of antilymphocytic antibody and antibody fragments on human lymphocytes in vitro. *Nature* **215**, 591–594 (1967).
65. Dintzis, H. M., Dintzis, R. Z. & Vogelstein, B. Molecular determinants of immunogenicity: the immunon model of immune response. *Proc. Natl. Acad. Sci. U. S. A.* **73**, 3671–3675 (1976).
66. Puffer, E. B., Pontrello, J. K., Hollenbeck, J. J., Kink, J. A. & Kiessling, L. L. Activating B cell signaling with defined multivalent ligands. *ACS Chem. Biol.* **2**, 252–262 (2007).
67. Kim, Y.-M. *et al.* Monovalent ligation of the B cell receptor induces receptor activation but fails to promote antigen presentation. *Proc. Natl. Acad. Sci. U. S. A.* **103**, 3327–3332 (2006).
68. Avalos, A. M. *et al.* Monovalent engagement of the BCR activates ovalbumin-specific transnuclear B cells. *J. Exp. Med.* **211**, 365–379 (2014).
69. Yang, J. & Reth, M. The dissociation activation model of B cell antigen receptor triggering.

## References

---

- FEBS Lett.* **584**, 4872–4877 (2010).
70. Yang, J. & Reth, M. Oligomeric organization of the B-cell antigen receptor on resting cells. *Nature* **467**, 465–469 (2010).
  71. Kläsener, K., Maity, P. C., Hobeika, E., Yang, J. & Reth, M. B cell activation involves nanoscale receptor reorganizations and inside-out signaling by Syk. *eLife* **3**, e02069 (2014).
  72. Kurosaki, T. Genetic Analysis of B Cell Antigen Receptor Signaling. *Annu. Rev. Immunol.* **17**, 555–592 (1999).
  73. Engels, N., Wollscheid, B. & Wienands, J. Association of SLP-65/BLNK with the B cell antigen receptor through a non-ITAM tyrosine of Ig- $\alpha$ . *Eur. J. Immunol.* **31**, 2126–2134 (2001).
  74. Sohn, H. W., Tolar, P. & Pierce, S. K. Membrane heterogeneities in the formation of B cell receptor-Lyn kinase microclusters and the immune synapse. *J. Cell Biol.* **182**, 367–379 (2008).
  75. Weber, M. *et al.* Phospholipase C-gamma2 and Vav cooperate within signaling microclusters to propagate B cell spreading in response to membrane-bound antigen. *J. Exp. Med.* **205**, 853–868 (2008).
  76. Depoil, D. *et al.* CD19 is essential for B cell activation by promoting B cell receptor-antigen microcluster formation in response to membrane-bound ligand. *Nat. Immunol.* **9**, 63–72 (2008).
  77. O'Rourke, L. M. *et al.* CD19 as a membrane-anchored adaptor protein of B lymphocytes: costimulation of lipid and protein kinases by recruitment of Vav. *Immunity* **8**, 635–645 (1998).
  78. Fruman, D. A. Phosphoinositide 3-kinase and its targets in B-cell and T-cell signaling. *Curr. Opin. Immunol.* **16**, 314–320 (2004).
  79. Scharenberg, A. M. *et al.* Phosphatidylinositol-3,4,5-trisphosphate (PtdIns-3,4,5-P3)/Tec kinase-dependent calcium signaling pathway: a target for SHIP-mediated inhibitory signals. *EMBO J.* **17**, 1961–1972 (1998).
  80. Takata, M. & Kurosaki, T. A role for Bruton's tyrosine kinase in B cell antigen receptor-mediated activation of phospholipase C-gamma 2. *J. Exp. Med.* **184**, 31–40 (1996).
  81. Kim, Y. J., Sekiya, F., Poulin, B., Bae, Y. S. & Rhee, S. G. Mechanism of B-Cell Receptor-Induced Phosphorylation and Activation of Phospholipase C- $\gamma$ 2. *Mol. Cell. Biol.* **24**, 9986–9999 (2004).
  82. Faccio, R. & Cremasco, V. PLC $\gamma$ 2: where bone and immune cells find their common ground: PLC $\gamma$ 2 in bone and immune cells. *Ann. N. Y. Acad. Sci.* **1192**, 124–130 (2010).
  83. Luik, R. M., Wang, B., Prakriya, M., Wu, M. M. & Lewis, R. S. Oligomerization of STIM1 couples ER calcium depletion to CRAC channel activation. *Nature* **454**, 538–542 (2008).
  84. Stathopulos, P. B. & Ikura, M. Structurally delineating stromal interaction molecules as the endoplasmic reticulum calcium sensors and regulators of calcium release-activated calcium entry. *Immunol. Rev.* **231**, 113–131 (2009).

85. Hashimoto, A. *et al.* Involvement of Guanosine Triphosphatases and Phospholipase C- $\gamma$ 2 in Extracellular Signal-regulated Kinase, c-Jun NH<sub>2</sub>-terminal Kinase, and p38 Mitogen-activated Protein Kinase Activation by the B Cell Antigen Receptor. *J. Exp. Med.* **188**, 1287–1295 (1998).
86. Dolmetsch, R. E., Lewis, R. S., Goodnow, C. C. & Healy, J. I. Differential activation of transcription factors induced by Ca<sup>2+</sup> response amplitude and duration. *Nature* **386**, 855–858 (1997).
87. Healy, J. I. *et al.* Different Nuclear Signals Are Activated by the B Cell Receptor during Positive Versus Negative Signaling. *Immunity* **6**, 419–428 (1997).
88. Engels, N. *et al.* Recruitment of the cytoplasmic adaptor Grb2 to surface IgG and IgE provides antigen receptor-intrinsic costimulation to class-switched B cells. *Nat. Immunol.* **10**, 1018–1025 (2009).
89. Engels, N. *et al.* The immunoglobulin tail tyrosine motif upgrades memory-type BCRs by incorporating a Grb2-Btk signalling module. *Nat. Commun.* **5**, 5456 (2014).
90. Martin, S. W. & Goodnow, C. C. Burst-enhancing role of the IgG membrane tail as a molecular determinant of memory. *Nat. Immunol.* **3**, 182–188 (2002).
91. Horikawa, K. *et al.* Enhancement and suppression of signaling by the conserved tail of IgG memory-type B cell antigen receptors. *J. Exp. Med.* **204**, 759–769 (2007).
92. Dogan, I. *et al.* Multiple layers of B cell memory with different effector functions. *Nat. Immunol.* **10**, 1292–1299 (2009).
93. Küppers, R. Mechanisms of B-cell lymphoma pathogenesis. *Nat. Rev. Cancer* **5**, 251–262 (2005).
94. Nogai, H., Dörken, B. & Lenz, G. Pathogenesis of Non-Hodgkin's Lymphoma. *J. Clin. Oncol.* **29**, 1803–1811 (2011).
95. Jemal, A., Siegel, R., Xu, J. & Ward, E. Cancer Statistics, 2010. *CA. Cancer J. Clin.* **60**, 277–300 (2010).
96. Non-Hodgkin lymphoma statistics. *Cancer Research UK* (2015). Available at: <http://www.cancerresearchuk.org/health-professional/non-hodgkin-lymphoma-statistics>. (Accessed: 2nd March 2016)
97. Shankland, K. R., Armitage, J. O. & Hancock, B. W. Non-Hodgkin lymphoma. *The Lancet* **380**, 848–857 (2012).
98. Chiu, B. C.-H. & Hou, N. Epidemiology and etiology of non-hodgkin lymphoma. *Cancer Treat. Res.* **165**, 1–25 (2015).
99. Guerard, E. J. & Bishop, M. R. Overview of Non-Hodgkin's Lymphoma. *Dis. Mon.* **58**, 208–218 (2012).
100. Ondrejka, S. L. & Hsi, E. D. Pathology of B-cell lymphomas: diagnosis and biomarker discovery. *Cancer Treat. Res.* **165**, 27–50 (2015).

## References

---

101. Dölken, G., Illerhaus, G., Hirt, C. & Mertelsmann, R. BCL-2/JH rearrangements in circulating B cells of healthy blood donors and patients with nonmalignant diseases. *J. Clin. Oncol. Off. J. Am. Soc. Clin. Oncol.* **14**, 1333–1344 (1996).
102. Limpens, J. *et al.* Lymphoma-associated translocation t(14;18) in blood B cells of normal individuals. *Blood* **85**, 2528–2536 (1995).
103. Roulland, S. *et al.* Follicular lymphoma-like B cells in healthy individuals: a novel intermediate step in early lymphomagenesis. *J. Exp. Med.* **203**, 2425–2431 (2006).
104. Alizadeh, A. A. *et al.* Distinct types of diffuse large B-cell lymphoma identified by gene expression profiling. *Nature* **403**, 503–511 (2000).
105. Davis, R. E., Brown, K. D., Siebenlist, U. & Staudt, L. M. Constitutive Nuclear Factor  $\kappa$ B Activity Is Required for Survival of Activated B Cell-like Diffuse Large B Cell Lymphoma Cells. *J. Exp. Med.* **194**, 1861–1874 (2001).
106. Davis, R. E. *et al.* Chronic Active B Cell Receptor Signaling in Diffuse Large B Cell Lymphoma. *Nature* **463**, 88–92 (2010).
107. Hamblin, T. J., Davis, Z., Gardiner, A., Oscier, D. G. & Stevenson, F. K. Unmutated Ig VH Genes Are Associated With a More Aggressive Form of Chronic Lymphocytic Leukemia. *Blood* **94**, 1848–1854 (1999).
108. Agathangelidis, A. *et al.* Stereotyped B-cell receptors in one-third of chronic lymphocytic leukemia: a molecular classification with implications for targeted therapies. *Blood* **119**, 4467–4475 (2012).
109. Hervé, M. *et al.* Unmutated and mutated chronic lymphocytic leukemias derive from self-reactive B cell precursors despite expressing different antibody reactivity. *J. Clin. Invest.* **115**, 1636–1643 (2005).
110. Catera, R. *et al.* Chronic lymphocytic leukemia cells recognize conserved epitopes associated with apoptosis and oxidation. *Mol. Med. Camb. Mass* **14**, 665–674 (2008).
111. Chu, C. C. *et al.* Many chronic lymphocytic leukemia antibodies recognize apoptotic cells with exposed nonmuscle myosin heavy chain IIA: implications for patient outcome and cell of origin. *Blood* **115**, 3907–3915 (2010).
112. Binder, M. *et al.* Stereotypical chronic lymphocytic leukemia B-cell receptors recognize survival promoting antigens on stromal cells. *PLoS One* **5**, e15992 (2010).
113. Minden, M. D. *et al.* Chronic lymphocytic leukaemia is driven by antigen-independent cell-autonomous signalling. *Nature* **489**, 309–312 (2012).
114. Binder, M. *et al.* CLL B-cell receptors can recognize themselves: alternative epitopes and structural clues for autostimulatory mechanisms in CLL. *Blood* **121**, 239–241 (2013).
115. Iacovelli, S. *et al.* Two types of BCR interactions are positively selected during leukemia development in the E $\mu$ -TCL1 transgenic mouse model of CLL. *Blood* **125**, 1578–1588 (2015).
116. Zhu, D. *et al.* Acquisition of potential N-glycosylation sites in the immunoglobulin variable

- region by somatic mutation is a distinctive feature of follicular lymphoma. *Blood* **99**, 2562–2568 (2002).
117. Radcliffe, C. M. *et al.* Human follicular lymphoma cells contain oligomannose glycans in the antigen-binding site of the B-cell receptor. *J. Biol. Chem.* **282**, 7405–7415 (2007).
  118. Coelho, V. *et al.* Glycosylation of surface Ig creates a functional bridge between human follicular lymphoma and microenvironmental lectins. *Proc. Natl. Acad. Sci. U. S. A.* **107**, 18587–18592 (2010).
  119. Schneider, D. *et al.* Lectins from opportunistic bacteria interact with acquired variable-region glycans of surface immunoglobulin in follicular lymphoma. *Blood* **125**, 3287–3296 (2015).
  120. The Non-Hodgkin's Lymphoma Classification Project. A Clinical Evaluation of the International Lymphoma Study Group Classification of Non-Hodgkin's Lymphoma. *Blood* **89**, 3909–3918 (1997).
  121. Vose, J. M. Mantle cell lymphoma: 2015 update on diagnosis, risk-stratification, and clinical management: Mantle cell lymphoma. *Am. J. Hematol.* **90**, 739–745 (2015).
  122. Velders, G. A. *et al.* Mantle-cell lymphoma: a population-based clinical study. *J. Clin. Oncol.* **14**, 1269–1274 (1996).
  123. Bertoni, F. & Ponzoni, M. The cellular origin of mantle cell lymphoma. *Int. J. Biochem. Cell Biol.* **39**, 1747–1753 (2007).
  124. Dreyling, M. & European Mantle Cell Lymphoma Network. Mantle cell lymphoma: biology, clinical presentation, and therapeutic approaches. *Am. Soc. Clin. Oncol. Educ. Book ASCO Am. Soc. Clin. Oncol. Meet.* 191–198 (2014). doi:10.14694/EdBook\_AM.2014.34.191
  125. Uchimaru, K. *et al.* Detection of Cyclin D1 (bcl-1, PRAD1) Overexpression by a Simple Competitive Reverse Transcription-Polymerase Chain Reaction Assay in t(11; 14)(q13; q32)-Bearing B-Cell Malignancies and/or Mantle Cell Lymphoma. *Blood* **89**, 965–974 (1997).
  126. Saba, N. & Wiestner, A. Do mantle cell lymphomas have an 'Achilles heel'? *Curr. Opin. Hematol.* **21**, 350–357 (2014).
  127. Meissner, B. *et al.* The E3 ubiquitin ligase UBR5 is recurrently mutated in mantle cell lymphoma. *Blood* **121**, 3161–3164 (2013).
  128. Dreyling, M. H. *et al.* Alterations of the cyclin D1/p16-pRB pathway in mantle cell lymphoma. *Cancer Res.* **57**, 4608–4614 (1997).
  129. Pinyol, M. *et al.* Deletions and Loss of Expression of P16INK4a and P21Waf1 Genes Are Associated With Aggressive Variants of Mantle Cell Lymphomas. *Blood* **89**, 272–280 (1997).
  130. Salaverria, I. *et al.* Specific secondary genetic alterations in mantle cell lymphoma provide prognostic information independent of the gene expression-based proliferation signature. *J. Clin. Oncol. Off. J. Am. Soc. Clin. Oncol.* **25**, 1216–1222 (2007).
  131. Seto, M. Cyclin D1-negative mantle cell lymphoma. *Blood* **121**, 1249–1250 (2013).
  132. Fu, K. *et al.* Cyclin D1-negative mantle cell lymphoma: a clinicopathologic study based on

## References

---

- gene expression profiling. *Blood* **106**, 4315–4321 (2005).
133. Salaverria, I. *et al.* CCND2 rearrangements are the most frequent genetic events in cyclin D1(-) mantle cell lymphoma. *Blood* **121**, 1394–1402 (2013).
134. Herens, C. *et al.* Cyclin D1-negative mantle cell lymphoma with cryptic t(12;14)(p13;q32) and cyclin D2 overexpression. *Blood* **111**, 1745–1746 (2008).
135. Orchard, J. *et al.* A subset of t(11;14) lymphoma with mantle cell features displays mutated IgVH genes and includes patients with good prognosis, nonnodal disease. *Blood* **101**, 4975–4981 (2003).
136. Fernández, V. *et al.* Genomic and gene expression profiling defines indolent forms of mantle cell lymphoma. *Cancer Res.* **70**, 1408–1418 (2010).
137. Nygren, L. *et al.* Prognostic role of SOX11 in a population-based cohort of mantle cell lymphoma. *Blood* **119**, 4215–4223 (2012).
138. Navarro, A. *et al.* Molecular subsets of mantle cell lymphoma defined by the IGHV mutational status and SOX11 expression have distinct biologic and clinical features. *Cancer Res.* **72**, 5307–5316 (2012).
139. Vegliante, M. C. *et al.* SOX11 regulates PAX5 expression and blocks terminal B-cell differentiation in aggressive mantle cell lymphoma. *Blood* **121**, 2175–2185 (2013).
140. Frater, J. L. & Hsi, E. D. Properties of the mantle cell and mantle cell lymphoma. *Curr. Opin. Hematol.* **9**, 56–62 (2002).
141. Hummel, M., Tamaru, J., Kalvelage, B. & Stein, H. Mantle cell (previously centrocytic) lymphomas express VH genes with no or very little somatic mutations like the physiologic cells of the follicle mantle. *Blood* **84**, 403–407 (1994).
142. Küppers, R. Ongoing somatic mutation in mantle cell lymphomas questioned. *Br. J. Haematol.* **97**, 932–934 (1997).
143. Pittaluga, S. *et al.* Blastic variant of mantle cell lymphoma shows a heterogenous pattern of somatic mutations of the rearranged immunoglobulin heavy chain variable genes. *Br. J. Haematol.* **102**, 1301–1306 (1998).
144. László, T., Nagy, M., Kelényi, G. & Matolcsy, A. Immunoglobulin V(H) gene mutational analysis suggests that blastic variant of mantle cell lymphoma derives from different stages of B-cell maturation. *Leuk. Res.* **24**, 27–31 (2000).
145. Thorsélius, M. *et al.* Somatic hypermutation and VH gene usage in mantle cell lymphoma. *Eur. J. Haematol.* **68**, 217–224 (2002).
146. Walsh, S. H. *et al.* Mutated VH genes and preferential VH3-21 use define new subsets of mantle cell lymphoma. *Blood* **101**, 4047–4054 (2003).
147. Kienle, D. *et al.* VH mutation status and VDJ rearrangement structure in mantle cell lymphoma: correlation with genomic aberrations, clinical characteristics, and outcome. *Blood* **102**, 3003–3009 (2003).

148. Schraders, M. *et al.* Hypermutation in mantle cell lymphoma does not indicate a clinical or biological subentity. *Mod. Pathol.* **22**, 416–425 (2009).
149. Hadzidimitriou, A. *et al.* Is there a role for antigen selection in mantle cell lymphoma? Immunogenetic support from a series of 807 cases. *Blood* **118**, 3088–3095 (2011).
150. Xochelli, A. *et al.* Molecular Evidence for Antigen Drive in the Natural History of Mantle Cell Lymphoma. *Am. J. Pathol.* **185**, 1740–1748 (2015).
151. Klapper, W. *et al.* Immunoglobulin class-switch recombination occurs in mantle cell lymphomas. *J. Pathol.* **209**, 250–257 (2006).
152. Babbage, G. *et al.* Mantle cell lymphoma with t(11;14) and unmutated or mutated VH genes expresses AID and undergoes isotype switch events. *Blood* **103**, 2795–2798 (2004).
153. Pighi, C. *et al.* Phospho-proteomic analysis of mantle cell lymphoma cells suggests a pro-survival role of B-cell receptor signaling. *Cell. Oncol. Dordr.* **34**, 141–153 (2011).
154. Ghilmini, M. *et al.* Effect of Single-Agent Rituximab Given at the Standard Schedule or As Prolonged Treatment in Patients With Mantle Cell Lymphoma: A Study of the Swiss Group for Clinical Cancer Research (SAKK). *J. Clin. Oncol.* **23**, 705–711 (2005).
155. Hallek, M. *et al.* Addition of rituximab to fludarabine and cyclophosphamide in patients with chronic lymphocytic leukaemia: a randomised, open-label, phase 3 trial. *The Lancet* **376**, 1164–1174 (2010).
156. Li, Z.-M., Zucca, E. & Ghilmini, M. Open questions in the management of mantle cell lymphoma. *Cancer Treat. Rev.* **39**, 602–609 (2013).
157. Mócsai, A., Ruland, J. & Tybulewicz, V. L. J. The SYK tyrosine kinase: a crucial player in diverse biological functions. *Nat. Rev. Immunol.* **10**, 387–402 (2010).
158. Rinaldi, A. *et al.* Genomic and expression profiling identifies the B-cell associated tyrosine kinase Syk as a possible therapeutic target in mantle cell lymphoma. *Br. J. Haematol.* **132**, 303–316 (2006).
159. Friedberg, J. W. *et al.* Inhibition of Syk with fostamatinib disodium has significant clinical activity in non-Hodgkin lymphoma and chronic lymphocytic leukemia. *Blood* **115**, 2578–2585 (2010).
160. Buchner, M. & Müschen, M. Targeting the B-cell receptor signaling pathway in B lymphoid malignancies. *Curr. Opin. Hematol.* (2014). doi:10.1097/MOH.0000000000000048
161. Pan, Z. *et al.* Discovery of Selective Irreversible Inhibitors for Bruton's Tyrosine Kinase. *ChemMedChem* **2**, 58–61 (2007).
162. Cinar, M. *et al.* Bruton tyrosine kinase is commonly overexpressed in mantle cell lymphoma and its attenuation by Ibrutinib induces apoptosis. *Leuk. Res.* **37**, 1271–1277 (2013).
163. Herman, S. E. M. *et al.* Bruton tyrosine kinase represents a promising therapeutic target for treatment of chronic lymphocytic leukemia and is effectively targeted by PCI-32765. *Blood* **117**, 6287–6296 (2011).

## References

---

164. Wang, M. L. *et al.* Targeting BTK with ibrutinib in relapsed or refractory mantle-cell lymphoma. *N. Engl. J. Med.* **369**, 507–516 (2013).
165. Hendriks, R. W., Yuvaraj, S. & Kil, L. P. Targeting Bruton's tyrosine kinase in B cell malignancies. *Nat. Rev. Cancer* **14**, 219–232 (2014).
166. Advani, R. H. *et al.* Bruton tyrosine kinase inhibitor ibrutinib (PCI-32765) has significant activity in patients with relapsed/refractory B-cell malignancies. *J. Clin. Oncol. Off. J. Am. Soc. Clin. Oncol.* **31**, 88–94 (2013).
167. Rahal, R. *et al.* Pharmacological and genomic profiling identifies NF- $\kappa$ B-targeted treatment strategies for mantle cell lymphoma. *Nat. Med.* **20**, 87–92 (2014).
168. Bojarczuk, K. *et al.* B-cell receptor signaling in the pathogenesis of lymphoid malignancies. *Blood Cells. Mol. Dis.* **55**, 255–265 (2015).
169. Marrack, P. & Kappler, J. The staphylococcal enterotoxins and their relatives. *Science* **248**, 705–711 (1990).
170. Huber, B. T., Hsu, P. N. & Sutkowski, N. Virus-encoded superantigens. *Microbiol. Rev.* **60**, 473–482 (1996).
171. Lowy, F. D. Staphylococcus aureus Infections. *N. Engl. J. Med.* **339**, 520–532 (1998).
172. van Belkum, A. *et al.* Co-evolutionary aspects of human colonisation and infection by Staphylococcus aureus. *Infect. Genet. Evol.* **9**, 32–47 (2009).
173. Silverman, G. J. & Goodyear, C. S. Confounding B-cell defences: lessons from a staphylococcal superantigen. *Nat. Rev. Immunol.* **6**, 465–475 (2006).
174. Graille, M. *et al.* Crystal structure of a Staphylococcus aureus protein A domain complexed with the Fab fragment of a human IgM antibody: structural basis for recognition of B-cell receptors and superantigen activity. *Proc. Natl. Acad. Sci. U. S. A.* **97**, 5399–5404 (2000).
175. Tashiro, M. & Montelione, G. T. Structures of bacterial immunoglobulin-binding domains and their complexes with immunoglobulins. *Curr. Opin. Struct. Biol.* **5**, 471–481 (1995).
176. Kristiansen, S. V., Pascual, V. & Lipsky, P. E. Staphylococcal protein A induces biased production of Ig by VH3-expressing B lymphocytes. *J. Immunol. Baltim. Md 1950* **153**, 2974–2982 (1994).
177. Goodyear, C. S. & Silverman, G. J. Death by a B cell superantigen: In vivo VH-targeted apoptotic supraclonal B cell deletion by a Staphylococcal Toxin. *J. Exp. Med.* **197**, 1125–1139 (2003).
178. Domiati-Saad, R. *et al.* Staphylococcal enterotoxin D functions as a human B cell superantigen by rescuing VH4-expressing B cells from apoptosis. *J. Immunol. Baltim. Md 1950* **156**, 3608–3620 (1996).
179. Björck, L. Protein L. A novel bacterial cell wall protein with affinity for Ig L chains. *J. Immunol. Baltim. Md 1950* **140**, 1194–1197 (1988).
180. Graille, M. *et al.* Complex between Peptostreptococcus magnus protein L and a human



- antibody reveals structural convergence in the interaction modes of Fab binding proteins. *Struct. Lond. Engl.* 1993 **9**, 679–687 (2001).
181. Beckingham, J. A., Bottomley, S. P., Hinton, R., Sutton, B. J. & Gore, M. G. Interactions between a single immunoglobulin-binding domain of protein L from *Peptostreptococcus magnus* and a human kappa light chain. *Biochem. J.* **340** ( Pt 1), 193–199 (1999).
182. Smith, D. *et al.* Whole-body autoradiography reveals that the *Peptostreptococcus magnus* immunoglobulin-binding domains of protein L preferentially target B lymphocytes in the spleen and lymph nodes in vivo. *Cell. Microbiol.* **6**, 609–623 (2004).
183. Goodyear, C. S., Narita, M. & Silverman, G. J. In vivo VL-targeted activation-induced apoptotic supraclonal deletion by a microbial B cell toxin. *J. Immunol. Baltim. Md 1950* **172**, 2870–2877 (2004).
184. Berberian, L., Goodglick, L., Kipps, T. J. & Braun, J. Immunoglobulin VH3 gene products: natural ligands for HIV gp120. *Science* **261**, 1588–1591 (1993).
185. Neshat, M. N., Goodglick, L., Lim, K. & Braun, J. Mapping the B cell superantigen binding site for HIV-1 gp120 on a V(H)3 Ig. *Int. Immunol.* **12**, 305–312 (2000).
186. Karray, S. *et al.* Structural basis of the gp120 superantigen-binding site on human immunoglobulins. *J. Immunol. Baltim. Md 1950* **161**, 6681–6688 (1998).
187. Osterroth, F. *et al.* Rapid expression cloning of human immunoglobulin Fab fragments for the analysis of antigen specificity of B cell lymphomas and anti-idiotypic lymphoma vaccination. *J. Immunol. Methods* **229**, 141–153 (1999).
188. OligoCalc: Oligonucleotide Properties Calculator. Available at: <http://biotools.nubic.northwestern.edu/OligoCalc.html>. (Accessed: 16th March 2016)
189. Brochet, X., Lefranc, M.-P. & Giudicelli, V. IMGT/V-QUEST: the highly customized and integrated system for IG and TR standardized V-J and V-D-J sequence analysis. *Nucleic Acids Res.* **36**, W503–508 (2008).
190. Giudicelli, V., Brochet, X. & Lefranc, M.-P. IMGT/V-QUEST: IMGT standardized analysis of the immunoglobulin (IG) and T cell receptor (TR) nucleotide sequences. *Cold Spring Harb. Protoc.* **2011**, 695–715 (2011).
191. Laemmli, U. K. Cleavage of structural proteins during the assembly of the head of bacteriophage T4. *Nature* **227**, 680–685 (1970).
192. Dyballa, N. & Metzger, S. Fast and sensitive colloidal coomassie G-250 staining for proteins in polyacrylamide gels. *J. Vis. Exp. JoVE* (2009). doi:10.3791/1431
193. Murphy, R. M. Static and dynamic light scattering of biological macromolecules: what can we learn? *Curr. Opin. Biotechnol.* **8**, 25–30 (1997).
194. Scott, J. K. & Smith, G. P. Searching for peptide ligands with an epitope library. *Science* **249**, 386–390 (1990).
195. Schepers, E., Glorieux, G., Dhondt, A., Leybaert, L. & Vanholder, R. Flow cytometric calcium

## References

---

- flux assay: Evaluation of cytoplasmic calcium kinetics in whole blood leukocytes. *J. Immunol. Methods* **348**, 74–82 (2009).
196. Gupta, R., Jung, E. & Brunak, S. Prediction of N-glycosylation sites in human proteins. (2004).
197. Nobbmann, U. *et al.* Dynamic light scattering as a relative tool for assessing the molecular integrity and stability of monoclonal antibodies. *Biotechnol. Genet. Eng. Rev.* **24**, 117–128 (2007).
198. Yadav, S., Shire, S. J. & Kalonia, D. S. Factors Affecting the Viscosity in High Concentration Solutions of Different Monoclonal Antibodies. *J. Pharm. Sci.* **99**, 4812–4829 (2010).
199. Chen, T. R. Re-evaluation of HeLa, HeLa S3, and HEp-2 karyotypes. *Cytogenet. Cell Genet.* **48**, 19–24 (1988).
200. Ulvestad, E. Performance characteristics and clinical utility of a hybrid ELISA for detection of ANA. *APMIS Acta Pathol. Microbiol. Immunol. Scand.* **109**, 217–222 (2001).
201. Pighi, C., Barbi, S., Bertolaso, A. & Zamò, A. Mantle cell lymphoma cell lines show no evident immunoglobulin heavy chain stereotypy but frequent light chain stereotypy. *Leuk. Lymphoma* **54**, 1747–1755 (2013).
202. Nollau, P. & Mayer, B. J. Profiling the global tyrosine phosphorylation state by Src homology 2 domain binding. *Proc. Natl. Acad. Sci. U. S. A.* **98**, 13531–13536 (2001).
203. Brown, J. R. *et al.* Idelalisib, an inhibitor of phosphatidylinositol 3-kinase p110 $\delta$ , for relapsed/refractory chronic lymphocytic leukemia. *Blood* **123**, 3390–3397 (2014).
204. Kahl, B. S. *et al.* A phase 1 study of the PI3K $\delta$  inhibitor idelalisib in patients with relapsed/refractory mantle cell lymphoma (MCL). *Blood* **123**, 3398–3405 (2014).
205. Byrd, J. C. *et al.* Ibrutinib versus ofatumumab in previously treated chronic lymphoid leukemia. *N. Engl. J. Med.* **371**, 213–223 (2014).
206. Damle, R. N. *et al.* Ig V Gene Mutation Status and CD38 Expression As Novel Prognostic Indicators in Chronic Lymphocytic Leukemia. *Blood* **94**, 1840–1847 (1999).
207. Camacho, F. I. *et al.* Molecular heterogeneity in MCL defined by the use of specific V H genes and the frequency of somatic mutations. *Blood* **101**, 4042–4046 (2003).
208. Lai, R. *et al.* Immunoglobulin VH somatic hypermutation in mantle cell lymphoma: mutated genotype correlates with better clinical outcome. *Mod. Pathol. Off. J. U. S. Can. Acad. Pathol. Inc* **19**, 1498–1505 (2006).
209. Chang, B. & Casali, P. The CDR1 sequences of a major proportion of human germline Ig VH genes are inherently susceptible to amino acid replacement. *Immunol. Today* **15**, 367–373 (1994).
210. Bose, B. & Sinha, S. Problems in using statistical analysis of replacement and silent mutations in antibody genes for determining antigen-driven affinity selection. *Immunology* **116**, 172–183 (2005).

- 
211. Messmer, B. T., Albesiano, E., Messmer, D. & Chiorazzi, N. The pattern and distribution of immunoglobulin VH gene mutations in chronic lymphocytic leukemia B cells are consistent with the canonical somatic hypermutation process. *Blood* **103**, 3490–3495 (2004).
212. Wu, Y.-C. *et al.* High-throughput immunoglobulin repertoire analysis distinguishes between human IgM memory and switched memory B-cell populations. *Blood* **116**, 1070–1078 (2010).
213. Bertoni, F. *et al.* Immunoglobulin light chain kappa deletion rearrangement as a marker of clonality in mantle cell lymphoma. *Leuk. Lymphoma* **36**, 147–150 (1999).
214. Tobin, G. *et al.* Somatic mutated Ig VH3-21 genes characterize a new subset of chronic lymphocytic leukemia. *Blood* **99**, 2262–2264 (2002).
215. William, J., Euler, C., Christensen, S. & Shlomchik, M. J. Evolution of Autoantibody Responses via Somatic Hypermutation Outside of Germinal Centers. *Science* **297**, 2066–2070 (2002).
216. Di Niro, R. *et al.* Salmonella Infection Drives Promiscuous B Cell Activation Followed by Extrafollicular Affinity Maturation. *Immunity* **43**, 120–131 (2015).
217. Zabalegui, N. *et al.* Acquired potential N-glycosylation sites within the tumor-specific immunoglobulin heavy chains of B-cell malignancies. *Haematologica* **89**, 541–546 (2004).
218. Loeffler, M. *et al.* Genomic and epigenomic co-evolution in follicular lymphomas. *Leukemia* **29**, 456–463 (2015).
219. Seiler, T. *et al.* Characterization of structurally defined epitopes recognized by monoclonal antibodies produced by chronic lymphocytic leukemia B cells. *Blood* **114**, 3615–3624 (2009).
220. Binder, M. *et al.* B-cell receptor epitope recognition correlates with the clinical course of chronic lymphocytic leukemia. *Cancer* **117**, 1891–1900 (2011).
221. Tanabe, S. Epitope peptides and immunotherapy. *Curr. Protein Pept. Sci.* **8**, 109–118 (2007).
222. Altschul, S. F., Gish, W., Miller, W., Myers, E. W. & Lipman, D. J. Basic local alignment search tool. *J. Mol. Biol.* **215**, 403–410 (1990).
223. Vodnik, M., Zager, U., Strukelj, B. & Lunder, M. Phage display: selecting straws instead of a needle from a haystack. *Mol. Basel Switz.* **16**, 790–817 (2011).
224. Cha, S.-C. *et al.* Nonstereotyped Lymphoma B Cell Receptors Recognize Vimentin as a Shared Autoantigen. *J. Immunol.* **190**, 4887–4898 (2013).
225. Wardemann, H. *et al.* Predominant Autoantibody Production by Early Human B Cell Precursors. *Science* **301**, 1374–1377 (2003).
226. Leslie, D., Lipsky, P. & Notkins, A. L. Autoantibodies as predictors of disease. *J. Clin. Invest.* **108**, 1417–1422 (2001).
227. Lohr, J. G. *et al.* Discovery and prioritization of somatic mutations in diffuse large B-cell lymphoma (DLBCL) by whole-exome sequencing. *Proc. Natl. Acad. Sci. U. S. A.* **109**, 3879–3884 (2012).

## References

---

228. Song, W. *et al.* Actin-mediated feedback loops in B-cell receptor signaling. *Immunol. Rev.* **256**, (2013).
229. Liu, C. *et al.* Actin Reorganization Is Required for the Formation of Polarized B Cell Receptor Signalosomes in Response to Both Soluble and Membrane-Associated Antigens. *J. Immunol.* **188**, 3237–3246 (2012).
230. George, J. N., Lyons, R. M. & Morgan, R. K. Membrane Changes Associated with Platelet Activation. *J. Clin. Invest.* **66**, 1–9 (1980).
231. Tykhomyrov, A. A. Dynamics of thrombin-induced exposition of actin on the platelet surface. *Ukr. Biochem. J.* **86**, 74–81 (2014).
232. Malara, A. *et al.* The secret life of a megakaryocyte: emerging roles in bone marrow homeostasis control. *Cell. Mol. Life Sci. CMLS* **72**, 1517–1536 (2015).
233. Myhrinder, A. L. *et al.* A new perspective: molecular motifs on oxidized LDL, apoptotic cells, and bacteria are targets for chronic lymphocytic leukemia antibodies. *Blood* **111**, 3838–3848 (2008).
234. Franke, W. W., Hergt, M. & Grund, C. Rearrangement of the vimentin cytoskeleton during adipose conversion: formation of an intermediate filament cage around lipid globules. *Cell* **49**, 131–141 (1987).
235. Mor-Vaknin, N., Punturieri, A., Sitwala, K. & Markovitz, D. M. Vimentin is secreted by activated macrophages. *Nat. Cell Biol.* **5**, 59–63 (2003).
236. Loeber, G., Dworkin, M. B., Infante, A. & Ahorn, H. Characterization of cytosolic malic enzyme in human tumor cells. *FEBS Lett.* **344**, 181–186 (1994).
237. Berglund, L. *et al.* A Genecentric Human Protein Atlas for Expression Profiles Based on Antibodies. *Mol. Cell. Proteomics* **7**, 2019–2027 (2008).
238. Uhlén, M. *et al.* Tissue-based map of the human proteome. *Science* **347**, 1260419 (2015).
239. Michaud, G. A. *et al.* Analyzing antibody specificity with whole proteome microarrays. *Nat. Biotechnol.* **21**, 1509–1512 (2003).
240. Predki, P. F., Mattoon, D., Bangham, R., Schweitzer, B. & Michaud, G. Protein microarrays: a new tool for profiling antibody cross-reactivity. *Hum. Antibodies* **14**, 7–15 (2005).
241. Montesinos-Rongen, M. *et al.* Primary Central Nervous System (CNS) Lymphoma B Cell Receptors Recognize CNS Proteins. *J. Immunol. Baltim. Md 1950* **195**, 1312–1319 (2015).
242. Goodyear, C. S. & Silverman, G. J. Staphylococcal toxin induced preferential and prolonged in vivo deletion of innate-like B lymphocytes. *Proc. Natl. Acad. Sci. U. S. A.* **101**, 11392–11397 (2004).
243. Potter, K. N., Hobby, P., Klijn, S., Stevenson, F. K. & Sutton, B. J. Evidence for involvement of a hydrophobic patch in framework region 1 of human V4-34-encoded Igs in recognition of the red blood cell I antigen. *J. Immunol. Baltim. Md 1950* **169**, 3777–3782 (2002).
244. Walboomers, J. M. *et al.* Human papillomavirus is a necessary cause of invasive cervical

- cancer worldwide. *J. Pathol.* **189**, 12–19 (1999).
245. Kusters, J. G., van Vliet, A. H. M. & Kuipers, E. J. Pathogenesis of *Helicobacter pylori* infection. *Clin. Microbiol. Rev.* **19**, 449–490 (2006).
246. Fischbach, W., Goebeler-Kolve, M.-E., Dragosics, B., Greiner, A. & Stolte, M. Long term outcome of patients with gastric marginal zone B cell lymphoma of mucosa associated lymphoid tissue (MALT) following exclusive *Helicobacter pylori* eradication therapy: experience from a large prospective series. *Gut* **53**, 34–37 (2004).
247. Machida, K., Khenkhar, M. & Nollau, P. Deciphering Phosphotyrosine-Dependent Signaling Networks in Cancer by SH2 Profiling. *Genes Cancer* **3**, 353–361 (2012).
248. Tisch, R., Roifman, C. M. & Hozumi, N. Functional differences between immunoglobulins M and D expressed on the surface of an immature B-cell line. *Proc. Natl. Acad. Sci. U. S. A.* **85**, 6914–6918 (1988).
249. Kim, K. M. *et al.* Growth regulation of a human mature B cell line, B104, by anti-IgM and anti-IgD antibodies. *J. Immunol. Baltim. Md 1950* **146**, 819–825 (1991).
250. Zupo, S. *et al.* Apoptosis or plasma cell differentiation of CD38-positive B-chronic lymphocytic leukemia cells induced by cross-linking of surface IgM or IgD. *Blood* **95**, 1199–1206 (2000).
251. Petlickovski, A. *et al.* Sustained signaling through the B-cell receptor induces Mcl-1 and promotes survival of chronic lymphocytic leukemia B cells. *Blood* **105**, 4820–4827 (2005).
252. Longo, P. G. *et al.* The Akt/Mcl-1 pathway plays a prominent role in mediating antiapoptotic signals downstream of the B-cell receptor in chronic lymphocytic leukemia B cells. *Blood* **111**, 846–855 (2008).
253. Kovalchuk, A. L. *et al.* Burkitt lymphoma in the mouse. *J. Exp. Med.* **192**, 1183–1190 (2000).

## 7 Appendix

### A Permissions from the publishers

Figure 1:

Reprinted from Bojarczuk, K. *et al.* B-cell receptor signaling in the pathogenesis of lymphoid malignancies. *Blood Cells. Mol. Dis.* **55**, 255–265 (2015), with permission from Elsevier.

Figure 3:

Reprinted by permission from Macmillan Publishers Ltd: *Nature Reviews Immunology*, Silverman, G. J. & Goodyear, C. S. Confounding B-cell defences: lessons from a staphylococcal superantigen. *Nat. Rev. Immunol.* **6**, 465–475 (2006).

## B List of additional primers used in this study

### Heavy chain amplification primer forward (pBud and pLeGO only):

Ramos-VH-P1	5'-GATCATTTAAATGTGTCCAGTGTGAGGTGCAGCTACAGCAGTG	MCL19, FL4
Pat8-VH-P1s	5'-GATCATTTAAATGTGTCCAGTGTGAAAGTGCAGCTGGTGGAGTC	FL8
CLL172 VH for	5'-GATCATTTAAATGTGTCCAGTGTGAGGTGCAGCTGGTGGAG	FL6
CLL 173 VH for	5'-GATCATTTAAATGTGTCCAGTGTGAGGTGCAGCTGGTGGAGTC	MCL11
G10 IgM for	5'-GATCATTTAAATGTGTCCAGTGTGAGGTGCAGCTGGTGGAG	FL10
G11 IgG for	5'-GATCATTTAAATGTGTCCAGTGTGAAATACAATTATTGGAGTCTGGG	FL11
FL191 VH fw	5'-GATCATTTAAATGTGTCCAGTGTGACGTACACTTGGTGGAGTC	FL101
MZL002 IgM for	5'-GATCATTTAAATGTGTCCAGTGTGAGGTGCAGTTGTTGGAGTC	MCL2

### Heavy chain amplification primer reverse

ST486-VH-P2	5'-GATCCTCGAGACGGTGACCAGGGTTC	MCL4, MCL5, MCL12, MCL18, MCL27, FL6, FL8, FL101,
Ramos-VH-P2	5'-GATCCTCGAGACGGTGACCAGGGTTC	MCL2, FL4
BL49-VH-P2	5'-GATCCTCGAGACGGTGACCATTGTCCCTTG	MCL23
VH145 reverse	5'-GATCCTCGAGACGGTGACCAGGG	MCL11, MCL24
G10 IgM back	5'-GATCCTCGAGACGACGACCGGGG	FL10
G11 IgG back	5'-GATCCTCGAGACGGTGACCAGGGTTC	FL11
MCL22 IgM rev	5'-GATCCTCGAGACGATGACCAGGGTTC	MCL22
MCL19 IgM rev	5'-GATCCTCGAGACGGTGACCAGGGTTC	MCL19

### Heavy chain amplification primer forward (pFBD only):

CA46 VH Sfi for	5'-GATCGGCCCATTCGGCCTTTGCGGAGGTGCAGCTGGTGC	MCL12
FL8 VH SfiI for	5'-GATCGGCCCATTCGGCCTTTGCGGAAAGTGCAGCTGGTGGAG	MCL23
PCNSL 0909 VH SfiI for	5'-GATCGGCCCATTCGGCCTTTGCGGAGGTGCAGCTGGTGG	MCL11, MCL18
MCL5 vH SfiI	5'-GATCGGCCCATTCGGCCTTTGCGGAGGTGCAACTGGTGGAGTC	MCL5
Alg1 QVQ SfiI fw	5'-GATCGGCCCATTCGGCCTTTGCGCAGGTGCAGCTGGTGC	MCL4
MCL22 IgM SfiI fw	5'-GATCGGCCCATTCGGCCTTTGCGCAGGTGCAGCTGGTGGAG	MCL22
MCL24 IgM SfiI fw	5'-GATCGGCCCATTCGGCCTTTGCGCAGGTGCAGCTACAGCAG	MCL19, MCL24
MCL002 IgM SfiI fw	5'-GATCGGCCCATTCGGCCTTTGCGGAGGTGCAGTTGTTGGAGTC	MCL2
MCL27 IgM SfiI fw	5'-GATCGGCCCATTCGGCCTTTGCGCAGGTGCAGCTGCAGGAG	MCL27

**Variable lambda light chain amplification primer forward (pBud and pLeGO only):**

MCL1 VL P1	5'-GATCCTGCAGGGTGCCAGATGTTCTTCTGAGCTGACTCAGG	MCL11, MCL19
Ramos-VL-P1	5'-GATCCTGCAGGGTGCCAGATGTCAGTCTGCCCTGACTCAGC	FL8
FL4 VL P1	5'-GATCCTGCAGGGTGCCAGATGTCAGTCTGTGCTGACGCAGC	FL4
G11 lambda for	5'-GATCCTGCAGGGTGCCAGATGTCAGTCTGTTCTGATTCAGCCAC	FL11
FL101 VL fw	5'-GATCCTGCAGGGTGCCAGATGTCAGTCTGCCCTGACTCAG	FL101

**Variable lambda light chain amplification primer reverse**

Ramos-VL-P2	5'-GATCGGCGCGCCCTTGGGCTGACCTAGGACG	MCL11, MCL12, MCL19, MCL24, FL101, FL8
FL4 VL back	5'-GATCGGCGCGCCACCTAGGACGGTCAGCTTGGTC	FL4
G11 lambda back	5'-GATCGGCGCGCCACCTAGGACGGTCAATGTGGTTC	FL11

**Variable kappa light chain amplification primer forward (pBud and pLeGO only):**

MCL2 VK for	5'-GATCCTGCAGGGTGCCAGATGTGACATCGTGATGACCCAGTCTCC	MCL2
G6 kappa for	5'-GATCCTGCAGGGTGCCAGATGTGACATCCAGATGACCCAGTC	FL6
G10 kappa for	5'-GATCCTGCAGGGTGCCAGATGTGATATTGCCTGACACAGTCTC	FL10

**Variable kappa light chain amplification primer reverse**

ST486-VK-P2	5'-GATCGGCGCGCCACAGTTCGTTTGATCTCCAG	MCL18, MCL27
DG75-VK-P2	5'-GATCGGCGCGCCACAGTTCGTTTGATCTCCAC	MCL4, MCL5
CLL173 VK rev	5'-GATCGGCGCGCCACAGTTCGTTTGATATCCAC	MCL22
G10 kappa reverse	5'-GATCGGCGCGCCACAGTTCGTTTAACTCCAATC	FL10
MZL002 kappa rev	5'-GATCGGCGCGCCACAGTTCGTTTGACTTCCAC	MCL2
G6-kappa rev	5'-GATCGGCGCGCCACAGTTCGTCTGATGTCCAC	FL6
MCL23 kappa back pFBD	5'-GATCGGCGCGCCACAGTTCGTTTGATTCCACC	MCL23



**Variable light chain amplification primer forward (pFBD):**

PCNSL 0532 VL NotI for	5'-GATCGCGGCCGCGGCTCACTCTGCTTTTCGCGCAGTCTGCCCTGACTCAG	MCL12
CA46 VL NotI for	5'-GATCGCGGCCGCGGCTCACTCTGCTTTTCGCGGATATTGTGATGACTCAGTCTC	MCL18
MCL2 VL NotI for	5'-GATCGCGGCCGCGGCTCACTCTGCTTTTCGCGTCTTCTGAGCTGACTCAGG	MCL11, MCL19
MCL4 VL NotI fw	5'-GATCGCGGCCGCGGCTCACTCTGCTTTTCGCGGACATCGTGATGACCCAGTC	MCL2, MCL4,
MCL5 kappa NotI fw	5'-GATCGCGGCCGCGGCTCACTCTGCTTTTCGCGGACATCCAGATGACCCAGTCTCC	MCL5, MCL22, MCL27
MCL24 VL NotI fw	5'-GATCGCGGCCGCGGCTCACTCTGCTTTTCGCGCAGTCTGTGCTGACGCAG	MCL24
MCL23 VL NotI fw	5'-GATCGCGGCCGCGGCTCACTCTGCTTTTCGCGGAAATTGTGTTGACGCAGTCTC	MCL23

**Primer used for Next-Generation Sequencing (NGS) sample preparation:**

Seq_PlugO_ 3M_elon_fw	5'- ACACTCTTCCCTACACGACGCTCTTCCGATCTACGCAGAGTGGCCATTAC
Seq_IGKC_ uni_rv	5'- TGA CTGGAGTTCAGACGTGTGCTCTTCCGATCTGGAAGATGAAGACAGATGGTGC
Seq_IGLC_ al2367_rv	5'- TGA CTGGAGTTCAGACGTGTGCTCTTCCGATCTGGGAACAGAGTGACCGAG
Seq_IGM_rv	5'- TGA CTGGAGTTCAGACGTGTGCTCTTCCGATCTGGGAATTCTCACAGGAGACG
Barcode Primer 102	5'- CAAGCAGAAGACGGCATAACGAGATGAGCTGCGTGACTGGAGTTCAGACGTGTG
Barcode Primer 103	5'- CAAGCAGAAGACGGCATAACGAGATTA ACTCCGTGACTGGAGTTCAGACGTGTG
Linker_seq_ neu_fw	5'- AATGATACGGCGACCACCGAGATCTCACTCTTCCCTACACGACGCTC

**C Origin of the patient samples**

<b>Sample</b>	<b>acquired from</b>
MCL4	lymph node
MCL21	tumor
MCL32	lymph node
MCL23	lymph node
MCL1	bone marrow
MCL8	lymph node
MCL11	base of the mouth (tumor)
MCL20	lymph node
MCL28	lymph node
MCL2	bone marrow
MCL22	spleen (tumor)
MCL13	gall bladder (tumor)
MCL5	spleen (tumor)
MCL31	lymph node
MCL16	lymph node
MCL19	lymph node
MCL24	lymph node
MCL29	lymph node
MCL25	lymph node
MCL14	lymph node
MCL30	lymph node
MCL27	base of the tongue (tumor)
MCL12	lymph node
MCL18	lymph node

## D Index of tables

Table 1: Common Non-Hodgkin-lymphomas categorised by indolent or aggressive behaviour.....	24
Table 2: B cell NHLs ordered by the suspected B cell development stage at genesis of the lymphoma.....	24
Table 3: Chromosomal translocations in B cell NHLs.....	25
Table 4: Summary of the successful determined variable heavy and light chain sequences of MCL-derived Igs.....	85
Table 5: Heavy chain complementarity determining regions (HCDRs) of a strongly biased subgroup.....	87
Table 6: Light chain complementarity determining regions (LCDRs) of a strongly biased subgroup.....	87
Table 7: IMGT clonotype summary of two MCL samples acquired from a patient in a 4 year interval.....	89
Table 8: Exclusive and common CDR3 clonotypes (AA) in the two MCL27 samples.....	90
Table 9: Summary of acquired and germline coded glycosylation sites in MCL-derived Igs.....	92
Table 10: The total obtained amount of recombinant antibodies after production in HEK293T or Sf9 cells..	93
Table 11 Selected phages with potential motifs after 4 selection rounds.....	95
Table 12: Proteins identified by mass spectrometric analysis of the obtained protein band after IP with an MCL22-Ig on HEp-2 cell lysate (Band 1, Figure 17A).....	106
Table 13: Proteins identified by mass spectrometric analysis of a band obtained with an IP of the MCL12 Ig on SK-BR-3 cell lysate (Band 3, Figure 17B).....	107
Table 14: Proteins identified by mass spectrometric analysis after an IP with the MCL12-Ig on lymph node protein lysates of FVB/N mice (Band4, Figure 17C).....	107
Table 15: Representation of SpA binding motif in lymphoma Igs expressing IGHV3-genes.....	109

## E Index of figures

Figure 1: Key molecules of the B cell antigen receptor signalling cascade.....	22
Figure 2: Incidence rates of NHL subtypes in the USA (2000-2011).....	24
Figure 3: Illustration of the complex between a Fab fragment, the SpA and PpL superantigens as well as a regular antigen.....	30
Figure 4: Maps of the vectors used for expression of recombinant antibodies and Fab fragments.....	45
Figure 5: Maps of the pLeGO vectors used for transduction of lymphoma cell lines.....	79
Figure 6: Exemplary nested-PCR result.....	83
Figure 7: Result of the colony PCR with subcloned IGLV-amplification products.....	84
Figure 8: Distribution of heavy and light chain gene families within the MCL patient cohort.....	86
Figure 9: Length distribution of the variable heavy chain CDR3-region in the whole MCL cohort.....	87
Figure 10: Boxplots representing the germline identity of the variable Ig sequences from three NHL cohorts.....	88
Figure 11: Anti-phage-ELISA with enriched phages at multiple dilutions.....	96
Figure 12: Cross-reactivity ELISA of enriched phages.....	98
Figure 13: Heatmap of calculated hydrodynamic radii of MCL-derived Igs in solution determined by dynamic light scattering measurements.....	100
Figure 14: Immunofluorescence assay of recombinant MCL-Igs with methanol-fixed HEp-2 cells.....	102
Figure 15: Immunofluorescence assay of MCL-derived Igs with PFA-fixed HEp-2 cells.....	103
Figure 16: Western Blots with different concentrations of MCL-derived Igs on HEp-2 cell lysates.....	104
Figure 17: Precipitated proteins after an immunoprecipitation with MCL-Igs on RIPA protein lysates.....	105
Figure 18: Anti-vimentin Western Blot with MCL-derived Igs.....	108
Figure 19: Anti-SpA ELISA with Fab fragments.....	110
Figure 20: Fluorescence activated cell sorting of different Burkitt lymphoma B cell lines.....	112
Figure 21: Flow cytometric analysis of human Ig light chain expression in lymphoma cell lines, sorted for Ig negativity.....	113
Figure 22: Western Blot analysis of sorted BCR-negative Ramos cells.....	114
Figure 23: Fluorescence activated cell sorting of transduced Ramos B cell lines.....	115
Figure 24: Flow cytometric analysis of Ramos cells transduced with recombinant Igs.....	116
Figure 25: Ca <sup>2+</sup> -mobilisation assay of Ramos cells expressing MCL-derived membrane bound immunoglobulins.....	117
Figure 26: Ca <sup>2+</sup> -mobilisation assay of MAVER-1 and Jeko-1 MCL cells.....	118
Figure 27: Far-Western Blot to detect altered phosphorylation patterns in stimulated and unstimulated Ramos cells.....	120
Figure 28: Proliferation of transduced and untransduced Ramos cells.....	121

## F Risk and safety statements












### GHS hazard statements

- H225: Highly flammable liquid and vapour
- H226: Flammable liquid and vapour
- H228: Flammable solid
- H272: May intensify fire; oxidizer
- H290: May be corrosive to metals
- H301: Toxic if swallowed
- H302: Harmful if swallowed
- H310: Fatal in contact with skin
- H311: Toxic in contact with skin
- H312: Harmful in contact with skin
- H314: Causes severe skin burns and eye damage
- H315: Causes skin irritation
- H316: Causes mild skin irritation
- H317: May cause an allergic skin reaction
- H318: Causes serious eye damage
- H319: Causes serious eye irritation
- H330: Fatal if inhaled
- H331: Toxic if inhaled
- H332: Harmful if inhaled
- H334: May cause allergy or asthma symptoms or breathing difficulties if inhaled
- H335: May cause respiratory irritation
- H336: May cause drowsiness or dizziness
- H340: May cause genetic defects
- H341: Suspected of causing genetic defects
- H350: May cause cancer
- H351: Suspected of causing cancer
- H360: May damage fertility or the unborn child
- H361: Suspected of damaging fertility or the unborn child
- H361D: Suspected of damaging the unborn child
- H370: Causes damage to organs
- H372: Causes damage to organs through prolonged or repeated exposure
- H373: May cause damage to organs through prolonged or repeated exposure
- H410: Very toxic to aquatic life with long-lasting effects
- H412: Harmful to aquatic life with long-lasting effects













### GHS precautionary statements

- P101: If medical advice is needed, have product container or label at hand.
- P102: Keep out of reach of children.
- P103: Read label before use.
- P201: Obtain special instructions before use.
- P210: Keep away from heat, hot surfaces, sparks, open flames and other ignition sources.  
No smoking.
- P233: Keep container tightly closed.
- P234: Keep only in original container.
- P240: Ground/bond container and receiving equipment.
- P260: Do not breathe dust/fumes/gas/mist/vapours/spray.
- P261: Avoid breathing dust/fumes/gas/mist/vapours/spray.
- P273: Avoid release to the environment.
- P280: Wear protective gloves/protective clothing/eye protection/face protection.
- P284: [In case of inadequate ventilation] wear respiratory protection.
- P301: IF SWALLOWED:
- P302: IF ON SKIN:
- P303: IF ON SKIN (or hair):
- P304: IF INHALED:
- P305: IF IN EYES:
- P308: If exposed or concerned:
- P310: Immediately call a POISON CENTRE/doctor/...
- P311: Call a POISON CENTRE/ doctor/...
- P313: Get medical advice/attention.
- P314: Get medical advice/attention if you feel unwell.
- P330: Rinse mouth.
- P331: Do NOT induce vomiting.
- P338: Remove contact lenses if present and easy to do. Continue rinsing.
- P340: Remove person to fresh air and keep comfortable for breathing.
- P342: If experiencing respiratory symptoms:
- P351: Rinse cautiously with water for several minutes.
- P352: Wash with plenty of water/...
- P353: Rinse skin with water/shower.
- P361: Take off immediately all contaminated clothing.
- P403: Store in a well ventilated place.
- P405: Store locked up.

## G Hazardous chemicals used in this study

chemical	CAS No.	GHS pictograms	Hazard statements	Precautionary statements
2-mercaptoethanol	60-24-2		H301, H310, H315, H317, H318, H330, H410	P260, P273, P280, P284, P301+310, P302+350
ABTS	30931-67-0		H315, H319, H335	P261, P305+351+338
acetic acid	64-19-7		H226, H314	P280, P305+351+338, P310
acrylamide (30%)	79-06-1		H301, H312, H316, H317, H319, H332, H340, H350, H361, H372	P201, P280, P301+310, P305+351+338, P308+313
aluminium sulfate	10043-01-3		H315, H318, H335, H412	P261, P273, P280, P305+351+338
ampicillin	69-52-3		H315, H317, H319, H334, H335	P261, P280, P305+P351+P388, P342+P311
APS	7727-54-0		H272, H302, H315, H317, H319, H334, H335	P280, P302+352, P304+341, P305+351+338, P342+311
boric acid	10043-35-3		H360	P201, P308+313
CaCl <sub>2</sub>	10043-52-4		H319	P305+351+338
chloroform	67-66-3		H302, H315, H319, H331, H351, 361D, H372	H302+352, H314
citric acid	77-92-9		H319	P305+351+338

## Appendix

chemical	CAS No.	GHS pictograms	Hazard statements	Precautionary statements
DTT	3483-12-3		H302, H315, H319	P302+352, P305+351+338
EDTA	60-00-4		H319	P305+351+338
ethanol	64-17-5		H225, H319	P210, P240, P305+351+338, P403+233
ethidiumbromide	1239-45-8		H302, H315, H319, H330, H335, H341	P281, P302+352, P305+351+338, P304+340, P309, P310
formamide	75-12-7		H351, H360D, H373	P201, P314
gentamycin	1403-66-3		H317, H334	P261, P280, P342+311
guanidine hydrochloride	50-01-1		H302, H319, H315	P302+352, P305+351+338
hydrochloric acid	7647-01-0		H290, H314, H335	P234, P260, P304+340, P303+361+353, P305+351+338, P309+311, P501
imidazole	288-32-4		H302, H314, H360D	P201, P280, P305+351+338, P310
isopropanol	67-63-0		H225, H319, H336	P101, P102, P103, P210, P261, P303+361+353, P305+351+338, P405, P501
kanamycin	8063-07-8		H360	P201, P308+313
methanol	67-56-1		H225, H301, H311, H331, H370	P210, P233, P280, P302+352



chemical	CAS No.	GHS pictograms	Hazard statements	Precautionary statements
PEI	9002-98-6		H301	P301+310
phenol	108-95-2		H301, H311, H314, H331, H341, H373	P280, P301+330+331, P302+352, P305+351+338, P309, P310
phosphoric acid	7664-38-2		H290, H314	P280, P301+330+331, P305+351+338, P309+310
SDS	151-21-3		H228, H302, H332, H315, H318, H335, H412	P210, P261, P273, P280, P305+351+338
silver nitrate	7761-88-8		H272, H314, H410	P273, P280, P301+330+331, P305+351+338, P309+310
sodium hydroxide	1310-73-2		H290, H314	P280, P301+330+331, P305+351+338, P308+310
TEMED	110-18-9		H225, H302, H314, H332	P210, P233, P280, P301+330+331, P305+351+338, P309+310
tetracycline	60-54-8		H302	-
trichloroacetic acid	76-03-9		H314, H410	P273, P280, P301+330+331, P305+351+338, P309+310
Tris	77-86-1		H315, H319, H335	P261, P305+351+338
zeocin	11031-11-1		H302	-

## Acknowledgements

Within the last four years of working on this project, I was accompanied and supported by several people which I would like to thank.

At first, I thank **Prof. Dr. Martin Trepel** for giving me the opportunity to work on this challenging and versatile project. I also thank him for the constant support, our scientific discussions, and his supervision of the project and this work.

I thank **Prof. Dr. Edzard Spillner** for taking the time to review my thesis and the supervision of the project.

Furthermore, I thank **Prof. Dr. Mascha Binder** for the supervision of my project and our useful discussions.

I also like to thank **Prof. Dr. Martin Dreyling** and **Prof. Dr. Wolfram Klapper** for providing most of the MCL samples.

Moreover, I thank **Dr. Kristoffer Riecken** for the transduction of the Burkitt lymphoma cell lines, and **Arne Düsedau** for the expert support in cell sorting.

I also thank **Prof. Christian Betzel** for the permission to use the DLS device of his group, and **Dr. Sven Falke** for his assistance during the measurements and his helpful explanations.

**Dr. Henning Seismann** deserves a big appreciation for supporting me the whole time. I thank him for his supervision, his great advises, his unlimited wisdom, and the fun we had inside and outside the lab.

I also thank **Dr. Elmar Spies** for his help, especially during the final phase of the project and of my thesis.

Moreover, I thank **Barbara Gösch**, **Carolina Janko** and **Michael Horn-Glander** for their assistance at different stages of my project.

I like to thank the rest of my colleagues of the **AG Trepel**, for their help, the funny and/or fruitful conversations and for cheering up some frustrating days.

Last but certainly not least, I thank **Grit Tanner** for always being there and listening to my complaints. Without your constant support and motivation, I wouldn't have made it through this. Thank you so much!

## **Eidesstattliche Versicherung**

Hiermit versichere ich an Eides statt, die vorliegende Dissertation selbst verfasst und keine anderen als die angegebenen Hilfsmittel benutzt zu haben. Die eingereichte schriftliche Fassung entspricht der auf dem elektronischen Speichermedium. Ich versichere, dass diese Dissertation nicht in einem früheren Promotionsverfahren eingereicht wurde.

Hamburg, 20.07.2016

---

Michael Fichtner